Introduction to Quantum Noise, Measurement and Amplification: Online Appendices

A.A. Clerk,[1] M.H. Devoret,[2] S.M. Girvin,[3] Florian Marquardt,[4] and R.J. Schoelkopf[2]
[1]*Department of Physics, McGill University, 3600 rue University Montréal, QC Canada H3A 2T8**
[2]*Department of Applied Physics, Yale University PO Box 208284, New Haven, CT 06520-8284*
[3]*Department of Physics, Yale University PO Box 208120, New Haven, CT 06520-8120*
[4]*Department of Physics, Center for NanoScience, and Arnold Sommerfeld Center for Theoretical Physics, Ludwig-Maximilians-Universität München Theresienstr. 37, D-80333 München, Germany*

(Dated: July 2, 2009)

Contents

A. Basics of Classical and Quantum Noise 1
1. Classical noise correlators 1
2. The Wiener-Khinchin Theorem 2
3. Square law detectors and classical spectrum analyzers 3

B. Quantum Spectrum Analyzers: Further Details 4
1. Two-level system as a spectrum analyzer 4
2. Harmonic oscillator as a spectrum analyzer 5
3. Practical quantum spectrum analyzers 6
a. Filter plus diode 6
b. Filter plus photomultiplier 7
c. Double sideband heterodyne power spectrum 7

C. Modes, Transmission Lines and Classical Input/Output Theory 8
1. Transmission lines and classical input-output theory 8
2. Lagrangian, Hamiltonian, and wave modes for a transmission line 10
3. Classical statistical mechanics of a transmission line 11
4. Amplification with a transmission line and a negative resistance 13

D. Quantum Modes and Noise of a Transmission Line 15
1. Quantization of a transmission line 15
2. Modes and the windowed Fourier transform 16
3. Quantum noise from a resistor 17

E. Back Action and Input-Output Theory for Driven Damped Cavities 18
1. Photon shot noise inside a cavity and back action 19
2. Input-output theory for a driven cavity 20
3. Quantum limited position measurement using a cavity detector 24
4. Back-action free single-quadrature detection 28

F. Information Theory and Measurement Rate 29
1. Method I 29
2. Method II 30

G. Number Phase Uncertainty 30

H. Using feedback to reach the quantum limit 31
1. Feedback using mirrors 31
2. Explicit examples 32
3. Op-amp with negative voltage feedback 33

I. Additional Technical Details 34
1. Proof of quantum noise constraint 34
2. Proof that a noiseless detector does not amplify 36
3. Simplifications for a quantum-limited detector 36
4. Derivation of non-equilibrium Langevin equation 37
5. Linear-response formulas for a two-port bosonic amplifier 37
a. Input and output impedances 38
b. Voltage gain and reverse current gain 38
6. Details for the two-port bosonic voltage amplifier with feedback 39

References 40

*Electronic address: clerk@physics.mcgill.ca

Appendix A: Basics of Classical and Quantum Noise

1. Classical noise correlators

Consider a classical random voltage signal $V(t)$. The signal is characterized by zero mean $\langle V(t)\rangle = 0$, and autocorrelation function

$$G_{VV}(t-t') = \langle V(t)V(t')\rangle \tag{A1}$$

whose sign and magnitude tells us whether the voltage fluctuations at time t and time t' are correlated, anti-correlated or statistically independent. We assume that the noise process is *stationary* (i.e., the statistical properties are time translation invariant) so that G_{VV} depends only on the time difference. If $V(t)$ is Gaussian distributed, then the mean and autocorrelation completely specify the statistical properties and the probability distribution. We will assume here that the noise is due to the sum of a very large number of fluctuating charges so that by the central limit theorem, it is Gaussian distributed. We also assume that G_{VV} decays (sufficiently rapidly) to zero on some characteristic correlation time scale τ_c which is finite.

The spectral density of the noise as measured by a spectrum analyzer is a measure of the intensity of the signal at different frequencies. In order to understand

the spectral density of a random signal, it is useful to define its 'windowed' Fourier transform as follows:

$$V_T[\omega] = \frac{1}{\sqrt{T}} \int_{-T/2}^{+T/2} dt\, e^{i\omega t} V(t), \tag{A2}$$

where T is the sampling time. In the limit $T \gg \tau_c$ the integral is a sum of a large number $N \approx \frac{T}{\tau_c}$ of random uncorrelated terms. We can think of the value of the integral as the end point of a random walk in the complex plane which starts at the origin. Because the distance traveled will scale with $\sqrt{T}$, our choice of normalization makes the statistical properties of $V[\omega]$ independent of the sampling time T (for sufficiently large T). Notice that $V_T[\omega]$ has the peculiar units of volts$\sqrt{\text{secs}}$ which is usually denoted volts$/\sqrt{\text{Hz}}$.

The spectral density (or 'power spectrum') of the noise is defined to be the ensemble averaged quantity

$$\mathcal{S}_{VV}[\omega] \equiv \lim_{T\to\infty} \langle |V_T[\omega]|^2 \rangle = \lim_{T\to\infty} \langle V_T[\omega] V_T[-\omega] \rangle \tag{A3}$$

The second equality follows from the fact that $V(t)$ is real valued. The Wiener-Khinchin theorem (derived in Appendix A.2) tells us that the spectral density is equal to the Fourier transform of the autocorrelation function

$$\mathcal{S}_{VV}[\omega] = \int_{-\infty}^{+\infty} dt\, e^{i\omega t} G_{VV}(t). \tag{A4}$$

The inverse transform relates the autocorrelation function to the power spectrum

$$G_{VV}(t) = \int_{-\infty}^{+\infty} \frac{d\omega}{2\pi}\, e^{-i\omega t} \mathcal{S}_{VV}[\omega]. \tag{A5}$$

We thus see that a short auto-correlation time implies a spectral density which is non-zero over a wide range of frequencies. In the limit of 'white noise'

$$G_{VV}(t) = \sigma^2 \delta(t) \tag{A6}$$

the spectrum is flat (independent of frequency)

$$\mathcal{S}_{VV}[\omega] = \sigma^2 \tag{A7}$$

In the opposite limit of a long autocorrelation time, the signal is changing slowly so it can only be made up out of a narrow range of frequencies (not necessarily centered on zero).

Because $V(t)$ is a real-valued classical variable, it naturally follows that $G_{VV}(t)$ is always real. Since $V(t)$ is not a quantum operator, it commutes with its value at other times and thus, $\langle V(t)V(t')\rangle = \langle V(t')V(t)\rangle$. From this it follows that $G_{VV}(t)$ is always symmetric in time and the power spectrum is always symmetric in frequency

$$\mathcal{S}_{VV}[\omega] = \mathcal{S}_{VV}[-\omega]. \tag{A8}$$

As a prototypical example of these ideas, let us consider a simple harmonic oscillator of mass M and frequency Ω. The oscillator is maintained in equilibrium with a large heat bath at temperature T via some infinitesimal coupling which we will ignore in considering the dynamics. The solution of Hamilton's equations of motion are

$$\begin{aligned} x(t) &= x(0)\cos(\Omega t) + p(0)\frac{1}{M\Omega}\sin(\Omega t) \\ p(t) &= p(0)\cos(\Omega t) - x(0)M\Omega \sin(\Omega t), \end{aligned} \tag{A9}$$

where $x(0)$ and $p(0)$ are the (random) values of the position and momentum at time $t = 0$. It follows that the position autocorrelation function is

$$\begin{aligned} G_{xx}(t) &= \langle x(t)x(0)\rangle \\ &= \langle x(0)x(0)\rangle \cos(\Omega t) + \langle p(0)x(0)\rangle \frac{1}{M\Omega}\sin(\Omega t). \end{aligned} \tag{A10}$$

Classically in equilibrium there are no correlations between position and momentum. Hence the second term vanishes. Using the equipartition theorem $\frac{1}{2}M\Omega^2\langle x^2\rangle = \frac{1}{2}k_B T$, we arrive at

$$G_{xx}(t) = \frac{k_B T}{M\Omega^2}\cos(\Omega t) \tag{A11}$$

which leads to the spectral density

$$\mathcal{S}_{xx}[\omega] = \pi \frac{k_B T}{M\Omega^2}\left[\delta(\omega - \Omega) + \delta(\omega + \Omega)\right] \tag{A12}$$

which is indeed symmetric in frequency.

2. The Wiener-Khinchin Theorem

From the definition of the spectral density in Eqs.(A2-A3) we have

$$\begin{aligned} \mathcal{S}_{VV}[\omega] &= \frac{1}{T}\int_0^T dt \int_0^T dt'\, e^{i\omega(t-t')}\langle V(t)V(t')\rangle \\ &= \frac{1}{T}\int_0^T dt \int_{-2B(t)}^{+2B(t)} d\tau\, e^{i\omega\tau}\,\langle V(t+\tau/2)V(t-\tau/2)\rangle \end{aligned} \tag{A13}$$

where

$$\begin{aligned} B(t) &= t \text{ if } t < T/2 \\ &= T - t \text{ if } t > T/2. \end{aligned}$$

If T greatly exceeds the noise autocorrelation time τ_c then it is a good approximation to extend the bound $B(t)$ in the second integral to infinity, since the dominant contribution is from small τ. Using time translation invariance gives

$$\begin{aligned} \mathcal{S}_{VV}[\omega] &= \frac{1}{T}\int_0^T dt \int_{-\infty}^{+\infty} d\tau\, e^{i\omega\tau}\,\langle V(\tau)V(0)\rangle \\ &= \int_{-\infty}^{+\infty} d\tau\, e^{i\omega\tau}\,\langle V(\tau)V(0)\rangle\,. \end{aligned} \tag{A14}$$

This proves the Wiener-Khinchin theorem stated in Eq. (A4).

A useful application of these ideas is the following. Suppose that we have a noisy signal $V(t) = \bar{V} + \eta(t)$ which we begin monitoring at time $t = 0$. The integrated signal up to time t is given by

$$I(T) = \int_0^T dt\, V(t) \tag{A15}$$

and has mean

$$\langle I(T)\rangle = \bar{V}T. \tag{A16}$$

Provided that the integration time greatly exceeds the autocorrelation time of the noise, $I(T)$ is a sum of a large number of uncorrelated random variables. The central limit theorem tells us in this case that $I(t)$ is gaussian distributed even if the signal itself is not. Hence the probability distribution for I is fully specified by its mean and its variance

$$\langle(\Delta I)^2\rangle = \int_0^T dtdt'\, \langle\eta(t)\eta(t')\rangle. \tag{A17}$$

From the definition of spectral density above we have the simple result that the variance of the integrated signal grows linearly in time with proportionality constant given by the noise spectral density at zero frequency

$$\langle(\Delta I)^2\rangle = \mathcal{S}_{VV}[0]\, T. \tag{A18}$$

As a simple application, consider the photon shot noise of a coherent laser beam. The total number of photons detected in time T is

$$N(T) = \int_0^T dt\, \dot{N}(t). \tag{A19}$$

The photo-detection signal $\dot{N}(t)$ is *not* gaussian, but rather is a *point process*, that is, a sequence of delta functions with random Poisson distributed arrival times and mean photon arrival rate $\overline{\dot{N}}$. Nevertheless at long times the mean number of detected photons

$$\langle N(T)\rangle = \overline{\dot{N}}T \tag{A20}$$

will be large and the photon number distribution will be gaussian with variance

$$\langle(\Delta N)^2\rangle = S_{\dot{N}\dot{N}}\, T. \tag{A21}$$

Since we know that for a Poisson process the variance is equal to the mean

$$\langle(\Delta N)^2\rangle = \langle N(T)\rangle, \tag{A22}$$

it follows that the shot noise power spectral density is

$$S_{\dot{N}\dot{N}}(0) = \overline{\dot{N}}. \tag{A23}$$

Since the noise is white this result happens to be valid at all frequencies, but the noise is gaussian distributed only at low frequencies.

3. Square law detectors and classical spectrum analyzers

Now that we understand the basics of classical noise, we can consider how one experimentally measures a classical noise spectral density. With modern high speed digital sampling techniques it is perfectly feasible to directly measure the random noise signal as a function of time and then directly compute the autocorrelation function in Eq. (A1). This is typically done by first performing an analog-to-digital conversion of the noise signal, and then numerically computing the autocorrelation function. One can then use Eq. (A4) to calculate the noise spectral density via a numerical Fourier transform. Note that while Eq. (A4) seems to require an ensemble average, in practice this is not explicitly done. Instead, one uses a sufficiently long averaging time T (i.e. much longer than the correlation time of the noise) such that a single time-average is equivalent to an ensemble average. This approach of measuring a noise spectral density directly from its autocorrelation function is most appropriate for signals at RF frequencies well below 1 MHz.

For microwave signals with frequencies well above 1 GHz, a very different approach is usually taken. Here, the standard route to obtain a noise spectral density involves first shifting the signal to a lower intermediate frequency via a technique known as heterodyning (we discuss this more in Sec. B.3.c). This intermediate-frequency signal is then sent to a filter which selects a narrow frequency range of interest, the so-called 'resolution bandwidth'. Finally, this filtered signal is sent to a square-law detector (e.g. a diode), and the resulting output is averaged over a certain time-interval (the inverse of the so-called 'video bandwidth'). It is this final output which is then taken to be a measure of the noise spectral density.

It helps to put the above into equations. Ignoring for simplicity the initial heterodyning step, let

$$V_{\rm f}[\omega] = f[\omega]V[\omega] \tag{A24}$$

be the voltage at the output of the filter and the input of the square law detector. Here, $f[\omega]$ is the (amplitude) transmission coefficient of the filter and $V[\omega]$ is the Fourier transform of the noisy signal we are measuring. From Eq. (A5) it follows that the output of the square law detector is proportional to

$$\langle I\rangle = \int_{-\infty}^{+\infty} \frac{d\omega}{2\pi} |f[\omega]|^2 \mathcal{S}_{VV}[\omega]. \tag{A25}$$

Approximating the narrow band filter centered on frequency $\pm\omega_0$ as[1]

$$|f[\omega]|^2 = \delta(\omega - \omega_0) + \delta(\omega + \omega_0) \tag{A26}$$

---

[1] A linear passive filter performs a convolution $V_{\rm out}(t) = \int_{-\infty}^{+\infty} dt'\, F(t - t')V_{\rm in}(t')$ where F is a real-valued (and causal) function. Hence it follows that $f[\omega]$, which is the Fourier transform of F, obeys $f[-\omega] = f^*[\omega]$ and hence $|f[\omega]|^2$ is symmetric in frequency.

we obtain

$$\langle I \rangle = \mathcal{S}_{VV}(-\omega_0) + \mathcal{S}_{VV}(\omega_0) \tag{A27}$$

showing as expected that the classical square law detector measures the symmetrized noise power.

We thus have two very different basic approaches for the measurement of classical noise spectral densities: for low RF frequencies, one can directly measure the noise autocorrelation, whereas for high microwave frequencies, one uses a filter and a square law detector. For noise signals in intermediate frequency ranges, a combination of different methods is generally used. The whole story becomes even more complicated, as at very high frequencies (e.g. in the far infrared), devices such as the so-called 'Fourier Transform spectrometer' are in fact based on a direct measurement of the equivalent of an autocorrelation function of the signal. In the infrared, visible and ultraviolet, noise spectrometers use gratings followed by a slit acting as a filter.

Appendix B: Quantum Spectrum Analyzers: Further Details

1. Two-level system as a spectrum analyzer

In this sub-appendix, we derive the Golden Rule transition rates Eqs. (2.6) describing a quantum two-level system coupled to a noise source (cf. Sec. II.B). Our derivation is somewhat unusual, in that the role of the continuum as a noise source is emphasized from the outset. We start by treating the noise $F(t)$ in Eq. (2.5) as being a classically noisy variable. We assume that the coupling A is under our control and can be made small enough that the noise can be treated in lowest order perturbation theory. We take the state of the two-level system to be

$$|\psi(t)\rangle = \begin{pmatrix} \alpha_g(t) \\ \alpha_e(t) \end{pmatrix}. \tag{B1}$$

In the interaction representation, first-order time-dependent perturbation theory gives

$$|\psi_{\rm I}(t)\rangle = |\psi(0)\rangle - \frac{i}{\hbar}\int_0^t d\tau\ \hat{V}(\tau)|\psi(0)\rangle. \tag{B2}$$

If we initially prepare the two-level system in its ground state, the amplitude to find it in its excited state at time t is from Eq. (B2)

$$\begin{aligned} \alpha_e &= -\frac{iA}{\hbar}\int_0^t d\tau\ \langle e|\hat{\sigma}_x(\tau)|g\rangle F(\tau), \\ &= -\frac{iA}{\hbar}\int_0^t d\tau\ e^{i\omega_{01}\tau}F(\tau). \end{aligned} \tag{B3}$$

Since the integrand in Eq. (B3) is random, α_e is a sum of a large number of random terms; i.e. its value is the endpoint of a random walk in the complex plane (as discussed above in defining the spectral density of classical noise). As a result, for times exceeding the autocorrelation time $\tau_{\rm c}$ of the noise, the integral will not grow linearly with time but rather only as the square root of time, as expected for a random walk. We can now compute the probability

$$p_e(t) \equiv |\alpha_e|^2 = \frac{A^2}{\hbar^2}\int_0^t\int_0^t d\tau_1 d\tau_2\, e^{-i\omega_{01}(\tau_1-\tau_2)}F(\tau_1)F(\tau_2) \tag{B4}$$

which we expect to grow quadratically for short times $t < \tau_{\rm c}$, but linearly for long times $t > \tau_{\rm c}$. Ensemble averaging the probability over the random noise yields

$$\bar{p}_e(t) = \frac{A^2}{\hbar^2}\int_0^t\int_0^t d\tau_1 d\tau_2\, e^{-i\omega_{01}(\tau_1-\tau_2)}\,\langle F(\tau_1)F(\tau_2)\rangle \tag{B5}$$

Introducing the noise spectral density

$$S_{FF}(\omega) = \int_{-\infty}^{+\infty} d\tau\, e^{i\omega\tau}\langle F(\tau)F(0)\rangle, \tag{B6}$$

and utilizing the Fourier transform defined in Eq. (A2) and the Wiener-Khinchin theorem from Appendix A.2, we find that the probability to be in the excited state indeed increases *linearly* with time at long times,[2]

$$\bar{p}_e(t) = t\frac{A^2}{\hbar^2}S_{FF}(-\omega_{01}) \tag{B7}$$

The time derivative of the probability gives the transition rate from ground to excited states

$$\Gamma_\uparrow = \frac{A^2}{\hbar^2}S_{FF}(-\omega_{01}) \tag{B8}$$

Note that we are taking in this last expression the spectral density on the negative frequency side. If F were a strictly classical noise source, $\langle F(\tau)F(0)\rangle$ would be real, and $S_{FF}(-\omega_{01}) = S_{FF}(+\omega_{01})$. However, because as we discuss below F is actually an operator acting on the environmental degrees of freedom, $\left[\hat{F}(\tau), \hat{F}(0)\right] \neq 0$ and $S_{FF}(-\omega_{01}) \neq S_{FF}(+\omega_{01})$.

Another possible experiment is to prepare the two-level system in its excited state and look at the rate of decay into the ground state. The algebra is identical to that above except that the sign of the frequency is reversed:

$$\Gamma_\downarrow = \frac{A^2}{\hbar^2}S_{FF}(+\omega_{01}). \tag{B9}$$

We now see that our two-level system does indeed act as a quantum spectrum analyzer for the noise. Operationally,

---

[2] Note that for very long times, where there is a significant depletion of the probability of being in the initial state, first-order perturbation theory becomes invalid. However, for sufficiently small A, there is a wide range of times $\tau_{\rm c} \ll t \ll 1/\Gamma$ for which Eq. B7 is valid. Eqs. (2.6a) and (2.6b) then yield well-defined rates which can be used in a master equation to describe the full dynamics including long times.

we prepare the system either in its ground state or in its excited state, weakly couple it to the noise source, and after an appropriate interval of time (satisfying the above inequalities) simply measure whether the system is now in its excited state or ground state. Repeating this protocol over and over again, we can find the probability of making a transition, and thereby infer the rate and hence the noise spectral density at positive and negative frequencies. Naively one imagines that a spectrometers measures the noise spectrum by extracting a small amount of the signal energy from the noise source and analyzes it. This is *not* the case however. There must be energy flowing in both directions if the noise is to be fully characterized.

We now rigorously treat the quantity $\hat{F}(\tau)$ as a quantum Heisenberg operator which acts in the Hilbert space of the noise source. The previous derivation is unchanged (the ordering of $\hat{F}(\tau_1)\hat{F}(\tau_2)$ having been chosen correctly in anticipation of the quantum treatment), and Eqs. (2.6a,2.6b) are still valid provided that we interpret the angular brackets in Eq. (B5,B6) as representing a quantum expectation value (evaluated in the absence of the coupling to the spectrometer):

$$S_{FF}(\omega) = \int_{-\infty}^{+\infty} d\tau\, e^{i\omega\tau} \sum_{\alpha,\gamma} \rho_{\alpha\alpha}\, \langle\alpha|\hat{F}(\tau)|\gamma\rangle\langle\gamma|\hat{F}(0)|\alpha\rangle. \tag{B10}$$

Here, we have assumed a stationary situation, where the density matrix ρ of the noise source is diagonal in the energy eigenbasis (in the absence of the coupling to the spectrometer). However, we do not necessarily assume that it is given by the equilibrium expression. This yields the standard quantum mechanical expression for the spectral density:

$$\begin{aligned} S_{FF}(\omega) &= \int_{-\infty}^{+\infty} d\tau\, e^{i\omega\tau} \sum_{\alpha,\gamma} \rho_{\alpha\alpha}\, e^{\frac{i}{\hbar}(\epsilon_\alpha - \epsilon_\gamma)\tau}\, |\langle\alpha|\hat{F}|\gamma\rangle|^2 \\ &= 2\pi\hbar \sum_{\alpha,\gamma} \rho_{\alpha\alpha}\, |\langle\alpha|\hat{F}|\gamma\rangle|^2 \delta(\epsilon_\gamma - \epsilon_\alpha - \hbar\omega) \end{aligned} \tag{B11}$$

Substituting this expression into Eqs. (2.6a,2.6b), we derive the familiar Fermi Golden Rule expressions for the two transition rates.

In standard courses, one is not normally taught that the transition rate of a discrete state into a continuum as described by Fermi's Golden Rule can (and indeed should!) be viewed as resulting from the continuum acting as a quantum noise source which causes the amplitudes of the different components of the wave function to undergo random walks. The derivation presented here hopefully provides a motivation for this interpretation. In particular, thinking of the perturbation (i.e. the coupling to the continuum) as quantum noise with a small but finite autocorrelation time (inversely related to the bandwidth of the continuum) neatly explains why the transition probability increases quadratically for very short times, but linearly for very long times.

It it is important to keep in mind that our expressions for the transition rates are only valid if the autocorrelation time of our noise is much shorter that the typical time we are interested in; this typical time is simply the inverse of the transition rate. The requirement of a short autocorrelation time in turn implies that our noise source must have a large bandwidth (i.e. there must be large number of available photon frequencies in the vacuum) and must not be coupled too strongly to our system. This is true despite the fact that our final expressions for the transition rates only depend on the spectral density at the transition frequency (a consequence of energy conservation).

One standard model for the continuum is an infinite collection of harmonic oscillators. The electromagnetic continuum in the hydrogen atom case mentioned above is a prototypical example. The vacuum electric field noise coupling to the hydrogen atom has an extremely short autocorrelation time because the range of mode frequencies ω_α (over which the dipole matrix element coupling the atom to the mode electric field $\vec{E}_\alpha$ is significant) is extremely large, ranging from many times smaller than the transition frequency to many times larger. Thus, the autocorrelation time of the vacuum electric field noise is considerably less than 10^{-15}s, whereas the decay time of the hydrogen 2p state is about 10^{-9}s. Hence the inequalities needed for the validity of our expressions are very easily satisfied.

2. Harmonic oscillator as a spectrum analyzer

We now provide more details on the system described in Sec. II.B, where a harmonic oscillator acts as a spectrometer of quantum noise. We start with the coupling Hamiltonian givein in Eq. (2.9). In analogy to the TLS spectrometer, noise in $\hat{F}$ at the oscillator frequency Ω can cause transitions between its eigenstates. We assume both that A is small, and that our noise source has a short autocorrelation time, so we may again use perturbation theory to derive rates for these transitions. There is a rate for increasing the number of quanta in the oscillator by one, taking a state $|n\rangle$ to $|n+1\rangle$:

$$\Gamma_{n\to n+1} = \frac{A^2}{\hbar^2}\left[(n+1)x_{\rm ZPF}^2\right] S_{FF}[-\Omega] \equiv (n+1)\Gamma_\uparrow \tag{B12}$$

As expected, this rate involves the noise at $-\Omega$, as energy is being *absorbed from* the noise source. Similarly, there is a rate for decreasing the number of quanta in the oscillator by one:

$$\Gamma_{n\to n-1} = \frac{A^2}{\hbar^2}\left(n x_{\rm ZPF}^2\right) S_{FF}[\Omega] \equiv n\Gamma_\downarrow \tag{B13}$$

This rate involves the noise at $+\Omega$, as energy is being *emitted to* the noise source.

Given these transition rates, we may immediately write a simple master equation for the probability $p_n(t)$ that

there are n quanta in the oscillator:

$$\begin{aligned}\frac{d}{dt}p_n &= [n\Gamma_\uparrow p_{n-1} + (n+1)\Gamma_\downarrow p_{n+1}] \\ &- [n\Gamma_\downarrow + (n+1)\Gamma_\uparrow]\, p_n \end{aligned} \tag{B14}$$

The first two terms describe transitions into the state $|n\rangle$ from the states $|n+1\rangle$ and $|n-1\rangle$, and hence increase p_n. In contrast, the last two terms describe transitions out of the state $|n\rangle$ to the states $|n+1\rangle$ and $|n-1\rangle$, and hence decrease p_n. The stationary state of the oscillator is given by solving Eq. (B14) for $\frac{d}{dt}p_n = 0$, yielding:

$$p_n = e^{-n\hbar\Omega/(k_B T_{\rm eff})}\left(1 - e^{-\hbar\Omega/(k_B T_{\rm eff})}\right) \tag{B15}$$

where the effective temperature $T_{\rm eff}[\Omega]$ is defined in Eq. (2.8). Eq. (B15) describes a thermal equilibrium distribution of the oscillator, with an effective oscillator temperature $T_{\rm eff}[\Omega]$ determined by the quantum noise spectrum of $\hat{F}$. This is the same effective temperature that emerged in our discussion of the TLS spectrum analyzer. As we have seen, if the noise source is in thermal equilibrium at a temperature $T_{\rm eq}$, then $T_{\rm eff}[\Omega] = T_{\rm eq}$. In the more general case where the noise source is not in thermal equilibrium, $T_{\rm eff}$ only serves to characterize the asymmetry of the quantum noise, and will vary with frequency [3].

We can learn more about the quantum noise spectrum of $\hat{F}$ by also looking at the dynamics of the oscillator. In particular, as the average energy $\langle E\rangle$ of the oscillator is just given by $\langle E(t)\rangle = \sum_{n=0}^{\infty}\hbar\Omega\left(n+\frac{1}{2}\right)p_n(t)$, we can use the master equation Eq. (B14) to derive an equation for its time dependence. One thus finds Eq. (2.10). By demanding $d\langle E\rangle/dt = 0$ in this equation, we find that the combination of damping and heating effects causes the energy to reach a steady state mean value of $\langle E\rangle = P/\gamma$. This implies that the finite ground state energy $\langle E\rangle = \hbar\Omega/2$ of the oscillator is determined via the balance between the 'heating' by the zero-point fluctuations of the environment (described by the symmetrized correlator at $T = 0$) and the dissipation. It is possible to take an alternative but equally correct viewpoint, where only the deviation $\langle\delta E\rangle = \langle E\rangle - \hbar\Omega/2$ from the ground state energy is considered. Its evolution equation

$$\frac{d}{dt}\langle\delta E\rangle = \langle\delta E\rangle(\Gamma_\uparrow - \Gamma_\downarrow) + \Gamma_\uparrow\hbar\Omega \tag{B16}$$

only contains a decay term at $T = 0$, leading to $\langle\delta E\rangle \to 0$.

3. Practical quantum spectrum analyzers

As we have seen, a 'quantum spectrum analyzer' can in principle be constructed from a two level system (or a harmonic oscillator) in which we can separately measure the up and down transition rates between states differing by some precise energy $\hbar\omega > 0$ given by the frequency of interest. The down transition rate tells us the noise spectral density at frequency $+\omega$ and the up transition rate tells us the noise spectral density at $-\omega$. While we have already discussed experimental implementation of these ideas using two-level systems and oscillators, similar schemes have been implemented in other systems. A number of recent experiments have made use of superconductor-insulator-superconductor junctions (Billangeon *et al.*, 2006; Deblock *et al.*, 2003; Onac *et al.*, 2006) to measure quantum noise, as the current-voltage characteristics of such junctions are very sensitive to the absorption or emission of energy (so-called photon-assisted transport processes). It has also been suggested that tunneling of flux in a SQUID can be used to measure quantum noise (Amin and Averin, 2008).

In this subsection, we discuss additional methods for the detection of quantum noise. Recall from Sec. A.3 that one of the most basic classical noise spectrum analyzers consists of a linear narrow band filter and a square law detector such as a diode. In what follows, we will consider a simplified quantum treatment of such a device where we do not explicitly model a diode, but instead focus on the energy of the filter circuit. We then turn to various noise detection schemes making use of a photomultiplier. We will show that depending on the detection scheme used, one can measure either the symmetrized quantum noise spectral density $\bar{S}[\omega]$, or the non-symmetrized spectral density $S[\omega]$.

a. Filter plus diode

Using the simple treatment we gave of a harmonic oscillator as a quantum spectrum analyzer in Sec. B.2, one can attempt to provide a quantum treatment of the classical 'filter plus diode' spectrum analyzer discussed in Sec. A.3. This approach is due to Lesovik and Loosen (1997) and Gavish *et al.* (2000). The analysis starts by modeling the spectrum analyzer's resonant filter circuit as a harmonic oscillator of frequency Ω weakly coupled to some equilibrium dissipative bath. The oscillator thus has an intrinsic damping rate $\gamma_0 \ll \Omega$, and is initially at a finite temperature $T_{\rm eq}$. One then drives this damped oscillator (i.e. the filter circuit) with the noisy quantum force $\hat{F}(t)$ whose spectrum at frequency Ω is to be measured.

In the classical 'filter plus diode' spectrum analyzer, the output of the filter circuit was sent to a square law detector, whose time-averaged output was then taken as the measured spectral density. To simplify the analysis, we can instead consider how the noise changes the average energy of the resonant filter circuit, taking this quantity as a proxy for the output of the diode. Sure enough, if we subject the filter circuit to purely classical noise, it would cause the average energy of the circuit

[3] Note that the effective temperature can become negative if the noise source prefers emitting energy versus absorbing it; in the present case, that would lead to an instability.

$\langle E\rangle$ to increase an amount directly proportional to the classical spectrum $\mathcal{S}_{FF}[\Omega]$. We now consider $\langle E\rangle$ in the case of a quantum noise source, and ask how it relates to the quantum noise spectral density $S_{FF}[\Omega]$.

The quantum case is straightforward to analyze using the approach of Sec. B.2. Unlike the classical case, the noise will both lead to additional fluctuations of the filter circuit *and* increase its damping rate by an amount γ (c.f. Eq. (2.12)). To make things quantitative, we let $n_{\rm eq}$ denote the average number of quanta in the filter circuit prior to coupling to $\hat{F}(t)$, i.e.

$$n_{\rm eq} = \frac{1}{\exp\left(\frac{\hbar\Omega}{k_B T_{\rm eq}}\right) - 1}, \tag{B17}$$

and let $n_{\rm eff}$ represent the Bose-Einstein factor associated with the effective temperature $T_{\rm eff}[\Omega]$ of the noise source $\hat{F}(t)$,

$$n_{\rm eff} = \frac{1}{\exp\left(\frac{\hbar\Omega}{k_B T_{\rm eff}[\Omega]}\right) - 1}. \tag{B18}$$

One then finds (Gavish *et al.*, 2000; Lesovik and Loosen, 1997):

$$\Delta\langle E\rangle \;=\; \hbar\Omega \cdot \frac{\gamma}{\gamma_0 + \gamma}(n_{\rm eff} - n_{\rm eq}) \tag{B19}$$

This equation has an extremely simple interpretation: the first term results from the expected heating effect of the noise, while the second term results from the noise source having increased the circuit's damping by an amount γ. Re-expressing this result in terms of the symmetric and anti-symmetric in frequency parts of the quantum noise spectral density $S_{FF}[\Omega]$, we have:

$$\Delta\langle E\rangle \;=\; \frac{\bar{S}_{FF}(\Omega) - \left(n_{\rm eq} + \frac{1}{2}\right)\left(S_{FF}[\Omega] - S_{FF}[-\Omega]\right)}{2m\left(\gamma_0 + \gamma\right)} \tag{B20}$$

We see that $\Delta\langle E\rangle$ is in general *not* simply proportional to the symmetrized noise $\bar{S}_{FF}[\Omega]$. Thus, the 'filter plus diode' spectrum analyzer does not simply measure the symmetrized quantum noise spectral density. We stress that there is nothing particularly quantum about this result. The extra term on the RHS of Eq. (B20) simply reflects the fact that coupling the noise source to the filter circuit could change the damping of this circuit; this could easily happen in a completely classical setting. As long as this additional damping effect is minimal, the second term in Eq. (B20) will be minimal, and our spectrum analyzer will (to a good approximation) measure the symmetrized noise. Quantitatively, this requires:

$$n_{\rm eff} \gg n_{\rm eq}. \tag{B21}$$

We now see where quantum mechanics enters: if the noise to be measured is close to being zero point noise (i.e. $n_{\rm eff} \to 0$), the above condition can never be satisfied, and thus it is *impossible* to ignore the damping effect of the noise source on the filter circuit. In the zero point limit, this damping effect (i.e. second term in Eq. (B20)) will always be greater than or equal to the expected heating effect of the noise (i.e. first term in Eq. (B20)).

b. Filter plus photomultiplier

We now turn to quantum spectrum analyzers involving a square law detector we can accurately model– a photomultiplier. As a first example of such a system, consider a photomultiplier with a narrow band filter placed in front of it. The mean photocurrent is then given by

$$\langle I\rangle = \int_{-\infty}^{+\infty} d\omega\, |f[\omega]|^2 r[\omega] S_{\rm VV}[\omega], \tag{B22}$$

where f is the filter (amplitude) transmission function defined previously and $r[\omega]$ is the response of the photodetector at frequency ω, and $S_{\rm VV}$ represents the electric field spectral density incident upon the photodetector. Naively one thinks of the photomultiplier as a square law detector with the square of the electric field representing the optical power. However, according to the Glauber theory of (ideal) photo-detection (Gardiner and Zoller, 2000; Glauber, 2006; Walls and Milburn, 1994), photocurrent is produced if, and only if, a photon is absorbed by the detector, liberating the initial photoelectron. Glauber describes this in terms of normal ordering of the photon operators in the electric field autocorrelation function. In our language of noise power at positive and negative frequencies, this requirement becomes simply that $r[\omega]$ vanishes for $\omega > 0$. Approximating the narrow band filter centered on frequency $\pm\omega_0$ as in Eq. (A26), we obtain

$$\langle I\rangle = r[-\omega_0] S_{\rm VV}[-\omega_0] \tag{B23}$$

which shows that this particular realization of a quantum spectrometer only measures electric field spectral density at negative frequencies since the photomultiplier never emits energy into the noise source. Also one does not see in the output any 'vacuum noise' and so the output (ideally) vanishes as it should at zero temperature. Of course real photomultipliers suffer from imperfect quantum efficiencies and have non-zero dark current. Note that we have assumed here that there are no additional fluctuations associated with the filter circuit. Our result thus coincides with what we found in the previous subsection for the 'filter plus diode' spectrum analyzer (c.f. Eq. (B20), in the limit where the filter circuit is initially at zero temperature (i.e. $n_{\rm eq} = 0$).

c. Double sideband heterodyne power spectrum

At RF and microwave frequencies, practical spectrometers often contain heterodyne stages which mix the initial

frequency down to a lower frequency $\omega_{\rm IF}$ (possibly in the classical regime). Consider a system with a mixer and local oscillator at frequency $\omega_{\rm LO}$ that mixes both the upper sideband input at $\omega_{\rm u} = \omega_{\rm LO}+\omega_{\rm IF}$ and the lower sideband input at $\omega_{\rm l} = \omega_{\rm LO} - \omega_{\rm IF}$ down to frequency $\omega_{\rm IF}$. This can be achieved by having a Hamiltonian with a 3-wave mixing term which (in the rotating wave approximation) is given by

$$V = \lambda[\hat{a}_{\rm IF}\hat{a}_{\rm l}\hat{a}^\dagger_{\rm LO} + \hat{a}^\dagger_{\rm IF}\hat{a}^\dagger_{\rm l}\hat{a}_{\rm LO}] + \lambda[\hat{a}^\dagger_{\rm IF}\hat{a}_{\rm u}\hat{a}^\dagger_{\rm LO} + \hat{a}_{\rm IF}\hat{a}^\dagger_{\rm u}\hat{a}_{\rm LO}] \tag{B24}$$

The interpretation of this term is that of a Raman process. Notice that there are two energy conserving processes that can create an IF photon which could then activate the photodetector. First, one can absorb an LO photon and *emit* two photons, one at the IF and one at the lower sideband. The second possibility is to *absorb* an upper sideband photon and create IF and LO photons. Thus we expect from this that the power in the IF channel detected by a photomultiplier would be proportional to the noise power in the following way

$$I \propto S[+\omega_{\rm l}] + S[-\omega_{\rm u}] \tag{B25}$$

since creation of an IF photon involves the signal source either absorbing a lower sideband photon from the mixer or the signal source emitting an upper sideband photon into the mixer. In the limit of small IF frequency this expression would reduce to the symmetrized noise power

$$I \propto S[+\omega_{\rm LO}] + S[-\omega_{\rm LO}] = 2\bar{S}[\omega_{\rm LO}] \tag{B26}$$

which is the same as for a 'classical' spectrum analyzer with a square law detector (c.f. Appendix A.3). For equilibrium noise spectral density from a resistance R_0 derived in Appendix D we would then have

$$S_{\rm VV}[\omega] + S_{\rm VV}[-\omega] = 2R_0\hbar|\omega|[2n_{\rm B}(\hbar|\omega|) + 1], \tag{B27}$$

Assuming our spectrum analyzer has high input impedance so that it does not load the noise source, this voltage spectrum will determine the output signal of the analyzer. This symmetrized quantity does *not* vanish at zero temperature and the output contains the vacuum noise from the input. This vacuum noise has been seen in experiment. (Schoelkopf *et al.*, 1997)

Appendix C: Modes, Transmission Lines and Classical Input/Output Theory

In this appendix we introduce a number of important classical concepts about electromagnetic signals which are essential to understand before moving on to the study of their quantum analogs. A signal at carrier frequency ω can be described in terms of its amplitude and phase or equivalently in terms of its two quadrature amplitudes

$$s(t) = X\cos(\omega t) + Y\sin(\omega t). \tag{C1}$$

We will see in the following that the physical oscillations of this signal in a transmission line are precisely the sinusoidal oscillations of a simple harmonic oscillator. Comparison of Eq. (C1) with $x(t) = x_0\cos\omega t + (p_0/M\omega)\sin\omega t$ shows that we can identify the quadrature amplitude X with the coordinate of this oscillator and thus the quadrature amplitude Y is proportional to the momentum conjugate to X. Quantum mechanically, X and Y become operators $\hat{X}$ and $\hat{Y}$ which do not commute. Thus their quantum fluctuations obey the Heisenberg uncertainty relation.

Ordinarily (e.g., in the absence of squeezing), the phase choice defining the two quadratures is arbitrary and so their vacuum (i.e. zero-point) fluctuations are equal

$$X_{\rm ZPF} = Y_{\rm ZPF}. \tag{C2}$$

Thus the canonical commutation relation becomes

$$[\hat{X}, \hat{Y}] = iX^2_{\rm ZPF}. \tag{C3}$$

We will see that the fact that X and Y are canonically conjugate has profound implications both classically and quantum mechanically. In particular, the action of any circuit element (beam splitter, attenuator, amplifier, etc.) must preserve the Poisson bracket (or in the quantum case, the commutator) between the signal quadratures. This places strong constraints on the properties of these circuit elements and in particular, forces every amplifier to add noise to the signal.

1. Transmission lines and classical input-output theory

We begin by considering a coaxial transmission line modeled as a perfectly conducting wire with inductance per unit length of ℓ and capacitance to ground per unit length c as shown in Fig. 1. If the voltage at position x at time t is $V(x,t)$, then the charge density is $q(x,t) = cV(x,t)$. By charge conservation the current I and the charge density are related by the continuity equation

$$\partial_t q + \partial_x I = 0. \tag{C4}$$

The constitutive relation (essentially Newton's law) gives the acceleration of the charges

$$\ell\partial_t I = -\partial_x V. \tag{C5}$$

We can decouple Eqs. (C4) and (C5) by introducing left and right propagating modes

$$V(x,t) = [V^{\rightarrow} + V^{\leftarrow}] \tag{C6}$$

$$I(x,t) = \frac{1}{Z_{\rm c}}[V^{\rightarrow} - V^{\leftarrow}] \tag{C7}$$

where $Z_{\rm c} \equiv \sqrt{\ell/c}$ is called the characteristic impedance of the line. In terms of the left and right propagating modes, Eqs. (C4) and C5 become

$$v_{\rm p}\partial_x V^{\rightarrow} + \partial_t V^{\rightarrow} = 0 \tag{C8}$$

$$v_{\rm p}\partial_x V^{\leftarrow} - \partial_t V^{\leftarrow} = 0 \tag{C9}$$

where $v_{\rm p} \equiv 1/\sqrt{\ell c}$ is the wave phase velocity. These equations have solutions which propagate by uniform translation without changing shape since the line is dispersionless

$$V^{\rightarrow}(x,t) \;=\; V_{\rm out}(t-\frac{x}{v_{\rm p}}) \qquad \text{(C10)}$$

$$V^{\leftarrow}(x,t) \;=\; V_{\rm in}(t+\frac{x}{v_{\rm p}}), \qquad \text{(C11)}$$

where $V_{\rm in}$ and $V_{\rm out}$ are *arbitrary* functions of their arguments. For an infinite transmission line, $V_{\rm out}$ and $V_{\rm in}$ are completely independent. However for the case of a semi-infinite line terminated at $x=0$ (say) by some system S, these two solutions are not independent, but rather related by the boundary condition imposed by the system. We have

$$V(x=0,t) \;=\; [V_{\rm out}(t)+V_{\rm in}(t)] \qquad \text{(C12)}$$

$$I(x=0,t) \;=\; \frac{1}{Z_{\rm c}}[V_{\rm out}(t)-V_{\rm in}(t)], \qquad \text{(C13)}$$

from which we may derive

$$V_{\rm out}(t) = V_{\rm in}(t) + Z_{\rm c} I(x=0,t). \qquad \text{(C14)}$$

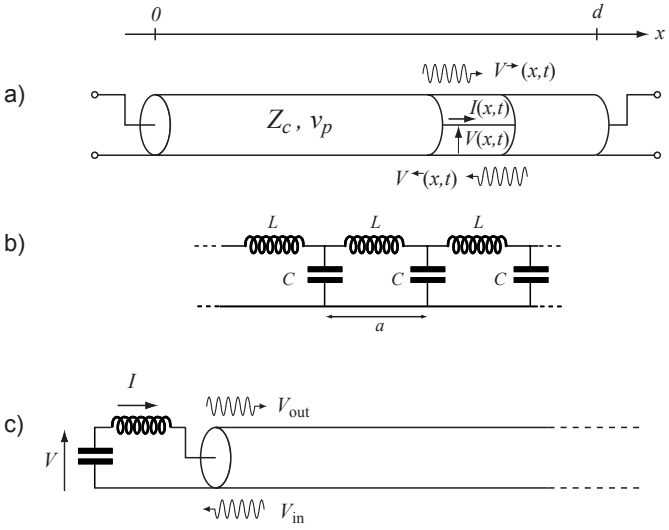

FIG. 1 a) Coaxial transmission line, indicating voltages and currents as defined in the main text. b) Lumped element representation of a transmission line with capacitance per unit length $c = C/a$ and inductance per unit length $\ell = L/a$. c) Discrete LC resonator terminating a transmission line.

If the system under study is just an open circuit so that $I(x=0,t)=0$, then $V_{\rm out} = V_{\rm in}$, meaning that the outgoing wave is simply the result of the incoming wave reflecting from the open circuit termination. In general however, there is an additional outgoing wave radiated by the current I that is injected by the system dynamics into the line. In the absence of an incoming wave we have

$$V(x=0,t) = Z_{\rm c} I(x=0,t), \qquad \text{(C15)}$$

indicating that the transmission line acts as a simple resistor which, instead of dissipating energy by Joule heating, carries the energy away from the system as propagating waves. The fact that the line can dissipate energy despite containing only purely reactive elements is a consequence of its infinite extent. One must be careful with the order of limits, taking the length to infinity *before* allowing time to go to infinity. In this way the outgoing waves never reach the far end of the transmission line and reflect back. Since this is a conservative Hamiltonian system, we will be able to quantize these waves and make a quantum theory of resistors (Caldeira and Leggett, 1983) in Appendix D. The net power flow carried to the right by the line is

$$P = \frac{1}{Z_{\rm c}}[V_{\rm out}^2(t) - V_{\rm in}^2(t)]. \qquad \text{(C16)}$$

The fact that the transmission line presents a dissipative impedance to the system means that it causes damping of the system. It also however opens up the possibility of controlling the system via the input field which partially determines the voltage driving the system. From this point of view it is convenient to eliminate the output field by writing the voltage as

$$V(x=0,t) = 2V_{\rm in}(t) + Z_{\rm c} I(x=0,t). \qquad \text{(C17)}$$

As we will discuss in more detail below, the first term drives the system and the second damps it. From Eq. (C14) we see that measurement of the outgoing field can be used to determine the current $I(x=0,t)$ injected by the system into the line and hence to infer the system dynamics that results from the input drive field.

As a simple example, consider the system consisting of an LC resonator shown in Fig. (1 c). This can be viewed as a simple harmonic oscillator whose coordinate Q is the charge on the capacitor plate (on the side connected to L_0). The current $I(x=0,t) = \dot{Q}$ plays the role of the velocity of the oscillator. The equation of motion for the oscillator is readily obtained from

$$Q = C_0[-V(x=0^+,t) - L_0 \dot{I}(x=0^+,t)]. \qquad \text{(C18)}$$

Using Eq. (C17) we obtain a harmonic oscillator damped by the transmission line and driven by the incoming waves

$$\ddot{Q} = -\Omega_0^2 Q - \gamma \dot{Q} - \frac{2}{L_0} V_{\rm in}(t), \qquad \text{(C19)}$$

where the resonant frequency is $\Omega_0^2 \equiv 1/\sqrt{L_0 C_0}$. Note that the term $Z_{\rm c} I(x=0,t)$ in Eq. (C17) results in the linear viscous damping rate $\gamma \equiv Z_{\rm c}/L_0$.

If we solve the equation of motion of the oscillator, we can predict the outgoing field. In the present instance of a simple oscillator we have a particular example of the general case where the system responds linearly to the input field. We can characterize any such system by a

complex, frequency dependent impedance $Z[\omega]$ defined by

$$Z[\omega] = -\frac{V(x=0,\omega)}{I(x=0,\omega)}. \tag{C20}$$

Note the peculiar minus sign which results from our definition of positive current flowing to the right (out of the system and into the transmission line). Using Eqs. (C12, C13) and Eq. (C20) we have

$$V_{\rm out}[\omega] = r[\omega] V_{\rm in}[\omega], \tag{C21}$$

where the reflection coefficient r is determined by the impedance mismatch between the system and the line and is given by the well known result

$$r[\omega] = \frac{Z[\omega] - Z_{\rm c}}{Z[\omega] + Z_{\rm c}}. \tag{C22}$$

If the system is constructed from purely reactive (i.e. lossless) components, then $Z[\omega]$ is purely imaginary and the reflection coefficient obeys $|r| = 1$ which is consistent with Eq. (C16) and the energy conservation requirement of no net power flow into the lossless system. For example, for the series LC oscillator we have been considering, we have

$$Z[\omega] = \frac{1}{j\omega C_0} + j\omega L_0, \tag{C23}$$

where, to make contact with the usual electrical engineering sign conventions, we have used $j = -i$. If the damping γ of the oscillator induced by coupling it to the transmission line is small, the quality factor of the resonance will be high and we need only consider frequencies near the resonance frequency $\Omega_0 \equiv 1/\sqrt{L_0 C_0}$ where the impedance has a zero. In this case we may approximate

$$Z[\omega] \approx \frac{2}{jC_0\Omega_0^2}[\Omega_0 - \omega] = 2jL_0(\omega - \Omega_0) \tag{C24}$$

which yields for the reflection coefficient

$$r[\omega] = \frac{\omega - \Omega_0 + j\gamma/2}{\omega - \Omega_0 - j\gamma/2} \tag{C25}$$

showing that indeed $|r| = 1$ and that the phase of the reflected signal winds by 2π upon passing through the resonance. [4]

Turning to the more general case where the system also contains lossy elements, one finds that $Z[\omega]$ is no longer purely imaginary, but has a real part satisfying $\mathrm{Re}\, Z[\omega] > 0$. This in turn implies via Eq. (C22) that $|r| < 1$. In the special case of impedance matching $Z[\omega] = Z_{\rm c}$, all the incident power is dissipated in the system and none is reflected. The other two limits of interest are open circuit termination with $Z = \infty$ for which $r = +1$ and short circuit termination $Z = 0$ for which $r = -1$.

Finally, if the system also contains an active device which has energy being pumped into it from a separate external source, it may under the right conditions be described by an effective *negative* resistance $\mathrm{Re}\, Z[\omega] < 0$ over a certain frequency range. Eq. (C22) then gives $|r| \geq 1$, implying $|V_{\rm out}| > |V_{\rm in}|$. Our system will thus act like the one-port amplifier discussed in Sec. V.D: it amplifies signals incident upon it. We will discuss this idea of negative resistance further in Sec. C.4; a physical realization is provided by the two-port reflection parametric amplifier discussed in Appendix V.C.

[4] For the case of resonant *transmission* through a symmetric cavity, the phase shift only winds by π.

2. Lagrangian, Hamiltonian, and wave modes for a transmission line

Prior to moving on to the case of quantum noise it is useful to review the classical statistical mechanics of transmission lines. To do this we need to write down the Lagrangian and then determine the canonical momenta and the Hamiltonian. Very conveniently, the system is simply a large collection of harmonic oscillators (the normal modes) and hence can be readily quantized. This representation of a physical resistor is essentially the one used by Caldeira and Leggett (Caldeira and Leggett, 1983) in their seminal studies of the effects of dissipation on tunneling. The only difference between this model and the vacuum fluctuations in free space is that the relativistic bosons travel in one dimension and do not carry a polarization label. This changes the density of states as a function of frequency, but has no other essential effect.

It is convenient to define a flux variable (Devoret, 1997)

$$\varphi(x,t) \equiv \int_{-\infty}^{t} d\tau\, V(x,\tau), \tag{C26}$$

where $V(x,t) = \partial_t \varphi(x,t)$ is the local voltage on the transmission line at position x and time t. Each segment of the line of length dx has inductance $\ell\, dx$ and the voltage drop along it is $-dx\, \partial_x \partial_t \varphi(x,t)$. The flux through this inductance is thus $-dx\, \partial_x \varphi(x,t)$ and the local value of the current is given by the constitutive equation

$$I(x,t) = -\frac{1}{\ell}\, \partial_x \varphi(x,t). \tag{C27}$$

The Lagrangian for the system is

$$L_g \equiv \int_0^\infty dx\, \mathcal{L}(x,t) = \int_0^\infty dx\, \left(\frac{c}{2} (\partial_t \varphi)^2 - \frac{1}{2\ell} (\partial_x \varphi)^2 \right), \tag{C28}$$

The Euler-Lagrange equation for this Lagrangian is simply the wave equation

$$v_{\rm p}^2 \partial_x^2 \varphi - \partial_t^2 \varphi = 0. \tag{C29}$$

The momentum conjugate to $\varphi(x)$ is simply the charge density

$$q(x,t) \equiv \frac{\delta \mathcal{L}}{\delta \partial_t \varphi} = c\partial_t \varphi = cV(x,t) \tag{C30}$$

and so the Hamiltonian is given by

$$H = \int dx \left\{ \frac{1}{2c} q^2 + \frac{1}{2\ell} (\partial_x \varphi)^2 \right\}. \tag{C31}$$

We know from our previous results that the charge density consists of left and right moving solutions of arbitrary fixed shape. For example we might have for the right moving case

$$q(t - x/v_{\rm p}) = \alpha_k \cos[k(x - v_{\rm p}t)] + \beta_k \sin[k(x - v_{\rm p}t)]. \tag{C32}$$

A confusing point is that since q is real valued, we see that it necessarily contains both e^{ikx} and e^{-ikx} terms even if it is only right moving. Note however that for $k > 0$ and a right mover, the e^{ikx} is associated with the positive frequency term $e^{-i\omega_k t}$ while the e^{-ikx} term is associated with the negative frequency term $e^{+i\omega_k t}$ where $\omega_k \equiv v_{\rm p}|k|$. For left movers the opposite holds. We can appreciate this better if we define

$$A_k \equiv \frac{1}{\sqrt{L}} \int dx\, e^{-ikx} \left\{ \frac{1}{\sqrt{2c}} q(x,t) - i\sqrt{\frac{k^2}{2\ell}} \varphi(x,t) \right\} \tag{C33}$$

where for simplicity we have taken the fields to obey periodic boundary conditions on a length L. Thus we have (in a form which anticipates the full quantum theory)

$$H = \frac{1}{2} \sum_k \left(A_k^* A_k + A_k A_k^* \right). \tag{C34}$$

The classical equation of motion (C29) yields the simple result

$$\partial_t A_k = -i\omega_k A_k. \tag{C35}$$

Thus

$$\begin{aligned} & q(x,t) \\ &= \sqrt{\frac{c}{2L}} \sum_k e^{ikx} \left[A_k(0) e^{-i\omega_k t} + A_{-k}^*(0) e^{+i\omega_k t} \right] && \text{(C36)} \\ &= \sqrt{\frac{c}{2L}} \sum_k \left[A_k(0) e^{+i(kx - \omega_k t)} + A_k^*(0) e^{-i(kx - \omega_k t)} \right]. && \text{(C37)} \end{aligned}$$

We see that for $k > 0$ ($k < 0$) the wave is right (left) moving, and that for right movers the e^{ikx} term is associated with positive frequency and the e^{-ikx} term is associated with negative frequency. We will return to this in the quantum case where positive (negative) frequency will refer to the destruction (creation) of a photon. Note that the right and left moving voltages are given by

$$V^{\rightarrow} = \sqrt{\frac{1}{2Lc}} \sum_{k>0} \left[A_k(0) e^{+i(kx - \omega_k t)} + A_k^*(0) e^{-i(kx - \omega_k t)} \right] \tag{C38}$$

$$V^{\leftarrow} = \sqrt{\frac{1}{2Lc}} \sum_{k<0} \left[A_k(0) e^{+i(kx - \omega_k t)} + A_k^*(0) e^{-i(kx - \omega_k t)} \right] \tag{C39}$$

The voltage spectral density for the right moving waves is thus

$$S_{VV}^{\rightarrow}[\omega] = \frac{2\pi}{2Lc} \sum_{k>0} \left\{ \langle A_k A_k^* \rangle \delta(\omega - \omega_k) + \langle A_k^* A_k \rangle \delta(\omega + \omega_k) \right\} \tag{C40}$$

The left moving spectral density has the same expression but $k < 0$.

Using Eq. (C16), the above results lead to a net power flow (averaged over one cycle) within a frequency band defined by a pass filter $G[\omega]$ of

$$P = P^{\rightarrow} - P^{\leftarrow} = \frac{v_{\rm p}}{2L} \sum_k {\rm sgn}(k) \left[G[\omega_k] \langle A_k A_k^* \rangle + G[-\omega_k] \langle A_k^* A_k \rangle \right]. \tag{C41}$$

3. Classical statistical mechanics of a transmission line

Now that we have the Hamiltonian, we can consider the classical statistical mechanics of a transmission line in thermal equilibrium at temperature T. Since each mode k is a simple harmonic oscillator we have from Eq. (C34) and the equipartition theorem

$$\langle A_k^* A_k \rangle = k_{\rm B} T. \tag{C42}$$

Using this, we see from Eq. (C40) that the right moving voltage signal has a simple white noise power spectrum. Using Eq. (C41) we have for the right moving power in a bandwidth B (in Hz rather than radians/sec) the very simple result

$$\begin{aligned} P^{\rightarrow} &= \frac{v_{\rm p}}{2L}\sum_{k>0}\langle G[\omega_k]A_k^*A_k + G[-\omega_k]A_kA_k^*\rangle \\ &= \frac{k_{\rm B}T}{2}\int_{-\infty}^{+\infty}\frac{d\omega}{2\pi}\,G[\omega] \\ &= k_{\rm B}TB. \end{aligned} \tag{C43}$$

where we have used the fact mentioned in connection with Eq. (A26) and the discussion of square law detectors that all passive filter functions are symmetric in frequency.

One of the basic laws of statistical mechanics is Kirchhoff's law stating that the ability of a hot object to emit radiation is proportional to its ability to absorb. This follows from very general thermodynamic arguments concerning the thermal equilibrium of an object with its radiation environment and it means that the best possible emitter is the black body. In electrical circuits this principle is simply a form of the fluctuation dissipation theorem which states that the electrical thermal noise produced by a circuit element is proportional to the dissipation it introduces into the circuit. Consider the example of a terminating resistor at the end of a transmission line. If the resistance R is matched to the characteristic impedance $Z_{\rm c}$ of a transmission line, the terminating resistor acts as a black body because it absorbs 100% of the power incident upon it. If the resistor is held at temperature T it will bring the transmission line modes into equilibrium at the same temperature (at least for the case where the transmission line has finite length). The rate at which the equilibrium is established will depend on the impedance mismatch between the resistor and the line, but the final temperature will not.

A good way to understand the fluctuation-dissipation theorem is to represent the resistor R which is terminating the $Z_{\rm c}$ line in terms of a second semi-infinite transmission line of impedance R as shown in Fig. (2). First consider the case when the R line is not yet connected to the $Z_{\rm c}$ line. Then according to Eq. (C22), the open termination at the end of the $Z_{\rm c}$ line has reflectivity $|r|^2 = 1$ so that it does not dissipate any energy. Additionally of course, this termination does not transmit any signals from the R line into the $Z_{\rm c}$. However when the two lines are connected the reflectivity becomes less than unity meaning that incoming signals on the $Z_{\rm c}$ line see a source of dissipation R which partially absorbs them. The absorbed signals are not turned into heat as in a true resistor but are partially transmitted into the R line which is entirely equivalent. Having opened up this port for energy to escape from the $Z_{\rm c}$ system, we have also allowed noise energy (thermal or quantum) from the R line to be transmitted into the $Z_{\rm c}$ line. This is completely equivalent to the effective circuit shown in Fig. (3 a) in which a real resistor has in parallel a random current generator representing thermal noise fluctuations of the electrons in the resistor. This is the essence of the fluctuation dissipation theorem.

In order to make a quantitative analysis in terms of the power flowing in the two lines, voltage is not the best variable to use since we are dealing with more than one value of line impedance. Rather we define incoming and outgoing fields via

$$A_{\rm in} = \frac{1}{\sqrt{Z_{\rm c}}}V_{\rm c}^{\leftarrow} \tag{C44}$$

$$A_{\rm out} = \frac{1}{\sqrt{Z_{\rm c}}}V_{\rm c}^{\rightarrow} \tag{C45}$$

$$B_{\rm in} = \frac{1}{\sqrt{R}}V_{\rm R}^{\rightarrow} \tag{C46}$$

$$B_{\rm out} = \frac{1}{\sqrt{R}}V_{\rm R}^{\leftarrow} \tag{C47}$$

Normalizing by the square root of the impedance allows us to write the power flowing to the right in each line in the simple form

$$P_{\rm c} = (A_{\rm out})^2 - (A_{\rm in})^2 \tag{C48}$$

$$P_R = (B_{\rm in})^2 - (B_{\rm out})^2 \tag{C49}$$

The out fields are related to the in fields by the s matrix

$$\begin{pmatrix} A_{\rm out} \\ B_{\rm out} \end{pmatrix} = s\begin{pmatrix} A_{\rm in} \\ B_{\rm in} \end{pmatrix} \tag{C50}$$

Requiring continuity of the voltage and current at the interface between the two transmission lines, we can solve for the scattering matrix s:

$$s = \begin{pmatrix} +r & t \\ t & -r \end{pmatrix} \tag{C51}$$

where

$$r = \frac{R - Z_{\rm c}}{R + Zc} \tag{C52}$$

$$t = \frac{2\sqrt{RZ_{\rm c}}}{R + Zc}. \tag{C53}$$

Note that $|r|^2 + |t|^2 = 1$ as required by energy conservation and that s is unitary with $\det(s) = -1$. By moving the point at which the phase of the $B_{\rm in}$ and $B_{\rm out}$ fields are determined one-quarter wavelength to the left, we can put s into different standard form

$$s' = \begin{pmatrix} +r & it \\ it & +r \end{pmatrix} \tag{C54}$$

which has $\det(s') = +1$.

As mentioned above, the energy absorbed from the $Z_{\rm c}$ line by the resistor R is not turned into heat as in a true resistor but is is simply transmitted into the R line, which is entirely equivalent. Kirchhoff's law is now easy

FIG. 2 (Color online) Semi-infinite transmission line of impedance Z_c terminated by a resistor R which is represented as a second semi-infinite transmission line.

to understand. The energy absorbed *from* the Z_c line by R, and the energy transmitted *into* it by thermal fluctuations in the R line are both proportional to the absorption coefficient

$$A = 1 - |r|^2 = |t|^2 = \frac{4RZ_c}{(R+Z_c)^2}. \tag{C55}$$

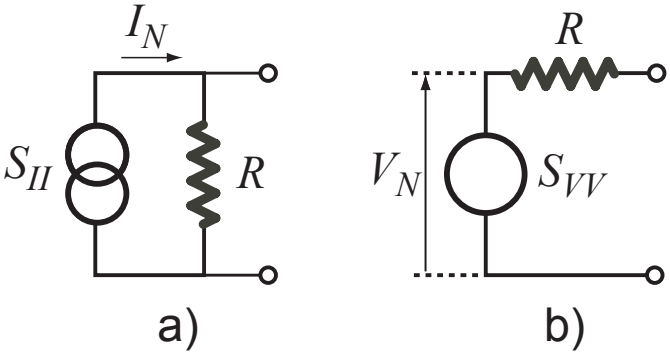

FIG. 3 Equivalent circuits for noisy resistors.

The requirement that the transmission line Z_c come to equilibrium with the resistor allows us to readily compute the spectral density of current fluctuations of the random current source shown in Fig. (3 a). The power dissipated in Z_c by the current source attached to R is

$$P = \int_{-\infty}^{+\infty} \frac{d\omega}{2\pi} S_{II}[\omega] \frac{R^2 Z_c}{(R+Z_c)^2} \tag{C56}$$

For the special case $R = Z_c$ we can equate this to the right moving power $P^{\rightarrow}$ in Eq. (C43) because left moving waves in the Z_c line are not reflected and hence cannot contribute to the right moving power. Requiring $P = P^{\rightarrow}$ yields the classical Nyquist result for the current noise of a resistor

$$\mathcal{S}_{II}[\omega] = \frac{2}{R} k_B T \tag{C57}$$

or in the electrical engineering convention

$$\mathcal{S}_{II}[\omega] + \mathcal{S}_{II}[-\omega] = \frac{4}{R} k_B T. \tag{C58}$$

We can derive the equivalent expression for the voltage noise of a resistor (see Fig. 3 b) by considering the voltage noise at the open termination of a semi-infinite transmission line with $Z_c = R$. For an open termination $V^{\rightarrow} = V^{\leftarrow}$ so that the voltage at the end is given by

$$V = 2V^{\leftarrow} = 2V^{\rightarrow} \tag{C59}$$

and thus using Eqs. (C40) and (C42) we find

$$\mathcal{S}_{VV} = 4\mathcal{S}^{\rightarrow}_{VV} = 2Rk_B T \tag{C60}$$

which is equivalent to Eq. (C57).

4. Amplification with a transmission line and a negative resistance

We close our discussion of transmission lines by further expanding upon the idea mentioned at the end of App. C.1 that one can view a one-port amplifier as a transmission line terminated by an effective negative resistance. The discussion here will be very general: we will explore what can be learned about amplification by simply extending the results we have obtained on transmission lines to the case of an effective negative resistance. Our general discussion will not address the important issues of *how* one achieves an effective negative resistance over some appreciable frequency range: for such questions, one must focus on a specific physical realization, such as the parametric amplifier discussed in Sec. V.C.

We start by noting that for the case $-Z_c < R < 0$ the power gain G is given by

$$G = |r|^2 > 1, \tag{C61}$$

and the s' matrix introduced in Eq. (C54) becomes

$$s' = -\begin{pmatrix} \sqrt{G} & \pm\sqrt{G-1} \\ \pm\sqrt{G-1} & \sqrt{G} \end{pmatrix} \tag{C62}$$

where the sign choice depends on the branch cut chosen in the analytic continuation of the off-diagonal elements. This transformation is clearly no longer unitary (because there is no energy conservation since we are ignoring the work done by the amplifier power supply). Note however that we still have $\det(s') = +1$. It turns out that this naive analytic continuation of the results from positive to negative resistance is not strictly correct. As we will show in the following, we must be more careful than we have been so far in order to insure that the transformation from the in fields to the out fields must be canonical.

In order to understand the canonical nature of the transformation between input and output modes, it is necessary to delve more deeply into the fact that the two quadrature amplitudes of a mode are canonically conjugate. Following the complex amplitudes defined in Eqs. (C44-C47), let us define a vector of real-valued quadrature amplitudes for the incoming and outgoing fields

$$\vec{q}^{\,\text{in}} = \begin{pmatrix} X_A^{\text{in}} \\ X_B^{\text{in}} \\ Y_B^{\text{in}} \\ Y_A^{\text{in}} \end{pmatrix}, \quad \vec{q}^{\,\text{out}} = \begin{pmatrix} X_A^{\text{out}} \\ X_B^{\text{out}} \\ Y_B^{\text{out}} \\ Y_A^{\text{out}} \end{pmatrix}. \tag{C63}$$

The Poisson brackets amongst the different quadrature amplitudes is given by

$$\{q_i^{\rm in}, q_j^{\rm in}\} \propto J_{ij}, \tag{C64}$$

or equivalently the quantum commutators are

$$[q_i^{\rm in}, q_j^{\rm in}] = iX_{\rm ZPF}^2 J_{ij}, \tag{C65}$$

where

$$J \equiv \begin{pmatrix} 0 & 0 & 0 & +1 \\ 0 & 0 & +1 & 0 \\ 0 & -1 & 0 & 0 \\ -1 & 0 & 0 & 0 \end{pmatrix}. \tag{C66}$$

In order for the transformation to be canonical, the same Poisson bracket or commutator relations must hold for the outgoing field amplitudes

$$[q_i^{\rm out}, q_j^{\rm out}] = iX_{\rm ZPF}^2 J_{ij}. \tag{C67}$$

In the case of a non-linear device these relations would apply to the small fluctuations in the input and output fields around the steady state solution. Assuming a linear device (or linearization around the steady state solution) we can define a 4×4 real-valued scattering matrix $\tilde{s}$ in analogy to the 2×2 complex-valued scattering matrix s in Eq. (C51) which relates the output fields to the input fields

$$q_i^{\rm out} = \tilde{s}_{ij} q_j^{\rm in}. \tag{C68}$$

Eq. (C67) puts a powerful constraint on on the $\tilde{s}$ matrix, namely that it must be symplectic. That is, $\tilde{s}$ and its transpose must obey

$$\tilde{s} J \tilde{s}^{\rm T} = J. \tag{C69}$$

From this it follows that

$$\det \tilde{s} = \pm 1. \tag{C70}$$

This in turn immediately implies Liouville's theorem that Hamiltonian evolution preserves phase space volume (since $\det \tilde{s}$ is the Jacobian of the transformation which propagates the amplitudes forward in time).

Let us further assume that the device is phase preserving, that is that the gain or attenuation is the same for both quadratures. One form for the $\tilde{s}$ matrix consistent with all of the above requirements is

$$\tilde{s} = \begin{pmatrix} +\cos\theta & \sin\theta & 0 & 0 \\ \sin\theta & -\cos\theta & 0 & 0 \\ 0 & 0 & -\cos\theta & \sin\theta \\ 0 & 0 & \sin\theta & +\cos\theta \end{pmatrix}. \tag{C71}$$

This simply corresponds to a beam splitter and is the equivalent of Eq. (C51) with $r = \cos\theta$. As mentioned in connection with Eq. (C51), the precise form of the scattering matrix depends on the choice of planes at which the phases of the various input and output waves are measured.

Another allowed form of the scattering matrix is:

$$\tilde{s}' = -\begin{pmatrix} +\cosh\theta & +\sinh\theta & 0 & 0 \\ +\sinh\theta & +\cosh\theta & 0 & 0 \\ 0 & 0 & +\cosh\theta & -\sinh\theta \\ 0 & 0 & -\sinh\theta & +\cosh\theta \end{pmatrix}. \tag{C72}$$

If one takes $\cosh\theta = \sqrt{G}$, this scattering matrix is essentially the canonically correct formulation of the negative-resistance scattering matrix we tried to write in Eq. (C62). Note that the off-diagonal terms have changed sign for the Y quadrature relative to the naive expression in Eq. (C62) (corresponding to the other possible analytic continuation choice). This is necessary to satisfy the symplecticity condition and hence make the transformation canonical. The scattering matrix $\tilde{s}'$ can describe amplification. Unlike the beam splitter scattering matrix $\tilde{s}$ above, $\tilde{s}'$ is not unitary (even though $\det \tilde{s}' = 1$). Unitarity would correspond to power conservation. Here, power is not conserved, as we are not explicitly tracking the power source supplying our active system.

The form of the negative-resistance amplifier scattering matrix $\tilde{s}'$ confirms many of the general statements we made about phase-preserving amplification in Sec. V.B. First, note that the requirement of finite gain $G > 1$ and phase preservation makes all the diagonal elements of $\tilde{s}'$ (i.e. $\cosh\theta$) equal. We see that to amplify the A mode, it is impossible to avoid coupling to the B mode (via the $\sinh\theta$ term) because of the requirement of symplecticity. We thus see that it is impossible classically or quantum mechanically to build a linear phase-preserving amplifier whose only effect is to amplify the desired signal. The presence of the $\sinh\theta$ term above means that the output signal is always contaminated by amplified noise from at least one other degree of freedom (in this case the B mode). If the thermal or quantum noise in A and B are equal in magnitude (and uncorrelated), then in the limit of large gain where $\cosh\theta \approx \sinh\theta$, the output noise (referred to the input) will be doubled. This is true for both classical thermal noise and quantum vacuum noise.

The negative resistance model of an amplifier here gives us another way to think about the noise added by an amplifier: crudely speaking, we can view it as being directly analogous to the fluctuation-dissipation theorem simply continued to the case of negative dissipation. Just as dissipation can occur only when we open up a new channel and thus we bring in new fluctuations, so amplification can occur only when there is coupling to an additional channel. Without this it is impossible to satisfy the requirement that the amplifier perform a canonical transformation.

Appendix D: Quantum Modes and Noise of a Transmission Line

1. Quantization of a transmission line

Recall from Eq. (C30) and the discussion in Appendix C that the momentum conjugate to the transmission line flux variable $\varphi(x,t)$ is the local charge density $q(x,t)$. Hence in order to quantize the transmission line modes we simply promote these two physical quantities to quantum operators obeying the commutation relation

$$[\hat{q}(x), \hat{\varphi}(x')] = -i\hbar\delta(x-x') \tag{D1}$$

from which it follows that the mode amplitudes defined in Eq. (C33) become quantum operators obeying

$$[\hat{A}_{k'}, \hat{A}_k^\dagger] = \hbar\omega_k \delta_{kk'} \tag{D2}$$

and we may identify the usual raising and lowering operators by

$$\hat{A}_k = \sqrt{\hbar\omega_k}\,\hat{b}_k \tag{D3}$$

where $\hat{b}_k$ destroys a photon in mode k. The quantum form of the Hamiltonian in Eq. (C34) is thus

$$H = \sum_k \hbar\omega_k \left[\hat{b}_k^\dagger \hat{b}_k + \frac{1}{2}\right]. \tag{D4}$$

For the quantum case the thermal equilibrium expression then becomes

$$\langle \hat{A}_k^\dagger \hat{A}_k \rangle = \hbar\omega_k n_{\rm B}(\hbar\omega_k), \tag{D5}$$

which reduces to Eq. (C42) in the classical limit $\hbar\omega_k \ll k_{\rm B}T$.

We have seen previously in Eqs. (C6) that the voltage fluctuations on a transmission line can be resolved into right and left moving waves which are functions of a combined space-time argument

$$V(x,t) = V^{\rightarrow}(t - \frac{x}{v_{\rm p}}) + V^{\leftarrow}(t + \frac{x}{v_{\rm p}}). \tag{D6}$$

Thus in an infinite transmission line, specifying $V^{\rightarrow}$ everywhere in space at $t=0$ determines its value for all times. Conversely specifying $V^{\rightarrow}$ at $x=0$ for all times fully specifies the field at all spatial points. In preparation for our study of the quantum version of input-output theory in Appendix E, it is convenient to extend Eqs. (C38-C39) to the quantum case ($x=0$):

$$\begin{aligned}\hat{V}^{\rightarrow}(t) &= \sqrt{\frac{1}{2Lc}} \sum_{k>0} \sqrt{\hbar\omega_k} \left[\hat{b}_k e^{-i\omega_k t} + h.c.\right] \\ &= \int_0^\infty \frac{d\omega}{2\pi} \sqrt{\frac{\hbar\omega Z_{\rm c}}{2}} \left[\hat{b}^{\rightarrow}[\omega] e^{-i\omega t} + h.c.\right] \end{aligned} \tag{D7}$$

In the second line, we have defined:

$$\hat{b}^{\rightarrow}[\omega] \equiv 2\pi \sqrt{\frac{v_p}{L}} \sum_{k>0} \hat{b}_k \delta(\omega - \omega_k) \tag{D8}$$

In a similar fashion, we have:

$$\hat{V}^{\leftarrow}(t) = \int_0^\infty \frac{d\omega}{2\pi} \sqrt{\frac{\hbar\omega Z_{\rm c}}{2}} \left[\hat{b}^{\leftarrow}[\omega] e^{-i\omega t} + h.c.\right] \tag{D9}$$

$$\hat{b}^{\leftarrow}[\omega] \equiv 2\pi \sqrt{\frac{v_p}{L}} \sum_{k<0} \hat{b}_k \delta(\omega - \omega_k) \tag{D10}$$

One can easily verify that among the $\hat{b}^{\rightarrow}[\omega], \hat{b}^{\leftarrow}[\omega]$ operators and their conjugates, the only non-zero commutators are given by:

$$\left[\hat{b}^{\rightarrow}[\omega], \left(\hat{b}^{\rightarrow}[\omega']\right)^\dagger\right] = \left[\hat{b}^{\leftarrow}[\omega], \left(\hat{b}^{\leftarrow}[\omega']\right)^\dagger\right] = 2\pi\delta(\omega-\omega') \tag{D11}$$

We have taken the continuum limit $L \to \infty$ here, allowing us to change sums on k to integrals. We have thus obtained the description of a quantum transmission line in terms of left and right-moving frequency resolved modes, as used in our discussion of amplifiers in Sec. VI (see Eqs. 6.2). Note that if the right-moving modes are further taken to be in thermal equilibrium, one finds (again, in the continuum limit):

$$\left\langle \left(\hat{b}^{\rightarrow}[\omega]\right)^\dagger \hat{b}^{\rightarrow}[\omega'] \right\rangle = 2\pi\delta(\omega-\omega') n_{\rm B}(\hbar\omega) \tag{D12a}$$

$$\left\langle \hat{b}^{\rightarrow}[\omega] \left(\hat{b}^{\rightarrow}[\omega']\right)^\dagger \right\rangle = 2\pi\delta(\omega-\omega') \left[1 + n_{\rm B}(\hbar\omega)\right] \tag{D12b}$$

.

We are typically interested in a relatively narrow band of frequencies centered on some characteristic drive or resonance frequency Ω_0. In this case, it is useful to work in the time-domain, in a frame rotating at Ω_0. Fourier transforming [5] Eqs. (D8) and (D10), one finds:

$$\hat{b}^{\rightarrow}(t) = \sqrt{\frac{v_{\rm p}}{L}} \sum_{k>0} e^{-i(\omega_k - \Omega_0)t} \hat{b}_k(0), \tag{D13a}$$

$$\hat{b}^{\leftarrow}(t) = \sqrt{\frac{v_{\rm p}}{L}} \sum_{k<0} e^{-i(\omega_k - \Omega_0)t} \hat{b}_k(0). \tag{D13b}$$

These represent temporal right and left moving modes. Note that the normalization factor in Eqs. (D13) has been chosen so that the right moving photon flux at $x=0$ and time t is given by

$$\langle \dot{N} \rangle = \langle \hat{b}^{\dagger\rightarrow}(t) \hat{b}^{\rightarrow}(t) \rangle \tag{D14}$$

In the same rotating frame, and within the approximation that all relevant frequencies are near Ω_0, Eq. (D7) becomes simply:

$$\hat{V}^{\rightarrow}(t) \approx \sqrt{\frac{\hbar\Omega_0 Z_{\rm c}}{2}} \left[\hat{b}^{\rightarrow}(t) + \hat{b}^{\dagger\rightarrow}(t)\right] \tag{D15}$$

---

[5] As in the main text, we use in this appendix a convention which differs from the one commonly used in quantum optics: $\hat{a}[\omega] = \int_{-\infty}^{+\infty} dt\, e^{+i\omega t} \hat{a}(t)$ and $\hat{a}^\dagger[\omega] = [\hat{a}[-\omega]]^\dagger = \int_{-\infty}^{+\infty} dt\, e^{+i\omega t} \hat{a}^\dagger(t)$.

We have already seen that using classical statistical mechanics, the voltage noise in equilibrium is white. The corresponding analysis of the temporal modes using Eqs. (D13) shows that the quantum commutator obeys

$$[\hat{b}^{\rightarrow}(t), \hat{b}^{\dagger\rightarrow}(t')] \;=\; \delta(t-t'). \tag{D16}$$

In deriving this result, we have converted summations over mode index to integrals over frequency. Further, because (for finite time resolution at least) the integral is dominated by frequencies near $+\Omega_0$ we can, within the Markov (Wigner Weisskopf) approximation, extend the lower limit of frequency integration to minus infinity and thus arrive at a delta function in time. If we further take the right moving modes to be in thermal equilibrium, then we may similarly approximate:

$$\langle \hat{b}^{\dagger\rightarrow}(t')\hat{b}^{\rightarrow}(t)\rangle \;=\; n_{\rm B}(\hbar\Omega_0)\delta(t-t') \tag{D17a}$$
$$\langle \hat{b}^{\rightarrow}(t)\hat{b}^{\dagger\rightarrow}(t')\rangle \;=\; [1+n_{\rm B}(\hbar\Omega_0)]\,\delta(t-t'). \tag{D17b}$$

Equations (D15) to (D17b) indicate that $\hat{V}^{\rightarrow}(t)$ can be treated as the quantum operator equivalent of white noise; a similar line of reasoning applies *mutatis mutandis* to the left moving modes. We stress that these results rely crucially on our assumption that we are dealing with a relatively narrow band of frequencies in the vicinity of Ω_0; the resulting approximations we have made are known as the Markov approximation. As one can already see from the form of Eqs. (D7,D9), and as will be discussed further, the actual spectral density of vacuum noise on a transmission line is not white, but is linear in frequency. The approximation made in Eq. (D16) treats it as a constant within the narrow band of frequencies of interest. If the range of frequencies of importance is large then the Markov approximation is not applicable.

2. Modes and the windowed Fourier transform

While delta function correlations can make the quantum noise relatively easy to deal with in both the time and frequency domain, it is sometimes the case that it is easier to deal with a 'smoothed' noise variable. The introduction of an ultraviolet cutoff regulates the mathematical singularities in the noise operators evaluated at equal times and is physically sensible because every real measurement apparatus has finite time resolution. A second motivation is that real spectrum analyzers output a time varying signal which represents the noise power in a certain frequency interval (the 'resolution bandwidth') averaged over a certain time interval (the inverse 'video bandwidth'). The mathematical tool of choice for dealing with such situations in which time and frequency both appear is the 'windowed Fourier transform'. The windowed transform uses a kernel which is centered on some frequency window and some time interval. By summation over all frequency and time windows it is possible to invert the transformation. The reader is directed to (Mallat, 1999) for the mathematical details.

For our present purposes where we are interested in just a single narrow frequency range centered on Ω_0, a convenient windowed transform kernel for smoothing the quantum noise is simply a box of width Δt representing the finite integration time of our detector. In the frame rotating at Ω_0 we can define

$$\hat{B}_j^{\rightarrow} = \frac{1}{\sqrt{\Delta t}} \int_{t_j}^{t_{j+1}} d\tau\, \hat{b}^{\rightarrow}(\tau) \tag{D18}$$

where $t_j = j(\Delta t)$ denotes the time of arrival of the jth temporal mode at the point $x = 0$. Recall that $\hat{b}^{\rightarrow}$ has a photon flux normalization and so $\hat{B}_j^{\rightarrow}$ is dimensionless. From Eq. (D16) we see that these smoothed operators obey the usual bosonic commutation relations

$$[\hat{B}_j^{\rightarrow}, \hat{B}_k^{\dagger\rightarrow}] = \delta_{jk}. \tag{D19}$$

The state $B_j^\dagger|0\rangle$ has a single photon occupying basis mode j, which is centered in frequency space at Ω_0 and in time space on the interval $j\Delta t < t < (j+1)\Delta t$ (i.e. this temporal mode passes the point $x = 0$ during the jth time interval.) This basis mode is much like a note in a musical score: it has a certain specified pitch and occurs at a specified time for a specified duration. Just as we can play notes of different frequencies simultaneously, we can define other temporal modes on the same time interval and they will be mutually orthogonal provided the angular frequency spacing is a multiple of $2\pi/\Delta t$. The result is a set of modes $B_{m,p}$ labeled by both a frequency index m and a time index p. p labels the time interval as before, while m labels the angular frequency:

$$\omega_m = \Omega_0 + m\frac{2\pi}{\Delta t} \tag{D20}$$

The result is, as illustrated in Fig. (4), a complete lattice of possible modes tiling the frequency-time phase space, each occupying area 2π corresponding to the time-frequency uncertainty principle.

We can form other modes of arbitrary shapes centered on frequency Ω_0 by means of linear superposition of our basis modes (as long as they are smooth on the time scale Δt). Let us define

$$\Psi = \sum_j \psi_j \hat{B}_j^{\rightarrow}. \tag{D21}$$

This is also a canonical bosonic mode operator obeying

$$[\Psi, \Psi^\dagger] = 1 \tag{D22}$$

provided that the coefficients obey the normalization condition

$$\sum_j |\psi_j|^2 = 1. \tag{D23}$$

We might for example want to describe a mode which is centered at a slightly higher frequency $\Omega_0 + \delta\Omega$ (obeying

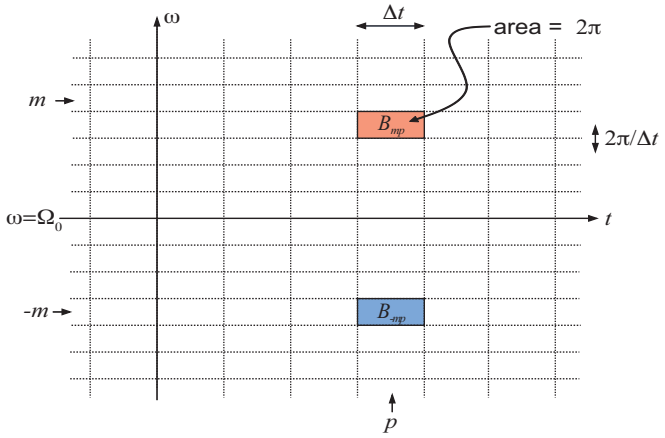

FIG. 4 (Color online) Schematic figure indicating how the various modes defined by the windowed Fourier transform tile the time-frequency plane. Each individual cell corresponds to a different mode, and has an area 2π.

$(\delta\Omega)(\Delta t) << 1$) and spread out over a large time interval T centered at time T_0. This could be given for example by

$$\psi_j = \mathcal{N} e^{-\frac{(j\Delta t - T_0)^2}{4T^2}} e^{-i(\delta\Omega)(j\Delta t)} \tag{D24}$$

where $\mathcal{N}$ is the appropriate normalization constant.

The state having n photons in the mode is simply

$$\frac{1}{\sqrt{n!}} \left(\Psi^\dagger\right)^n |0\rangle. \tag{D25}$$

The concept of 'wave function of the photon' is fraught with dangers. In the very special case where we restrict attention solely to the subspace of single photon Fock states, we can usefully think of the amplitudes $\{\psi_j\}$ as the 'wave function of the photon' (Cohen-Tannoudji *et al.*, 1989) since it tells us about the spatial mode which is excited. In the general case however it is essential to keep in mind that the transmission line is a collection of coupled LC oscillators with an infinite number of degrees of freedom. Let us simplify the argument by considering a single LC oscillator. We can perfectly well write a wave function for the system as a function of the coordinate (say the charge q on the capacitor). The ground state wave function $\chi_0(q)$ is a gaussian function of the coordinate. The one photon state created by $\Psi^\dagger$ has a wave function $\chi_1(q) \sim q\chi_0(q)$ proportional to the coordinate times the same gaussian. In the general case χ is a *wave functional* of the charge distribution $q(x)$ over the entire transmission line.

Using Eq. (D17a) we have

$$\langle \hat{B}_j^{\dagger\rightarrow} \hat{B}_k^{\rightarrow} \rangle = n_{\rm B}(\hbar\Omega_0)\delta_{jk} \tag{D26}$$

independent of our choice of the coarse-graining time window Δt. This result allows us to give meaning to the phrase one often hears bandied about in descriptions of amplifiers that 'the noise temperature corresponds to a mode occupancy of X photons'. This simply means that the photon flux *per unit bandwidth* is X. Equivalently the flux in bandwidth B is

$$\overline{\dot{N}} = \frac{X}{\Delta t}(B\Delta t) = XB. \tag{D27}$$

The interpretation of this is that X photons in a temporal mode of duration Δt pass the origin in time Δt. Each mode has bandwidth $\sim \frac{1}{\Delta t}$ and so there are $B\Delta t$ independent temporal modes in bandwidth B all occupying the same time interval Δt. The longer is Δt the longer it takes a given mode to pass the origin, but the more such modes fit into the frequency window.

As an illustration of these ideas, consider the following elementary question: What is the mode occupancy of a laser beam of power P and hence photon flux $\overline{\dot{N}} = \frac{P}{\hbar\Omega_0}$? We cannot answer this without knowing the coherence time or equivalently the bandwidth. The output of a good laser is like that of a radio frequency oscillator–it has essentially no amplitude fluctuations. The frequency is nominally set by the physical properties of the oscillator, but there is nothing to pin the phase which consequently undergoes slow diffusion due to unavoidable noise perturbations. This leads to a finite phase coherence time τ and corresponding frequency spread $1/\tau$ of the laser spectrum. (A laser beam differs from a thermal source that has been filtered to have the same spectrum in that it has smaller amplitude fluctuations.) Thus we expect that the mode occupancy is $X = \overline{\dot{N}}\tau$. A convenient approximate description in terms of temporal modes is to take the window interval to be $\Delta t = \tau$. Within the jth interval we take the phase to be a (random) constant φ_j so that (up to an unimportant normalization constant) we have the coherent state

$$\prod_j e^{\sqrt{X} e^{i\varphi_j} \hat{B}_j^{\dagger\rightarrow}} |0\rangle \tag{D28}$$

which obeys

$$\langle \hat{B}_k^{\rightarrow} \rangle = \sqrt{X} e^{i\varphi_k} \tag{D29}$$

and

$$\langle \hat{B}_k^{\dagger\rightarrow} \hat{B}_k^{\rightarrow} \rangle = X. \tag{D30}$$

3. Quantum noise from a resistor

Let us consider the quantum equivalent to Eq. (C60), $\mathcal{S}_{VV} = 2Rk_{\rm B}T$, for the case of a semi-infinite transmission line with open termination, representing a resistor. From Eq. (C27) we see that the proper boundary condition for the φ field is $\partial_x\varphi(0,t) = \partial_x\varphi(L,t) = 0$. (We have temporarily made the transmission line have a large but finite length L.) The normal mode expansion that satisfies these boundary conditions is

$$\varphi(x,t) = \sqrt{\frac{2}{L}} \sum_{n=1}^{\infty} \varphi_n(t) \cos(k_n x), \tag{D31}$$

where φ_n is the normal coordinate and $k_n \equiv \frac{\pi n}{L}$. Substitution of this form into the Lagrangian and carrying out the spatial integration yields a set of independent harmonic oscillators representing the normal modes.

$$L_g = \sum_{n=1}^{\infty} \left(\frac{c}{2}\dot{\varphi}_n^2 - \frac{1}{2\ell}k_n^2\varphi_n^2 \right). \tag{D32}$$

From this we can find the momentum operator $\hat{p}_n$ canonically conjugate to the coordinate operator $\hat{\varphi}_n$ and quantize the system to obtain an expression for the operator representing the voltage at the end of the transmission line in terms of the mode creation and destruction operators

$$\hat{V} = \sum_{n=1}^{\infty} \sqrt{\frac{\hbar\Omega_n}{Lc}} i(\hat{b}_n^\dagger - \hat{b}_n). \tag{D33}$$

The spectral density of voltage fluctuations is then found to be

$$S_{\rm VV}[\omega] = \frac{2\pi}{L}\sum_{n=1}^{\infty} \frac{\hbar\Omega_n}{c}\big\{ n_{\rm B}(\hbar\Omega_n)\delta(\omega+\Omega_n) + [n_{\rm B}(\hbar\Omega_n)+1]\delta(\omega-\Omega_n)\big\}, \tag{D34}$$

where $n_{\rm B}(\hbar\omega)$ is the Bose occupancy factor for a photon with energy $\hbar\omega$. Taking the limit $L\to\infty$ and converting the summation to an integral yields

$$S_{\rm VV}(\omega) = 2Z_{\rm c}\hbar|\omega|\big\{ n_{\rm B}(\hbar|\omega|)\Theta(-\omega) + [n_{\rm B}(\hbar|\omega|)+1]\Theta(\omega)\big\}, \tag{D35}$$

where Θ is the step function. We see immediately that at zero temperature there is no noise at negative frequencies because energy can not be extracted from zero-point motion. However there remains noise at positive frequencies indicating that the vacuum is capable of absorbing energy from another quantum system. The voltage spectral density at both zero and non-zero temperature is plotted in Fig. (1).

Eq. (D35) for this 'two-sided' spectral density of a resistor can be rewritten in a more compact form

$$S_{\rm VV}[\omega] = \frac{2Z_{\rm c}\hbar\omega}{1-e^{-\hbar\omega/k_{\rm B}T}}, \tag{D36}$$

which reduces to the more familiar expressions in various limits. For example, in the classical limit $k_{\rm B}T \gg \hbar\omega$ the spectral density is equal to the Johnson noise result[6]

$$S_{\rm VV}[\omega] = 2Z_{\rm c}k_{\rm B}T, \tag{D37}$$

in agreement with Eq. (C60). In the quantum limit it reduces to

$$S_{\rm VV}[\omega] = 2Z_{\rm c}\hbar\omega\Theta(\omega). \tag{D38}$$

[6] Note again that in the engineering convention this would be $S_{\rm VV}[\omega] = 4Z_{\rm c}k_{\rm B}T$.

Again, the step function tells us that the resistor can only absorb energy, not emit it, at zero temperature.

If we use the engineering convention and add the noise at positive and negative frequencies we obtain

$$S_{\rm VV}[\omega] + S_{\rm VV}[-\omega] = 2Z_{\rm c}\hbar\omega\coth\frac{\hbar\omega}{2k_{\rm B}T} \tag{D39}$$

for the symmetric part of the noise, which appears in the quantum fluctuation-dissipation theorem (cf. Eq. (2.16)). The antisymmetric part of the noise is simply

$$S_{\rm VV}[\omega] - S_{\rm VV}[-\omega] = 2Z_{\rm c}\hbar\omega, \tag{D40}$$

yielding

$$\frac{S_{\rm VV}[\omega] - S_{\rm VV}[-\omega]}{S_{\rm VV}[\omega] + S_{\rm VV}[-\omega]} = \tanh\frac{\hbar\omega}{2k_{\rm B}T}. \tag{D41}$$

This quantum treatment can also be applied to any arbitrary dissipative network (Burkhard *et al.*, 2004; Devoret, 1997). If we have a more complex circuit containing capacitors and inductors, then in all of the above expressions, $Z_{\rm c}$ should be replaced by $\mathrm{Re}\, Z[\omega]$ where $Z[\omega]$ is the complex impedance presented by the circuit.

In the above we have explicitly quantized the standing wave modes of a finite length transmission line. We could instead have used the running waves of an infinite line and recognized that, as the in classical treatment in Eq. (C59), the left and right movers are not independent. The open boundary condition at the termination requires $V^{\leftarrow} = V^{\rightarrow}$ and hence $b^{\rightarrow} = b^{\leftarrow}$. We then obtain

$$S_{VV}[\omega] = 4S^{\rightarrow}_{VV}[\omega] \tag{D42}$$

and from the quantum analog of Eq. (C40) we have

$$\begin{aligned} S_{VV}[\omega] &= \frac{4\hbar|\omega|}{2cv_{\rm p}}\left\{\Theta(\omega)(n_{\rm B}+1) + \Theta(-\omega)n_{\rm B}\right\} \\ &= 2Z_c\hbar|\omega|\left\{\Theta(\omega)(n_{\rm B}+1) + \Theta(-\omega)n_{\rm B}\right\} \end{aligned} \tag{D43}$$

in agreement with Eq. (D35).

Appendix E: Back Action and Input-Output Theory for Driven Damped Cavities

A high Q cavity whose resonance frequency can be parametrically controlled by an external source can act as a very simple quantum amplifier, encoding information about the external source in the phase and amplitude of the output of the driven cavity. For example, in an optical cavity, one of the mirrors could be moveable and the external source could be a force acting on that mirror. This defines the very active field of optomechanics, which also deals with microwave cavities coupled to nanomechanical systems and other related setups (Arcizet *et al.*, 2006; Brown *et al.*, 2007; Gigan *et al.*,

2006; Harris *et al.*, 2007; Höhberger-Metzger and Karrai, 2004; Marquardt *et al.*, 2007, 2006; Meystre *et al.*, 1985; Schliesser *et al.*, 2006; Teufel *et al.*, 2008; Thompson *et al.*, 2008; Wilson-Rae *et al.*, 2007). In the case of a microwave cavity containing a qubit, the state-dependent polarizability of the qubit acts as a source which shifts the frequency of the cavity (Blais *et al.*, 2004; Schuster *et al.*, 2005; Wallraff *et al.*, 2004).

The dephasing of a qubit in a microwave cavity and the fluctuations in the radiation pressure in an optical cavity both depend on the quantum noise in the number of photons inside the cavity. We here use a simple equation of motion method to exactly solve for this quantum noise in the perturbative limit where the dynamics of the qubit or mirror degree of freedom has only a weak back action effect on the cavity.

In the following, we first give a basic discussion of the cavity field noise spectrum, deferring the detailed microscopic derivation to subsequent subsections. We then provide a review of the input-output theory for driven cavities, and employ this theory to analyze the important example of a dispersive position measurement, where we demonstrate how the standard quantum limit can be reached. Finally, we analyze an example where a modified dispersive scheme is used to detect only one quadrature of a harmonic oscillator's motion, such that this quadrature does not feel any back-action.

1. Photon shot noise inside a cavity and back action

Consider a degree of freedom $\hat{z}$ coupled parametrically with strength A to the cavity oscillator

$$\hat{H}_{\rm int} = \hbar\omega_{\rm c}(1 + A\hat{z})\,[\hat{a}^\dagger\hat{a} - \langle\hat{a}^\dagger\hat{a}\rangle] \tag{E1}$$

where following Eq. (3.12), we have taken A to be dimensionless, and use $\hat{z}$ to denote the dimensionless system variable that we wish to probe. For example, $\hat{z}$ could represent the dimensionless position of a mechanical oscillator

$$\hat{z} \equiv \frac{\hat{x}}{x_{\rm ZPF}}. \tag{E2}$$

We have subtracted the $\langle\hat{a}^\dagger\hat{a}\rangle$ term so that the mean force on the degree of freedom is zero. To obtain the full Hamiltonian, we would have to add the cavity damping and driving terms, as well as the Hamiltonian governing the intrinsic dynamics of the system $\hat{z}$. From Eq. (3.18) we know that the back action noise force acting on $\hat{z}$ is proportional to the quantum fluctuations in the number of photons $\hat{n} = \hat{a}^\dagger\hat{a}$ in the cavity,

$$S_{nn}(t) = \langle\hat{a}^\dagger(t)\hat{a}(t)\hat{a}^\dagger(0)\hat{a}(0)\rangle - \langle\hat{a}^\dagger(t)\hat{a}(t)\rangle^2. \tag{E3}$$

For the case of continuous wave driving at frequency $\omega_{\rm L} = \omega_{\rm c} + \Delta$ detuned by Δ from the resonance, the cavity is in a coherent state $|\psi\rangle$ obeying

$$\hat{a}(t) = e^{-i\omega_{\rm L}t}[\bar{a} + \hat{d}(t)] \tag{E4}$$

where the first term is the 'classical part' of the mode amplitude $\psi(t) = \bar{a}e^{-i\omega_{\rm L}t}$ determined by the strength of the drive field, the damping of the cavity and the detuning Δ, and d is the quantum part. By definition,

$$\hat{a}|\psi\rangle = \psi|\psi\rangle \tag{E5}$$

so the coherent state is annihilated by $\hat{d}$:

$$\hat{d}|\psi\rangle = 0. \tag{E6}$$

That is, in terms of the operator $\hat{d}$, the coherent state looks like the undriven quantum ground state . The displacement transformation in Eq. (E4) is canonical since

$$[\hat{a}, \hat{a}^\dagger] = 1 \;\Rightarrow\; [\hat{d}, \hat{d}^\dagger] = 1. \tag{E7}$$

Substituting the displacement transformation into Eq. (E3) and using Eq. (E6) yields

$$S_{nn}(t) = \bar{n}\langle\hat{d}(t)\hat{d}^\dagger(0)\rangle, \tag{E8}$$

where $\bar{n} = |\bar{a}|^2$ is the mean cavity photon number. If we set the cavity energy damping rate to be κ, such that the amplitude damping rate is $\kappa/2$, then the undriven state obeys

$$\langle\hat{d}(t)\hat{d}^\dagger(0)\rangle = e^{+i\Delta t}e^{-\frac{\kappa}{2}|t|}. \tag{E9}$$

This expression will be justified formally in the subsequent subsection, after introducing input-output theory. We thus arrive at the very simple result

$$S_{nn}(t) = \bar{n}e^{i\Delta t - \frac{\kappa}{2}|t|}. \tag{E10}$$

The power spectrum of the noise is, via the Wiener-Khinchin theorem (Appendix A.2), simply the Fourier transform of the autocorrelation function given in Eq. (E10)

$$S_{nn}[\omega] = \int_{-\infty}^{+\infty} dt\, e^{i\omega t} S_{nn}(t) = \bar{n}\frac{\kappa}{(\omega+\Delta)^2 + (\kappa/2)^2}. \tag{E11}$$

As can be seen in Fig. 5a, for positive detuning $\Delta = \omega_L - \omega_{\rm c} > 0$, i.e. for a drive that is blue-detuned with respect to the cavity, the noise peaks at *negative* ω. This means that the noise tends to pump energy into the degree of freedom $\hat{z}$ (i.e. it contributes negative damping). For negative detuning the noise peaks at positive ω corresponding to the cavity absorbing energy from $\hat{z}$. Basically, the interaction with $\hat{z}$ (three wave mixing) tries to Raman scatter the drive photons into the high density of states at the cavity frequency. If this is uphill in energy, then $\hat{z}$ is cooled.

As discussed in Sec. B.2 (c.f. Eq. (2.8)), at each frequency ω, we can use detailed balance to assign the noise an effective temperature $T_{\rm eff}[\omega]$:

$$\begin{aligned} \frac{S_{nn}[\omega]}{S_{nn}[-\omega]} &= e^{\hbar\omega/k_B T_{\rm eff}[\omega]} \Leftrightarrow \\ k_{\rm B}T_{\rm eff}[\omega] &\equiv \frac{\hbar\omega}{\log\left[\frac{S_{nn}[\omega]}{S_{nn}[-\omega]}\right]} \end{aligned} \tag{E12}$$

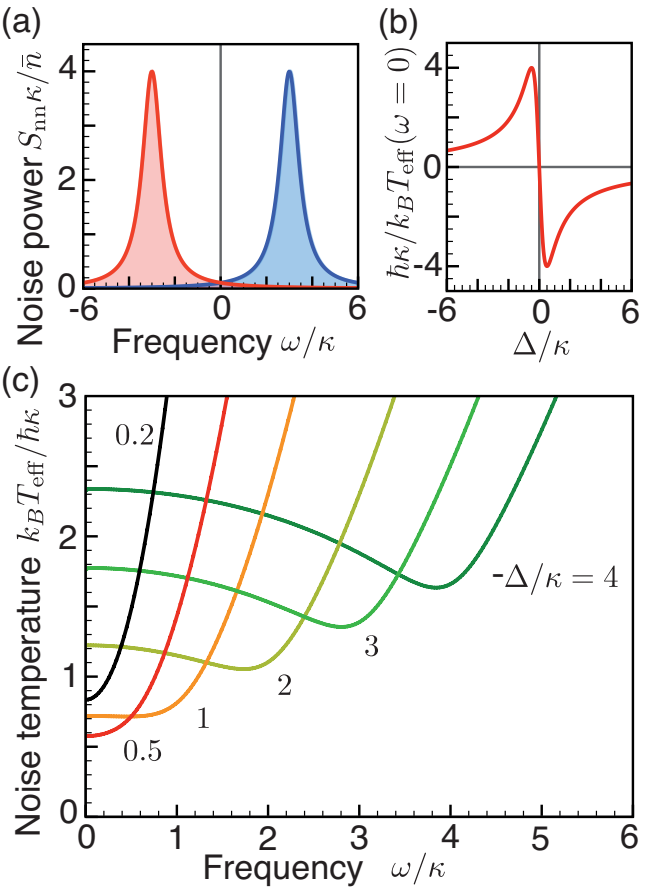

FIG. 5 (Color online) (a) Noise spectrum of the photon number in a driven cavity as a function of frequency when the cavity drive frequency is detuned from the cavity resonance by $\Delta = +3\kappa$ (left peak) and $\Delta = -3\kappa$ (right peak). (b) Effective temperature $T_{\rm eff}$ of the low frequency noise, $\omega \to 0$, as a function of the detuning Δ of the drive from the cavity resonance. (c) Frequency-dependence of the effective noise temperature, for different values of the detuning.

or equivalently

$$\frac{S_{nn}[\omega] - S_{nn}[-\omega]}{S_{nn}[\omega] + S_{nn}[-\omega]} = \tanh(\beta\hbar\omega/2). \qquad \text{(E13)}$$

If $\hat{z}$ is the coordinate of a harmonic oscillator of frequency ω (or some non-conserved observable of a qubit with level splitting ω), then that system will acquire a temperature $T_{\rm eff}[\omega]$ in the absence of coupling to any other environment. In particular, if the characteristic oscillation frequency of the system $\hat{z}$ is much smaller than κ, then we have the simple result

$$\begin{aligned}\frac{1}{k_{\rm B}T_{\rm eff}} &= \lim_{\omega\to 0^+} \frac{2}{\hbar\omega}\frac{S_{nn}[\omega] - S_{nn}[-\omega]}{S_{nn}[\omega] + S_{nn}[-\omega]} \\ &= 2\frac{d\ln S_{nn}[\omega]}{d\hbar\omega} \\ &= \frac{1}{\hbar}\frac{-4\Delta}{\Delta^2 + (\kappa/2)^2}. \end{aligned} \qquad \text{(E14)}$$

As can be seen in Fig. 5, the asymmetry in the noise changes sign with detuning, which causes the effective temperature to change sign.

First we discuss the case of a positive $T_{\rm eff}$, where this mechanism can be used to laser cool an oscillating mechanical cantilever, provided $T_{\rm eff}$ is lower than the intrinsic equilibrium temperature of the cantilever. (Arcizet *et al.*, 2006; Brown *et al.*, 2007; Gigan *et al.*, 2006; Harris *et al.*, 2007; Höhberger-Metzger and Karrai, 2004; Marquardt *et al.*, 2007; Schliesser *et al.*, 2006; Thompson *et al.*, 2008; Wilson-Rae *et al.*, 2007). A simple classical argument helps us understand this cooling effect. Suppose that the moveable mirror is at the right hand end of a cavity being driven below the resonance frequency. If the mirror moves to the right, the resonance frequency will fall and the number of photons in the cavity will rise. There will be a time delay however to fill the cavity and so the extra radiation pressure will not be fully effective in doing work on the mirror. During the return part of the oscillation as the mirror moves back to the left, the time delay in emptying the cavity will cause the mirror to have to do extra work against the radiation pressure. At the end of the cycle it ends up having done net positive work on the light field and hence is cooled. The effect can therefore be understood as being due to the introduction of some extra optomechanical damping.

The signs reverse (and $T_{\rm eff}$ becomes negative) if the cavity is driven above resonance, and consequently the cantilever motion is heated up. In the absence of intrinsic mechanical losses, negative values of the effective temperature indicate a dynamical instability of the cantilever (or population inversion in the case of a qubit), where the amplitude of motion grows until it is finally stabilized by nonlinear effects. This can be interpreted as negative damping introduced by the optomechanical coupling and can be used to create parametric amplification of mechanical forces acting on the oscillator.

Finally, we mention that cooling towards the quantum ground state of a mechanical oscillator (where phonon numbers become much less than one), is only possible (Marquardt *et al.*, 2007; Wilson-Rae *et al.*, 2007) in the "far-detuned regime", where $-\Delta = \omega \gg \kappa$ (in contrast to the $\omega \ll \kappa$ regime discussed above).

2. Input-output theory for a driven cavity

The results from the previous section can be more formally and rigorously derived in a full quantum theory of a cavity driven by an external coherent source. The theory relating the drive, the cavity and the outgoing waves radiated by the cavity is known as input-output theory and the classical description was presented in Appendix C. The present quantum discussion closely follows standard references on the subject (Walls and Milburn, 1994; Yurke, 1984; Yurke and Denker, 1984). The crucial feature that distinguishes such an approach from many other treatments of quantum-dissipative systems

is the goal of keeping the bath modes instead of tracing them out. This is obviously necessary for the situations we have in mind, where the output field emanating from the cavity contains the information acquired during a measurement of the system coupled to the cavity. As we learned from the classical treatment, we can eliminate the outgoing waves in favor of a damping term for the system. However we can recover the solution for the outgoing modes completely from the solution of the equation of motion of the damped system being driven by the incoming waves.

In order to drive the cavity we must partially open one of its ports which exposes the cavity both to the external drive and to the vacuum noise outside which permits energy in the cavity to leak out into the surrounding bath. We will formally separate the degrees of freedom into internal cavity modes and external bath modes. Strictly speaking, once the port is open, these modes are not distinct and we only have 'the modes of the universe' (Gea-Banacloche *et al.*, 1990a,b; Lang *et al.*, 1973). However for high Q cavities, the distinction is well-defined and we can model the decay of the cavity in terms of a spontaneous emission process in which an internal boson is destroyed and an external bath boson is created. We assume a single-sided cavity. For a high Q cavity, this physics is accurately captured in the following Hamiltonian

$$\hat{H} = \hat{H}_{\rm sys} + \hat{H}_{\rm bath} + \hat{H}_{\rm int}. \tag{E15}$$

The bath Hamiltonian is

$$\hat{H}_{\rm bath} = \sum_q \hbar\omega_q \hat{b}_q^\dagger \hat{b}_q \tag{E16}$$

where q labels the quantum numbers of the independent harmonic oscillator bath modes obeying

$$[\hat{b}_q, \hat{b}_{q'}^\dagger] = \delta_{q,q'}. \tag{E17}$$

Note that since the bath terminates at the system, there is no translational invariance, the normal modes are standing not running waves, and the quantum numbers q are not necessarily wave vectors.

The coupling Hamiltonian is (within the rotating wave approximation)

$$\hat{H}_{\rm int} = -i\hbar \sum_q \left[f_q \hat{a}^\dagger \hat{b}_q - f_q^* \hat{b}_q^\dagger \hat{a} \right]. \tag{E18}$$

For the moment we will leave the system (cavity) Hamiltonian to be completely general, specifying only that it consists of a single degree of freedom (i.e. we concentrate on only a single resonance of the cavity with frequency $\omega_{\rm c}$) obeying the usual bosonic commutation relation

$$[\hat{a}, \hat{a}^\dagger] = 1. \tag{E19}$$

(N.B. this does not imply that it is a harmonic oscillator. We will consider both linear and non-linear cavities.)

Note that the most general linear coupling to the bath modes would include terms of the form $\hat{b}_q^\dagger \hat{a}^\dagger$ and $\hat{b}_q a$ but these are neglected within the rotating wave approximation because in the interaction representation they oscillate at high frequencies and have little effect on the dynamics.

The Heisenberg equation of motion (EOM) for the bath variables is

$$\dot{\hat{b}}_q = \frac{i}{\hbar}[\hat{H}, \hat{b}_q] = -i\omega_{\rm q}\hat{b}_q + f_q^* \hat{a} \tag{E20}$$

We see that this is simply the EOM of a harmonic oscillator driven by a forcing term due to the motion of the cavity degree of freedom. Since this is a linear system, the EOM can be solved exactly. Let $t_0 < t$ be a time in the distant past before any wave packet launched at the cavity has reached it. The solution of Eq. (E20) is

$$\hat{b}_q(t) = e^{-i\omega_{\rm q}(t-t_0)}\hat{b}_q(t_0) + \int_{t_0}^{t} d\tau\, e^{-i\omega_{\rm q}(t-\tau)} f_q^*\, \hat{a}(\tau). \tag{E21}$$

The first term is simply the free evolution of the bath while the second represents the waves radiated by the cavity into the bath.

The EOM for the cavity mode is

$$\dot{\hat{a}} = \frac{i}{\hbar}[\hat{H}_{\rm sys}, \hat{a}] - \sum_q f_q \hat{b}_q. \tag{E22}$$

Substituting Eq. (E21) into the last term above yields

$$\sum_q f_q \hat{b}_q = \sum_q f_q e^{-i\omega_{\rm q}(t-t_0)}\hat{b}_q(t_0) + \sum_q |f_q|^2 \int_{t_0}^{t} d\tau\, e^{-i(\omega_{\rm q}-\omega_{\rm c})(t-\tau)}[e^{+i\omega_{\rm c}(\tau-t)}\hat{a}(\tau)], \tag{E23}$$

where the last term in square brackets is a slowly varying function of τ. To simplify our result, we note that if the cavity system were a simple harmonic oscillator of frequency $\omega_{\rm c}$ then the decay rate from the $n = 1$ single photon excited state to the $n = 0$ ground state would be given by the following Fermi Golden Rule expression

$$\kappa(\omega_{\rm c}) = 2\pi \sum_q |f_q|^2 \delta(\omega_{\rm c} - \omega_{\rm q}). \tag{E24}$$

From this it follows that

$$\int_{-\infty}^{+\infty} \frac{d\nu}{2\pi} \kappa(\omega_{\rm c} + \nu) e^{-i\nu(t-\tau)} = \sum_q |f_q|^2 e^{-i(\omega_{\rm q}-\omega_{\rm c})(t-\tau)}. \tag{E25}$$

We now make the Markov approximation which assumes that $\kappa(\nu) = \kappa$ is a constant over the range of frequencies relevant to the cavity so that Eq. (E25) may be represented as

$$\sum_q |f_q|^2 e^{-i(\omega_{\rm q}-\omega_{\rm c})(t-\tau)} = \kappa\delta(t-\tau). \tag{E26}$$

Using

$$\int_{-\infty}^{x_0} dx\, \delta(x - x_0) = \frac{1}{2} \tag{E27}$$

we obtain for the cavity EOM

$$\dot{\hat{a}} = \frac{i}{\hbar}[\hat{H}_{\rm sys}, \hat{a}] - \frac{\kappa}{2}\hat{a} - \sum_q f_q e^{-i\omega_{\rm q}(t-t_0)}\hat{b}_q(t_0). \tag{E28}$$

The second term came from the part of the bath motion representing the wave radiated by the cavity and, within the Markov approximation, has become a simple linear damping term for the cavity mode. Note the important factor of 2. The amplitude decays at half the rate of the intensity (the energy decay rate κ).

Within the spirit of the Markov approximation it is further convenient to treat $f \equiv \sqrt{|f_q|^2}$ as a constant and define the density of states (also taken to be a constant) by

$$\rho = \sum_q \delta(\omega_{\rm c} - \omega_{\rm q}) \tag{E29}$$

so that the Golden Rule rate becomes

$$\kappa = 2\pi f^2 \rho. \tag{E30}$$

We can now define the so-called 'input mode'

$$\hat{b}_{\rm in}(t) \equiv \frac{1}{\sqrt{2\pi\rho}} \sum_q e^{-i\omega_{\rm q}(t-t_0)}\hat{b}_q(t_0)\,. \tag{E31}$$

For the case of a transmission line treated in Appendix D, this coincides with the field $\hat{b}^{\rightarrow}$ moving towards the cavity [see Eq. (D13a)]. We finally have for the cavity EOM

$$\dot{\hat{a}} = \frac{i}{\hbar}[\hat{H}_{\rm sys}, \hat{a}] - \frac{\kappa}{2}\hat{a} - \sqrt{\kappa}\,\hat{b}_{\rm in}(t). \tag{E32}$$

Note that when a wave packet is launched from the bath towards the cavity, causality prevents it from knowing about the cavity's presence until it reaches the cavity. Hence the input mode evolves freely as if the cavity were not present until the time of the collision at which point it begins to drive the cavity. Since $\hat{b}_{\rm in}$(t) evolves under the free bath Hamiltonian and acts as the driving term in the cavity EOM, we interpret it physically as the input mode. Eq. (E32) is the quantum analog of the classical equation (C19), for our previous example of an LC-oscillator driven by a transmission line. The latter would also have been first order in time if as in Eq. (C35) we had worked with the complex amplitude A instead of the coordinate Q.

Eq. (E31) for the input mode contains a time label just as in the interaction representation. However it is best interpreted as simply labeling the particular linear combination of the bath modes which is coupled to the system at time t. Some authors even like to think of the bath modes as non-propagating while the cavity flies along the bath (taken to be 1D) at a velocity v. The system then only interacts briefly with the local mode positioned at $x = vt$ before moving on and interacting with the next local bath mode. We will elaborate on this view further at the end of this subsection.

The expression for the power $P_{\rm in}$ (energy per time) impinging on the cavity depends on the normalization chosen in our definition of $\hat{b}_{\rm in}$. It can be obtained, for example, by imagining the bath modes $\hat{b}_q$ to live on a one-dimensional waveguide with propagation velocity v and length L (using periodic boundary conditions). In that case we have to sum over all photons to get the average power flowing through a cross-section of the waveguide, $P_{\rm in} = \sum_q \hbar\omega_q(v_p/L)\left\langle \hat{b}_q^\dagger \hat{b}_q \right\rangle$. Inserting the definition for $\hat{b}_{\rm in}$, Eq. (E31), the expression for the input power carried by a monochromatic beam at frequency ω is

$$P_{\rm in}(t) = \hbar\omega \left\langle \hat{b}_{\rm in}^\dagger(t)\hat{b}_{\rm in}(t) \right\rangle \tag{E33}$$

Note that this has the correct dimensions due to our choice of normalization for $\hat{b}_{\rm in}$ (with dimensions $\sqrt{\omega}$). In the general case, an integration over frequencies is needed (as will be discussed further below). An analogous formula holds for the power radiated by the cavity, to be discussed now.

The output mode $\hat{b}_{\rm out}(t)$ is radiated into the bath and evolves freely after the system interacts with $\hat{b}_{\rm in}(t)$. If the cavity did not respond at all, then the output mode would simply be the input mode reflected off the cavity mirror. If the mirror is partially transparent then the output mode will also contain waves radiated by the cavity (which is itself being driven by the input mode partially transmitted into the cavity through the mirror) and hence contains information about the internal dynamics of the cavity. To analyze this output field, let $t_1 > t$ be a time in the distant future after the input field has interacted with the cavity. Then we can write an alternative solution to Eq. (E20) in terms of the final rather than the initial condition of the bath

$$\hat{b}_q(t) = e^{-i\omega_q(t-t_1)}\hat{b}_q(t_1) - \int_t^{t_1} d\tau\, e^{-i\omega_{\rm q}(t-\tau)} f_q^* \hat{a}(\tau). \tag{E34}$$

Note the important minus sign in the second term associated with the fact that the time t is now the lower limit of integration rather than the upper as it was in Eq. (E21).

Defining

$$\hat{b}_{\rm out}(t) \equiv \frac{1}{\sqrt{2\pi\rho}} \sum_q e^{-i\omega_{\rm q}(t-t_1)}\hat{b}_q(t_1), \tag{E35}$$

we see that this is simply the free evolution of the bath modes from the distant future (after they have interacted with the cavity) back to the present, indicating that it is indeed appropriate to interpret this as the outgoing field.

Proceeding as before we obtain

$$\dot{\hat{a}} = \frac{i}{\hbar}[\hat{H}_{\rm sys}, \hat{a}] + \frac{\kappa}{2}\hat{a} - \sqrt{\kappa}\,\hat{b}_{\rm out}(t). \tag{E36}$$

Subtracting Eq. (E36) from Eq. (E32) yields

$$\hat{b}_{\rm out}(t) = \hat{b}_{\rm in}(t) + \sqrt{\kappa}\,\hat{a}(t) \tag{E37}$$

which is consistent with our interpretation of the outgoing field as the reflected incoming field plus the field radiated by the cavity out through the partially reflecting mirror.

The above results are valid for any general cavity Hamiltonian. The general procedure is to solve Eq. (E32) for $\hat{a}(t)$ for a given input field, and then solve Eq. (E37) to obtain the output field. For the case of an empty cavity we can make further progress because the cavity mode is a harmonic oscillator

$$\hat{H}_{\rm sys} = \hbar\omega_{\rm c}\hat{a}^\dagger\hat{a}. \tag{E38}$$

In this simple case, the cavity EOM becomes

$$\dot{\hat{a}} = -i\omega_{\rm c}\hat{a} - \frac{\kappa}{2}\hat{a} - \sqrt{\kappa}\,\hat{b}_{\rm in}(t). \tag{E39}$$

Eq. (E39) can be solved by Fourier transformation, yielding

$$\begin{aligned}\hat{a}[\omega] &= -\frac{\sqrt{\kappa}}{i(\omega_{\rm c}-\omega)+\kappa/2}\,\hat{b}_{\rm in}[\omega] &\text{(E40)}\\ &= -\sqrt{\kappa}\chi_{\rm c}[\omega-\omega_{\rm c}]\hat{b}_{\rm in}[\omega] &\text{(E41)}\end{aligned}$$

and

$$\hat{b}_{\rm out}[\omega] = \frac{\omega-\omega_{\rm c}-i\kappa/2}{\omega-\omega_{\rm c}+i\kappa/2}\,\hat{b}_{\rm in}[\omega] \tag{E42}$$

which is the result for the reflection coefficient quoted in Eq. (3.13). For brevity, here and in the following, we will sometimes use the susceptibility of the cavity, defined as

$$\chi_{\rm c}[\omega-\omega_{\rm c}] \equiv \frac{1}{-i(\omega-\omega_{\rm c})+\kappa/2} \tag{E43}$$

For the case of steady driving on resonance where $\omega = \omega_{\rm c}$, the above equations yield

$$\hat{b}_{\rm out}[\omega] = \frac{\sqrt{\kappa}}{2}\hat{a}[\omega]. \tag{E44}$$

In steady state, the incoming power equals the outgoing power, and both are related to the photon number inside the single-sided cavity by

$$P = \hbar\omega\left\langle\hat{b}^\dagger_{\rm out}(t)\hat{b}_{\rm out}(t)\right\rangle = \hbar\omega\frac{\kappa}{4}\left\langle\hat{a}^\dagger(t)\hat{a}(t)\right\rangle \tag{E45}$$

Note that this does not coincide with the naive expectation, which would be $P = \hbar\omega\kappa\left\langle\hat{a}^\dagger\hat{a}\right\rangle$. The reason for this discrepancy is the the interference between the part of the incoming wave which is promptly reflected from the cavity and the field radiated by the cavity. The naive expression becomes correct after the drive has been switched off (where ignoring the effect of the incoming vacuum noise, we would have $\hat{b}_{\rm out} = \sqrt{\kappa}\hat{a}$). We note in passing that for a driven two-sided cavity with coupling constants κ_L and κ_R (where $\kappa = \kappa_L + \kappa_R$), the incoming power sent into the left port is related to the photon number by

$$P = \hbar\omega\kappa^2/(4\kappa_L)\left\langle\hat{a}^\dagger\hat{a}\right\rangle. \tag{E46}$$

Here for $\kappa_L = \kappa_R$ the interference effect completely eliminates the reflected beam and we have in contrast to Eq. (E45)

$$P = \hbar\omega\frac{\kappa}{2}\left\langle\hat{a}^\dagger\hat{a}\right\rangle. \tag{E47}$$

Eq. (E39) can also be solved in the time domain to obtain

$$\begin{aligned}\hat{a}(t) &= e^{-(i\omega_{\rm c}+\kappa/2)(t-t_0)}\hat{a}(t_0)\\ &- \sqrt{\kappa}\int_{t_0}^{t} d\tau\, e^{-(i\omega_{\rm c}+\kappa/2)(t-\tau)}\hat{b}_{\rm in}(\tau). &\text{(E48)}\end{aligned}$$

If we take the input field to be a coherent drive at frequency $\omega_{\rm L} = \omega_{\rm c} + \Delta$ so that its amplitude has a classical and a quantum part

$$\hat{b}_{\rm in}(t) = e^{-i\omega_{\rm L}t}[\bar{b}_{\rm in} + \hat{\xi}(t)] \tag{E49}$$

and if we take the limit $t_0 \to \infty$ so that the initial transient in the cavity amplitude has damped out, then the solution of Eq. (E48) has the form postulated in Eq. (E4) with

$$\bar{a} = -\frac{\sqrt{\kappa}}{-i\Delta+\kappa/2}\bar{b}_{\rm in} \tag{E50}$$

and (in the frame rotating at the drive frequency)

$$\hat{d}(t) = -\sqrt{\kappa}\int_{-\infty}^{t} d\tau\, e^{+(i\Delta-\kappa/2)(t-\tau)}\hat{\xi}(\tau). \tag{E51}$$

Even in the absence of any classical drive, the input field delivers vacuum fluctuation noise to the cavity. Notice that from Eqs. (E31, E49)

$$\begin{aligned}[\hat{b}_{\rm in}(t), \hat{b}^\dagger_{\rm in}(t')] &= [\hat{\xi}(t), \hat{\xi}^\dagger(t')]\\ &= \frac{1}{2\pi\rho}\sum_q e^{-i(\omega_{\rm q}-\omega_{\rm L})(t-t')}\\ &= \delta(t-t'), &\text{(E52)}\end{aligned}$$

which is similar to Eq. (D16) for a quantum transmission line. This is the operator equivalent of white noise. Using Eq. (E48) in the limit $t_0 \to -\infty$ in Eqs. (E4,E51) yields

$$\begin{aligned}[\hat{a}(t), \hat{a}^\dagger(t)] &= [\hat{d}(t), \hat{d}^\dagger(t)]\\ &= \kappa\int_{-\infty}^{t} d\tau\int_{-\infty}^{t} d\tau'\, e^{-(-i\Delta+\kappa/2)(t-\tau)}\\ &\quad e^{-(+i\Delta+\kappa/2)(t-\tau')}\delta(\tau-\tau')\\ &= 1 &\text{(E53)}\end{aligned}$$

as is required for the cavity bosonic quantum degree of freedom. We can interpret this as saying that the cavity zero-point fluctuations arise from the vacuum noise that enters through the open port. We also now have a simple physical interpretation of the quantum noise in the number of photons in the driven cavity in Eqs. (E3,E8,E11). It is due to the vacuum noise which enters the cavity through the same ports that bring in the classical drive. The interference between the vacuum noise and the classical drive leads to the photon number fluctuations in the cavity.

In thermal equilibrium, $\hat{\xi}$ also contains thermal radiation. If the bath is being probed only over a narrow range of frequencies centered on ω_c (which we have assumed in making the Markov approximation) then we have to a good approximation (consistent with the above commutation relation)

$$\langle \hat{\xi}^\dagger(t)\hat{\xi}(t')\rangle = N\delta(t-t') \tag{E54}$$

$$\langle \hat{\xi}(t)\hat{\xi}^\dagger(t')\rangle = (N+1)\delta(t-t') \tag{E55}$$

where $N = n_B(\hbar\omega_c)$ is the thermal equilibrium occupation number of the mode at the frequency of interest. We can gain a better understanding of Eq. (E54) by Fourier transforming it to obtain the spectral density

$$S[\omega] = \int_{-\infty}^{+\infty} dt\, \langle \hat{\xi}^\dagger(t)\hat{\xi}(t')\rangle e^{i\omega(t-t')} = N. \tag{E56}$$

As mentioned previously, this dimensionless quantity is the spectral density that would be measured by a photomultiplier: it represents the number of thermal photons passing a given point per unit time per unit bandwidth. Equivalently the thermally radiated power in a narrow bandwidth B is

$$P = \hbar\omega N B. \tag{E57}$$

One often hears the confusing statement that the noise added by an amplifier is a certain number N of photons ($N = 20$, say for a good cryogenic HEMT amplifier operating at 5 GHz). This means that the excess output noise (referred back to the input by dividing by the power gain) produces a flux of N photons per second in a 1 Hz bandwidth, or $10^6 N$ photons per second in 1 MHz of bandwidth (see also Eq. (D27)).

We can gain further insight into input-output theory by using the following picture. The operator $\hat{b}_{in}(t)$ represents the classical drive plus vacuum fluctuations which are just about to arrive at the cavity. We will be able to show that the output field is simply the input field a short while later after it has interacted with the cavity. Let us consider the time evolution over a short time period Δt which is very long compared to the inverse bandwidth of the vacuum noise (i.e., the frequency scale beyond which the vacuum noise cannot be treated as constant due to some property of the environment) but very short compared to the cavity system's slow dynamics. In this circumstance it is useful to introduce the quantum Wiener increment related to Eq. (D18)

$$d\widehat{W} \equiv \int_t^{t+\Delta t} d\tau\, \hat{\xi}(\tau) \tag{E58}$$

which obeys

$$[d\widehat{W}, d\widehat{W}^\dagger] = \Delta t. \tag{E59}$$

In the interaction picture (in a displaced frame in which the classical drive has been removed) the Hamiltonian term that couples the cavity to the quantum noise of the environment is from Eq. (E18)

$$\hat{V} = -i\hbar\sqrt{\kappa}(\hat{a}^\dagger\hat{\xi} - \hat{a}\hat{\xi}^\dagger). \tag{E60}$$

Thus the time evolution operator (in the interaction picture) on the jth short time interval $[t_j, t_j + \Delta t]$ is

$$\hat{U}_j = e^{\sqrt{\kappa}(\hat{a}\, d\widehat{W}^\dagger - \hat{a}^\dagger\, d\widehat{W})} \tag{E61}$$

Using this we can readily evolve the incoming temporal mode forward in time by a small step Δt

$$d\widehat{W}' = \hat{U}^\dagger d\widehat{W}\hat{U} \approx d\widehat{W} + \sqrt{\kappa}\Delta t\, \hat{a}. \tag{E62}$$

Recall that in input-output theory we formally defined the outgoing field as the bath field far in the future propagated back (using the free field time evolution) to the present, which yielded

$$\hat{b}_{out} = \hat{b}_{in} + \sqrt{\kappa}\hat{a}. \tag{E63}$$

Eq. (E62) is completely equivalent to this. Thus we confirm our understanding that the incoming field is the bath temporal mode just before it interacts with the cavity and the outgoing field is the bath temporal mode just after it interacts with the cavity.

This leads to the following picture which is especially useful in the quantum trajectory approach to conditional quantum evolution of a system subject to weak continuous measurement (Gardiner *et al.*, 1992; Walls and Milburn, 1994). On top of the classical drive $\bar{b}_{in}(t)$, the bath supplies to the system a continuous stream of "fresh" harmonic oscillators, each in their ground state (if $T = 0$). Each oscillator with its quantum fluctuation $d\widehat{W}$ interacts briefly for a period Δt with the system and then is disconnected to propagate freely thereafter, never interacting with the system again. Within this picture it is useful to think of the oscillators arrayed in an infinite stationary line and the cavity flying over them at speed v_p and touching each one for a time Δt.

3. Quantum limited position measurement using a cavity detector

We will now apply the input-output formalism introduced in the previous section to the important example

of a dispersive position measurement, which employs a cavity whose resonance frequency shifts in response to the motion of a harmonic oscillator. This physical system was considered heuristically in Sec. III.B.3. Here we will present a rigorous derivation using the (linearized) equations of motion for the coupled cavity and oscillator system.

Let the dimensionless position operator

$$\hat{z} = \frac{1}{x_{\rm ZPF}}\hat{x} = [\hat{c}^\dagger + \hat{c}] \tag{E64}$$

be the coordinate of a harmonic oscillator whose energy is

$$H_{\rm M} = \hbar\omega_{\rm M}\hat{c}^\dagger\hat{c} \tag{E65}$$

and whose position uncertainty in the quantum ground state is $x_{\rm ZPF} = \sqrt{\langle 0|\hat{x}^2|0\rangle}$.

This Hamiltonian could be realized for example by mounting one of the cavity mirrors on a flexible cantilever (see the discussion above).

When the mirror moves, the cavity resonance frequency shifts,

$$\tilde{\omega}_{\rm c} = \omega_{\rm c}[1 + A\hat{z}(t)] \tag{E66}$$

where for a cavity of length L, $A = -x_{\rm ZPF}/L$.

Assuming that the mirror moves slowly enough for the cavity to adiabatically follow its motion (i.e. $\Omega \ll \kappa$), the outgoing light field suffers a phase shift which follows the changes in the mirror position. This phase shift can be detected in the appropriate homodyne set up as discussed in Sec. III.B, and from this phase shift we can determine the position of the mechanical oscillator. In addition to the actual zero-point fluctuations of the oscillator, our measurement will suffer from shot noise in the homodyne signal and from additional uncertainty due to the back action noise of the measurement acting on the oscillator. All of these effects will appear naturally in the derivation below.

We begin by considering the optical cavity equation of motion based on Eq. (E32) and the optomechanical coupling Hamiltonian in Eq. (E1). These yield

$$\dot{\hat{a}} = -i\omega_{\rm c}(1 + A\hat{z})\hat{a} - \frac{\kappa}{2}\hat{a} - \sqrt{\kappa}\hat{b}_{\rm in}. \tag{E67}$$

Let the cavity be driven by a laser at a frequency $\omega_{\rm L} = \omega_{\rm c} + \Delta$ detuned from the cavity by Δ. Moving to a frame rotating at $\omega_{\rm L}$ we have

$$\dot{\hat{a}} = +i(\Delta - A\omega_{\rm c}\hat{z})\hat{a} - \frac{\kappa}{2}\hat{a} - \sqrt{\kappa}\hat{b}_{\rm in}. \tag{E68}$$

and we can write the incoming field as a constant plus white noise vacuum fluctuations (again, in the rotating frame)

$$\hat{b}_{\rm in} = \bar{b}_{\rm in} + \hat{\xi} \tag{E69}$$

and similarly for the cavity field following Eq. (E4)

$$\hat{a} = \bar{a} + \hat{d}. \tag{E70}$$

Substituting these expressions into the equation of motion, we find that the constant classical fields obey

$$\bar{a} = -\frac{\sqrt{\kappa}}{\kappa/2 - i\Delta}\bar{b}_{\rm in} \tag{E71}$$

and the new quantum equation of motion is, after neglecting a small term $\hat{d}\hat{z}$:

$$\dot{\hat{d}} = +i\Delta\hat{d} - iA\omega_{\rm c}\bar{a}\hat{z} - \frac{\kappa}{2}\hat{d} - \sqrt{\kappa}\hat{\xi}. \tag{E72}$$

The quantum limit for position measurement will be reached only at zero detuning, so we specialize to the case $\Delta = 0$. We also choose the incoming field amplitude and phase to obey

$$\bar{b}_{\rm in} = -i\sqrt{\overline{\dot{N}}}, \tag{E73}$$

so that

$$\bar{a} = +2i\sqrt{\frac{\overline{\dot{N}}}{\kappa}}, \tag{E74}$$

where $\overline{\dot{N}}$ is the incoming photon number flux. The quantum equation of motion for the cavity then becomes

$$\dot{\hat{d}} = +g\hat{z} - \frac{\kappa}{2}\hat{d} - \sqrt{\kappa}\hat{\xi}, \tag{E75}$$

where the opto-mechanical coupling constant is proportional to the laser drive amplitude

$$g \equiv 2A\omega_{\rm c}\sqrt{\frac{\overline{\dot{N}}}{\kappa}} = A\omega_{\rm c}\sqrt{\bar{n}}. \tag{E76}$$

and

$$\bar{n} = |\bar{a}|^2 = 4\frac{\overline{\dot{N}}}{\kappa} \tag{E77}$$

is the mean cavity photon number. Eq. (E75) is easily solved by Fourier transformation

$$\hat{d}[\omega] = \frac{1}{[\kappa/2 - i\omega]}\left\{g\hat{z}[\omega] - \sqrt{\kappa}\hat{\xi}[\omega]\right\}. \tag{E78}$$

Let us assume that we are in the limit of low mechanical frequency relative to the cavity damping, $\Omega \ll \kappa$, so that the cavity state adiabatically follows the motion of the mechanical oscillator. Then we obtain to a good approximation

$$\hat{d}[\omega] = \frac{2}{\kappa}\left\{g\hat{z}[\omega] - \sqrt{\kappa}\hat{\xi}[\omega]\right\} \tag{E79}$$

$$\hat{d}^\dagger[\omega] = \frac{2}{\kappa}\left\{g\hat{z}[\omega] - \sqrt{\kappa}\hat{\xi}^\dagger[\omega]\right\} \tag{E80}$$

The mechanical oscillator equation of motion which is identical in form to that of the optical cavity

$$\partial_t \hat{c} = -[\frac{\gamma_0}{2} + i\Omega]\hat{c} - \sqrt{\gamma_0}\hat{\eta}(t) + \frac{i}{\hbar}[\hat{H}_{\rm int}, \hat{c}(t)], \quad \text{(E81)}$$

where $\hat{H}_{\rm int}$ is the Hamiltonian in Eq. (E1) and $\hat{\eta}$ is the mechanical vacuum noise from the (zero temperature) bath which is causing the mechanical damping at rate γ_0. Using Eq. (E70) and expanding to first order in small fluctuations yields the equation of motion linearized about the steady state solution

$$\partial_t \hat{c} = -[\frac{\gamma_0}{2} + i\Omega]\hat{c} - \sqrt{\gamma_0}\hat{\eta}(t) + 2\frac{g}{\sqrt{\kappa}}[\hat{\xi}(t) - \hat{\xi}^\dagger(t)]. \quad \text{(E82)}$$

It is useful to consider an equivalent formulation in which we expand the Hamiltonian in Eq. (E1) to second order in the quantum fluctuations about the classical solution

$$\hat{H}_{\rm int} \approx \hbar\omega_{\rm c}\hat{d}^\dagger\hat{d} + \hat{x}\hat{F}, \quad \text{(E83)}$$

where the force (including the coupling A) is (up to a sign)

$$\hat{F} = -i\frac{\hbar g}{x_{\rm ZPF}}[\hat{d} - \hat{d}^\dagger]. \quad \text{(E84)}$$

Note that the radiation pressure fluctuations (photon shot noise) inside the cavity provide a forcing term. The state of the field inside the cavity in general depends on the past history of the cantilever position. However for this special case of driving the cavity on resonance, the dependence of the cavity field on the cantilever history is such that the latter drops out of the radiation pressure. To see this explicitly, consider the equation of motion for the force obtained from Eq. (E75)

$$\dot{\hat{F}} = -\frac{\kappa}{2}\hat{F} + i\frac{\hbar g}{x_{\rm ZPF}}\sqrt{\kappa}[\hat{\xi} - \hat{\xi}^\dagger]. \quad \text{(E85)}$$

Within our linearization approximation, the position of the mechanical oscillator has no effect on the radiation pressure (photon number in the cavity), but of course it does affect the *phase* of the cavity field (and hence the outgoing field) which is what we measure in the homodyne detection.

Thus for this special case $\hat{z}$ does not appear on the RHS of either Eq. (E85) or Eq. (E82), which means that there is no optical renormalization of the cantilever frequency ('optical spring') or optical damping of the cantilever. The lack of back-action damping in turn implies that the effective temperature $T_{\rm eff}$ of the cavity detector is infinite (cf. Eq. (2.8)). For this special case of zero detuning the back action force noise is controlled by a single quadrature of the incoming vacuum noise (which interferes with the classical drive to produce photon number fluctuations). This is illustrated in the cavity amplitude phasor diagram of Fig. (6). We see that the vacuum noise quadrature $\hat{\xi} + \hat{\xi}^\dagger$ conjugate to $\hat{F}$ controls the

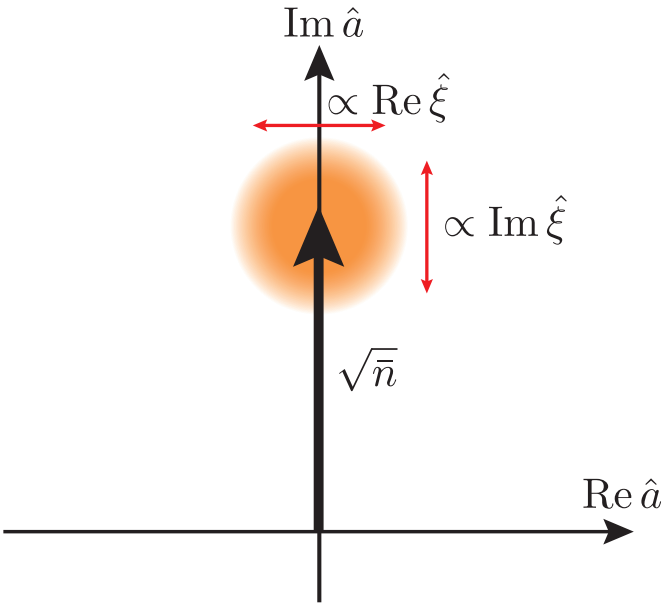

FIG. 6 (Color online) Phasor diagram for the cavity amplitude showing that (for our choice of parameters) the imaginary quadrature of the vacuum noise $\hat{\xi}$ interferes with the classical drive to produce photon number fluctuations while the real quadrature produces phase fluctuations which lead to measurement imprecision. The quantum fluctuations are illustrated in the usual fashion, depicting the Gaussian Wigner density of the coherent state in terms of color intensity.

phase noise which determines the measurement imprecision (shot noise in the homodyne signal). This will be discussed further below.

The solution for the cantilever position can again be obtained by Fourier transformation. For frequencies small on the scale of κ the solution of Eq. (E85) is

$$\hat{F}[\omega] = \frac{2i\hbar g}{x_{\rm ZPF}\sqrt{\kappa}}\left\{\hat{\xi}[\omega] - \hat{\xi}^\dagger[\omega]\right\} \quad \text{(E86)}$$

and hence the back action force noise spectral density is at low frequencies

$$S_{FF}[\omega] = \frac{4\hbar^2 g^2}{x_{\rm ZPF}^2 \kappa} \quad \text{(E87)}$$

in agreement with Eq. (3.18).

Introducing a quantity proportional to the cantilever (mechanical) susceptibility (within the rotating wave approximation we are using)

$$\chi_{\rm M}[\omega - \Omega] \equiv \frac{1}{-i(\omega - \Omega) + \frac{\gamma_0}{2}}, \quad \text{(E88)}$$

we find from Eq. (E82)

$$\hat{z}[\omega] = \hat{z}_0[\omega] - \frac{i}{\hbar}x_{\rm ZPF}\left\{\chi_{\rm M}[\omega - \Omega] - \chi_{\rm M}[\omega + \Omega]\right\}\hat{F}[\omega], \quad \text{(E89)}$$

where the equilibrium fluctuations in position are given by

$$\hat{z}_0[\omega] \equiv -\sqrt{\gamma_0}\left\{\chi_{\rm M}[\omega-\Omega]\hat{\eta}[\omega]+\chi_{\rm M}[\omega+\Omega]\hat{\eta}^\dagger[\omega]\right\}. \tag{E90}$$

We can now obtain the power spectrum S_{zz} describing the total position fluctuations of the cantilever driven by the mechanical vacuum noise plus the radiation pressure shot noise. From Eqs. (E89, E90) we find

$$\begin{aligned}\frac{S_{xx}[\omega]}{x_{\rm ZPF}^2} &= S_{zz}[\omega] \\ &= \gamma_0|\chi[\omega-\Omega]|^2 \\ &\quad +\frac{x_{\rm ZPF}^2}{\hbar^2}\left|\chi_{\rm M}[\omega-\Omega]-\chi_{\rm M}[\omega+\Omega]\right|^2 S_{FF}.\end{aligned} \tag{E91}$$

Note that (assuming high mechanical Q, i.e. $\gamma_0 \ll \Omega$) the equilibrium part has support only at positive frequencies while the back action induced position noise is symmetric in frequency reflecting the effective infinite temperature of the back action noise. Symmetrizing this result with respect to frequency (and using $\gamma_0 \ll \Omega$) we have

$$\bar{S}_{xx}[\omega] \approx \bar{S}^0_{xx}[\omega]\left(1+\frac{\bar{S}^0_{xx}[\Omega]}{\hbar^2}\bar{S}_{FF}\right), \tag{E92}$$

where $\bar{S}^0_{xx}[\omega]$ is the symmetrized spectral density for position fluctuations in the ground state given by Eq. (3.54).

Now that we have obtained the effect of the back action noise on the position fluctuations, we must turn our attention to the imprecision of the measurement due to shot noise in the output. The appropriate homodyne quadrature variable to monitor to be sensitive to the output phase shift caused by position fluctuations is

$$\hat{I} = \hat{b}_{\rm out}+\hat{b}^\dagger_{\rm out}, \tag{E93}$$

which, using the input-output results above, can be written

$$\hat{I} = -(\hat{\xi}+\hat{\xi}^\dagger)+\lambda\hat{x}. \tag{E94}$$

We see that the cavity homodyne detector system acts as a position transducer with gain

$$\lambda = \frac{4g}{x_{\rm ZPF}\sqrt{\kappa}}. \tag{E95}$$

The first term in Eq. (E94) represents the vacuum noise that mixes with the homodyne local oscillator to produce the shot noise in the output. The resulting measurement imprecision (symmetrized) spectral density referred back to the position of the oscillator is

$$\bar{S}^{\rm I}_{xx} = \frac{1}{\lambda^2}. \tag{E96}$$

Comparing this to Eq. (E87) we see that we reach the quantum limit relating the imprecision noise to the back action noise

$$\bar{S}^{\rm I}_{xx}\bar{S}_{FF} = \frac{\hbar^2}{4} \tag{E97}$$

in agreement with Eq. (3.10).

Notice also from Eq. (E94) that the quadrature of the vacuum noise which leads to the measurement imprecision is conjugate to the one which produces the back action force noise as illustrated previously in Fig. (6). Recall that the two quadratures of motion of a harmonic oscillator in its ground state have no classical (i.e., symmetrized) correlation. Hence the symmetrized cross correlator

$$\bar{S}_{IF}[\omega] = 0 \tag{E98}$$

vanishes. Because there is no correlation between the output imprecision noise and the forces controlling the position fluctuations, the total output noise referred back to the position of the oscillator is simply

$$\begin{aligned}\bar{S}_{xx,{\rm tot}}[\omega] &= \bar{S}_{xx}[\omega]+\bar{S}^{\rm I}_{xx} \\ &= \bar{S}^0_{xx}[\omega]\left(1+\frac{\bar{S}^0_{xx}[\Omega]}{\hbar^2}\bar{S}_{FF}\right)+\frac{\hbar^2}{4\bar{S}_{FF}}.\end{aligned} \tag{E99}$$

This expression again clearly illustrates the competition between the back action noise proportional to the drive laser intensity and the measurement imprecision noise which is inversely proportional. We again emphasize that all of the above relations are particular to the case of zero detuning of the cavity drive field from the cavity.

The total output noise at some particular frequency will be a minimum at some optimal drive intensity. The precise optimal value depends on the frequency chosen. Typically this is taken to be the mechanical resonance frequency where we find that the optimal coupling leads to an optimal back action noise

$$\bar{S}_{FF,{\rm opt}} = \frac{\hbar^2}{2\bar{S}^0_{xx}[\Omega]} = \frac{\hbar^2\gamma_0}{4x^2_{\rm ZPF}}. \tag{E100}$$

This makes sense because the higher the damping the less susceptible the oscillator is to back action forces. At this optimal coupling the total output noise spectral density at frequency Ω referred to the position is simply twice the vacuum value

$$\bar{S}_{xx,{\rm tot}}[\Omega] = 2\bar{S}^0_{xx}[\Omega], \tag{E101}$$

in agreement with Eq. (3.62). Evaluation of Eq. (E100) at the optimal coupling yields the graph shown in Fig. (6). The background noise floor is due to the frequency independent imprecision noise with value $\frac{1}{2}\bar{S}^0_{xx}[\Omega]$. The peak value at $\omega=\Omega$ rises a factor of three above this background.

We derived the gain λ in Eq. (E95) by direct solution of the equations of motion. With the results we have derived above, it is straightforward to show that the Kubo formula in Eq. (4.3) yields equivalent results. We have already seen that the classical (i.e. symmetrized) correlations between the output signal $\hat{I}$ and the force $\hat{F}$ which couples to the position vanishes. However the Kubo formula evaluates the *quantum* (i.e. antisymmetric) correlations for the uncoupled system ($A = g = 0$). Hence we have

$$\chi_{IF}(t) = -\frac{i}{\hbar}\theta(t)\left\langle\left[-\big(\hat{\xi}(t-\delta t)+\hat{\xi}^\dagger(t-\delta t)\big), \frac{2i\hbar g}{x_{\rm ZPF}\sqrt{\kappa}}\big(\hat{\xi}(0)-\hat{\xi}^\dagger(0)\big)\right]\right\rangle_0, \tag{E102}$$

where δt is a small (positive) time representing the delay between the time when the vacuum noise impinges on the cavity and when the resulting outgoing wave reaches the homodyne detector. (More precisely it also compensates for certain small retardation effects neglected in the limit $\omega \ll \kappa$ used in several places in the above derivations.) Using the fact that the commutator between the two quadratures of the vacuum noise is a delta function, Fourier transformation of the above yields (in the limit $\omega\,\delta t \ll 1$ the desired result

$$\chi_{IF}[\omega] = \lambda. \tag{E103}$$

Similarly we readily find that the small retardation causes the reverse gain to vanish. Hence all our results are consistent with the requirements needed to reach the standard quantum limit.

Thus with this study of the specific case of an oscillator parametrically coupled to a cavity, we have reproduced all of the key results in Sec. V.E derived from completely general considerations of linear response theory.

4. Back-action free single-quadrature detection

We now provide details on the cavity single-quadrature detection scheme discussed in Sec. V.H.2. We again consider a high-Q cavity whose resonance frequency is modulated by a high-Q mechanical oscillator with co-ordinate $\hat{x}$ (cf. Eqs. (E1) and (E64)). To use this system for amplification of a single quadrature, we will consider the typical case of a fast cavity ($\omega_{\rm c} \gg \Omega$), and take the "good cavity" limit, where $\Omega \gg \kappa$. As explained in the main text, the crucial ingredient for single-quadrature detection is to take an amplitude-modulated cavity drive described by the classical input field $\bar{b}_{\rm in}$ given in Eq. (5.101). As before (cf. Eq. (E4)), we may write the cavity annihilation operator $\hat{a}$ as the sum of a classical piece $\bar{a}(t)$ and a quantum piece $\hat{d}$; only $\hat{d}$ is influenced by the mechanical oscillator. $\bar{a}(t)$ is easily found from the classical (noise-free) equations of motion for the isolated cavity; making use of the conditions $\omega_{\rm c} \gg \Omega \gg \kappa$, we have

$$\bar{a}(t) \;\simeq\; \frac{\sqrt{\dot{N}\kappa}}{2\Omega}\cos(\Omega t+\delta)\, e^{-i\omega_c t} \tag{E104}$$

To proceed with our analysis, we work in an interaction picture with respect to the uncoupled cavity and oscillator Hamiltonians. Making standard rotating-wave approximations, the Hamiltonian in the interaction picture takes the simple form corresponding to Eq. (5.102b):

$$\begin{aligned} H_{\rm int} &= \hbar\tilde{A}\left(\hat{d}+\hat{d}^\dagger\right)\left(e^{i\delta}\hat{c}+e^{-i\delta}\hat{c}^\dagger\right) \\ &= \hbar\tilde{A}\left(\hat{d}+\hat{d}^\dagger\right)\frac{\hat{X}_\delta}{x_{\rm ZPF}}, \end{aligned} \tag{E105}$$

where

$$\tilde{A} \;=\; A\cdot\omega_{\rm c}\frac{\sqrt{\dot{N}\kappa}}{4\Omega}, \tag{E106}$$

and in the second line, we have made use of the definition of the quadrature operators $\hat{X}_\delta, \hat{Y}_\delta$ given in Eqs. (5.92). The form of $H_{\rm int}$ was discussed heuristically in the main text in terms of Raman processes where photons are removed from the classical drive $\bar{b}_{\rm in}$ and either up or down converted to the cavity frequency via absorption or emission of a mechanical phonon. Alternatively, we can think of the drive yielding a time-dependent cavity-oscillator coupling which "follows" the X_δ quadrature. Note that we made crucial of use of the good cavity limit ($\kappa \ll \Omega$) to drop terms in $\hat{H}_{int}$ which oscillate at frequencies $\pm 2\Omega$. These terms represent Raman sidebands which are away from the cavity resonance by a distance $\pm 2\Omega$. In the good cavity limit, the density of photon states is negligible so far off resonance and these processes are suppressed.

Similar to Eqs. (E39) and (E81), the Heisenberg equations of motion (in the rotating frame) follow directly from $H_{\rm int}$ and the dissipative terms in the total Hamiltonian:

$$\partial_t\hat{d} \;=\; -\frac{\kappa}{2}\hat{d} - \sqrt{\kappa}\hat{\xi}(t)e^{i\omega_{\rm c}t} - i\tilde{A}\left(e^{i\delta}\hat{c}+e^{-i\delta}\hat{c}^\dagger\right) \tag{E107a}$$

$$\partial_t\hat{c} \;=\; -\frac{\gamma_0}{2}\hat{c} - \sqrt{\gamma_0}\hat{\eta}(t)e^{i\Omega t} - ie^{-i\delta}\left[\tilde{A}\left(\hat{d}+\hat{d}^\dagger\right) - f(t)\right] \tag{E107b}$$

As before, $\hat{\xi}(t)$ represents the unavoidable noise in the cavity drive, and $\hat{\eta}(t)$, γ_0 are the noisy force and damping resulting from an equilibrium bath coupled to the mechanical oscillator. Note from Eq. (E107a) that as anticipated, the cavity is only driven by one quadrature of the oscillator's motion. We have also included a driving force $F(t)$ on the mechanical oscillator which has some narrow bandwidth centered on the oscillator frequency; this force is parameterized as:

$$F(t) = \frac{2\hbar}{x_{\rm ZPF}}{\rm Re}\left[f(t)e^{-i\Omega t}e^{-i\delta}\right] \tag{E108}$$

where $f(t)$ is a complex function which is slowly varying on the scale of an oscillator period.

The equations of motion are easily solved upon Fourier transformation, resulting in:

$$\hat{X}_\delta[\omega] = -x_{\rm ZPF}\cdot\chi_M[\omega]\Big[i\left(f^*[-\omega]-f[\omega]\right) + \sqrt{\gamma_0}\left(e^{i\delta}\hat{\eta}(\omega+\Omega)+e^{-i\delta}\hat{\eta}^\dagger(\omega-\Omega)\right)\Big] \quad \text{(E109a)}$$

$$\hat{Y}_\delta[\omega] = ix_{\rm ZPF}\cdot\chi_M[\omega]\Big[(-i)\left(f[\omega]+f^*[-\omega]\right) + \sqrt{\gamma_0}\left(e^{i\delta}\hat{\eta}(\omega+\Omega)-e^{-i\delta}\hat{\eta}^\dagger(\omega-\Omega)\right) - 2i\tilde{A}\chi_{\rm c}[\omega]\sqrt{\kappa}\left(\hat{\xi}(\omega+\omega_{\rm c})+\hat{\xi}^\dagger(\omega-\omega_{\rm c})\right)\Big] \quad \text{(E109b)}$$

where the cavity and mechanical susceptibilities $\chi_{\rm c}, \chi_{\rm M}$ are defined in Eqs. (E43) and (E88).

As anticipated, the detected quadrature $\hat{X}_\delta$ is *completely* unaffected by the measurement: Eq. (E109a) is identical to what we would have if there were no coupling between the oscillator and the cavity. In contrast, the conjugate quadrature $\hat{Y}_\delta$ experiences an extra stochastic force due to the cavity: this is the measurement back-action.

Turning now to the output field from the cavity $\hat{b}_{\rm out}$, we use the input-output relation Eq. (E37) to find in the *lab* (i.e. non-rotating) frame:

$$\hat{b}_{\rm out}[\omega] = \bar{b}_{\rm out}[\omega] + \left[\frac{-i(\omega-\omega_{\rm c})-\kappa/2}{-i(\omega-\omega_{\rm c})+\kappa/2}\right]\hat{\xi}[\omega] - i\frac{\tilde{A}\sqrt{\kappa}}{x_{\rm ZPF}}\chi_{\rm c}[\omega-\omega_{\rm c}]\cdot\hat{X}_\delta(\omega-\omega_{\rm c}) \quad \text{(E110)}$$

The first term on the RHS simply represents the output field from the cavity in the absence of the mechanical oscillator and any fluctuations. It will yield sharp peaks at the two sidebands associated with the drive, $\omega=\omega_{\rm c}\pm\Omega$. The second term on the RHS of Eq. (E110) represents the reflected noise of the incident cavity drive. This noise will play the role of the "intrinsic ouput noise" of this amplifier.

Finally, the last term on the RHS of Eq. (E110) is the amplified signal: it is simply the amplified quadrature $\hat{X}_\delta$ of the oscillator. This term will result in a peak in the output spectrum at the resonance frequency of the cavity, $\omega_{\rm c}$. As there is no back-action on the measured $\hat{X}_\delta$ quadrature, the added noise can be made arbitrarily small by simply increasing the drive strength $\dot{N}$ (and hence $\tilde{A}$).

Appendix F: Information Theory and Measurement Rate

Suppose that we are measuring the state of a qubit via the phase shift $\pm\theta_0$ from a one-sided cavity. Let $I(t)$ be the homodyne signal integrated up to time t as in Sec. III.B. We would like to understand the relationship between the signal-to-noise ratio defined in Eq. (3.23), and the rate at which information about the state of the qubit is being gained. The probability distribution for I conditioned on the state of the qubit $\sigma=\pm1$ is

$$p(I|\sigma) = \frac{1}{\sqrt{2\pi S_{\theta\theta}t}}\exp\left[\frac{-(I-\sigma\theta_0 t)^2}{2S_{\theta\theta}t}\right]. \quad \text{(F1)}$$

Based on knowledge of this conditional distribution, we now present two distinct but equivalent approaches to giving an information theoretic basis for the definition of the measurement rate.

1. Method I

Suppose we start with an initial qubit density matrix

$$\rho_0 = \begin{pmatrix} \frac{1}{2} & 0 \\ 0 & \frac{1}{2}\end{pmatrix}. \quad \text{(F2)}$$

After measuring for a time t, the new density matrix conditioned on the results of the measurement is

$$\rho_1 = \begin{pmatrix} p_+ & 0 \\ 0 & p_-\end{pmatrix} \quad \text{(F3)}$$

where it will be convenient to parameterize the two probabilities by the polarization $m\equiv{\rm Tr}(\sigma_z\rho_1)$ by

$$\mathbf{p}_\pm = \frac{1\pm m}{2}. \quad \text{(F4)}$$

The information gained by the measurement is the entropy loss[7] of the qubit

$$\mathcal{I} = {\rm Tr}(\rho_1\ln\rho_1-\rho_0\ln\rho_0). \quad \text{(F5)}$$

We are interested in the initial rate of gain of information at short times $\theta_0^2 t\ll S_{\theta\theta}$ where m will be small. In this limit we have

$$\mathcal{I}\approx\frac{m^2}{2}. \quad \text{(F6)}$$

We must now calculate m conditioned on the measurement result I

$$m_I\equiv\sum_\sigma\sigma p(\sigma|I). \quad \text{(F7)}$$

From Bayes theorem we can express this in terms of $p(I|\sigma)$, which is the quantity we know,

$$p(\sigma|I) = \frac{p(I|\sigma)p(\sigma)}{\sum_{\sigma'}p(I|\sigma')p(\sigma')}. \quad \text{(F8)}$$

[7] It is important to note that we use throughout here the physicist's entropy with the natural logarithm rather than the log base 2 which gives the information in units of bits.

Using Eq. (F1) the polarization is easily evaluated

$$m_I = \tanh\left(\frac{I\theta_0}{S_{\theta\theta}}\right). \tag{F9}$$

The information gain is thus

$$\mathcal{I}_I = \frac{1}{2}\tanh^2\left(\frac{I\theta_0}{S_{\theta\theta}}\right) \approx \frac{I^2}{2}\left(\frac{\theta_0}{S_{\theta\theta}}\right)^2 \tag{F10}$$

where the second equality is only valid for small $|m|$. Ensemble averaging this over all possible measurement results yields the mean information gain at short times

$$\mathcal{I} \approx \frac{1}{2}\frac{\theta_0^2}{S_{\theta\theta}}t \tag{F11}$$

which justifies the definition of the measurement rate given in Eq. (3.24).

2. Method II

An alternative information theoretic derivation is to consider the qubit plus measurement device to be a signaling channel. The two possible inputs to the channel are the two states of the qubit. The output of the channel is the result of the measurement of I. By toggling the qubit state back and forth, one can send information through the signal channel to another party. The channel is noisy because even for a fixed state of the qubit, the measured values of the signal I have intrinsic fluctuations. Shannon's noisy channel coding theorem (Cover and Thomas, 1991) tells us the maximum rate at which information can be reliably sent down the channel by toggling the state of the qubit and making measurements of I. It is natural to take this rate as defining the measurement rate for our detector.

The reliable information gain by the receiver on a noisy channel is a quantity known as the 'mutual information' of the communication channel (Clerk *et al.*, 2003; Cover and Thomas, 1991)

$$R = -\int_{-\infty}^{+\infty} dI \left\{ p(I)\ln p(I) - \sum_\sigma p(\sigma)\left[p(I|\sigma)\ln p(I|\sigma)\right]\right\} \tag{F12}$$

The first term is the Shannon entropy in the signal I when we do not know the input signal (the value of the qubit). The second term represents the entropy given that we do know the value of the qubit (averaged over the two possible input values). Thus the first term is signal plus noise, the second is just the noise. Subtracting the two gives the net information gain. Expanding this expression for short times yields

$$\begin{aligned} R &= \frac{1}{8}\frac{(\langle I(t)\rangle_+ - \langle I(t)\rangle_-)^2}{S_{\theta\theta}t} \\ &= \frac{\theta_0^2}{2S_{\theta\theta}}t \\ &= \Gamma_{\rm meas}t \end{aligned} \tag{F13}$$

exactly the same result as Eq. (F11). (Here $\langle I(t)\rangle_\sigma$ is the mean value of I given that the qubit is in state σ.)

Appendix G: Number Phase Uncertainty

In this appendix, we briefly review the number-phase uncertainty relation, and from it we derive the relationship between the spectral densities describing the photon number fluctuations and the phase fluctuations. Consider a coherent state labeled by its classical amplitude α

$$|\alpha\rangle = \exp\left\{-\frac{|\alpha|^2}{2}\right\}\exp\{\alpha\hat{a}^\dagger\}|0\rangle. \tag{G1}$$

This is an eigenstate of the destruction operator

$$\hat{a}|\alpha\rangle = \alpha|\alpha\rangle. \tag{G2}$$

It is convenient to make the unitary displacement transformation which maps the coherent state onto a new vacuum state and the destruction operator onto

$$\hat{a} = \alpha + \hat{d} \tag{G3}$$

where d annihilates the new vacuum. Then we have

$$\bar{N} = \langle\hat{N}\rangle = \langle 0|(\alpha^* + \hat{d}^\dagger)(\alpha + \hat{d})|0\rangle = |\alpha|^2, \tag{G4}$$

and

$$(\Delta N)^2 = \langle(\hat{N} - \bar{N})^2\rangle = |\alpha|^2\langle 0|\hat{d}\hat{d}^\dagger|0\rangle = \bar{N}. \tag{G5}$$

Now define the two quadrature amplitudes

$$\hat{X} = \frac{1}{\sqrt{2}}(\hat{a} + \hat{a}^\dagger) \tag{G6}$$

$$\hat{Y} = \frac{i}{\sqrt{2}}(\hat{a}^\dagger - \hat{a}). \tag{G7}$$

Each of these amplitudes can be measured in a homodyne experiment. For convenience, let us take α to be real and positive. Then

$$\langle\hat{X}\rangle = \sqrt{2}\alpha \tag{G8}$$

and

$$\langle\hat{Y}\rangle = 0. \tag{G9}$$

If the phase of this wave undergoes a small modulation due for example to weak parametric coupling to a qubit then one can estimate the phase by

$$\langle\theta\rangle = \frac{\langle\hat{Y}\rangle}{\langle\hat{X}\rangle}. \tag{G10}$$

This result is of course only valid for small angles, $\theta \ll 1$. For $\bar{N} \gg 1$, the uncertainty will be

$$(\Delta\theta)^2 = \frac{\langle\hat{Y}^2\rangle}{(\langle\hat{X}\rangle)^2} = \frac{\frac{1}{2}\langle 0|\hat{d}\hat{d}^\dagger|0\rangle}{2\bar{N}} = \frac{1}{4\bar{N}}. \tag{G11}$$

Thus using Eq. (G5) we arrive at the fundamental quantum uncertainty relation

$$\Delta\theta\Delta N = \frac{1}{2}. \tag{G12}$$

Using the input-output theory described in Appendix E we can restate the results above in terms of noise spectral densities. Let the amplitude of the field coming in to the homodyne detector be

$$\hat{b}_{\rm in} = \bar{b}_{\rm in} + \hat{\xi}(t) \tag{G13}$$

where $\hat{\xi}(t)$ is the vacuum noise obeying

$$[\hat{\xi}(t), \hat{\xi}^\dagger(t')] = \delta(t-t'). \tag{G14}$$

We are using a flux normalization for the field operators so

$$\overline{\dot{N}} = \langle \hat{b}^\dagger_{\rm in}\hat{b}_{\rm in}\rangle = |\bar{b}_{\rm in}|^2 \tag{G15}$$

and

$$\langle \dot{N}(t)\dot{N}(0)\rangle - \overline{\dot{N}}^2 = \langle 0|(\bar{b}^*_{\rm in}+\hat{\xi}^\dagger(t))(\bar{b}_{\rm in}+\hat{\xi}(t))(\bar{b}^*_{\rm in}+\hat{\xi}^\dagger(0))(\bar{b}_{\rm in}+\hat{\xi}(0))|0\rangle - \left|\bar{b}_{\rm in}\right|^4 = \overline{\dot{N}}\delta(t). \tag{G16}$$

From this it follows that the shot noise spectral density is

$$S_{\dot{N}\dot{N}} = \overline{\dot{N}}. \tag{G17}$$

Similarly the phase can be estimated from the quadrature operator

$$\hat{\theta} = \frac{i(\hat{b}^\dagger_{\rm in} - \hat{b}_{\rm in})}{\langle \hat{b}^\dagger_{\rm in} + \hat{b}_{\rm in}\rangle} = \langle\hat{\theta}\rangle + i\frac{(\hat{\xi}^\dagger - \hat{\xi})}{2\bar{b}_{\rm in}} \tag{G18}$$

which has noise correlator

$$\langle \delta\hat{\theta}(t)\delta\hat{\theta}(0)\rangle = \frac{1}{4\overline{\dot{N}}}\delta(t) \tag{G19}$$

corresponding to the phase imprecision spectral density

$$S_{\theta\theta} = \frac{1}{4\overline{\dot{N}}}. \tag{G20}$$

We thus arrive at the fundamental quantum limit relation

$$\sqrt{S_{\theta\theta}S_{\dot{N}\dot{N}}} = \frac{1}{2}. \tag{G21}$$

Appendix H: Using feedback to reach the quantum limit

In Sec. (VI.B), we demonstrated that any two port amplifier whose scattering matrix has $s_{11} = s_{22} = s_{12} = 0$ will fail to reach quantum limit when used as a weakly coupled op-amp; at best, it will miss optimizing the quantum noise constraint of Eq. (5.88) by a factor of two. Reaching the quantum limit thus requires at least one of s_{11}, s_{22} and s_{12} to be non-zero. In this subsection, we demonstrate how this may be done. We show that by introducing a form of negative feedback to the "minimal" amplifier of the previous subsection, one can take advantage of noise correlations to reduce the back-action current noise S_{II} by a factor of two. As a result, one is able to reach the weak-coupling (i.e. op-amp) quantum limit. Note that quantum amplifiers with feedback are also treated in Courty *et al.* (1999); Grassia (1998).

On a heuristic level, we can understand the need for either reflections or reverse gain to reach the quantum limit. A problem with the "minimal" amplifier of the last subsection was that its input impedance was too low in comparison to its noise impedance $Z_{\rm N} \sim Z_a$. From general expression for the input impedance, Eq. (6.7d), we see that having non-zero reverse gain (i.e. $s_{12} \neq 0$) and/or non-zero reflections (i.e. $s_{11} \neq 0$ and/or $s_{22} \neq 0$) could lead to $Z_{\rm in} \gg Z_a$. This is exactly what occurs when feedback is used to reach the quantum limit. Keep in mind that having non-vanishing reverse gain is dangerous: as we discussed earlier, an appreciable non-zero λ'_I can lead to the highly undesirable consequence that the amplifier's input impedance depends on the impedance of the load connected to its output (cf. Eq. (6.6)).

1. Feedback using mirrors

To introduce reverse gain and reflections into the "minimal" two-port bosonic amplifier of the previous subsection, we will insert mirrors in three of the four arms leading from the circulator: the arm going to the input line, the arm going to the output line, and the arm going to the auxiliary "cold load" (Fig. 7). Equivalently, one could imagine that each of these lines is not perfectly impedance matched to the circulator. Each mirror will be described by a 2×2 unitary scattering matrix:

$$\begin{pmatrix} \hat{a}_{j,\rm out} \\ \hat{b}_{j,\rm out}\end{pmatrix} = U_j \cdot \begin{pmatrix} \hat{b}_{j,\rm in} \\ \hat{a}_{j,\rm in}\end{pmatrix} \tag{H1}$$

$$U_j = \begin{pmatrix} \cos\theta_j & -\sin\theta_j \\ \sin\theta_j & \cos\theta_j\end{pmatrix} \tag{H2}$$

Here, the index j can take on three values: $j = z$ for the mirror in the input line, $j = y$ for the mirror in the arm

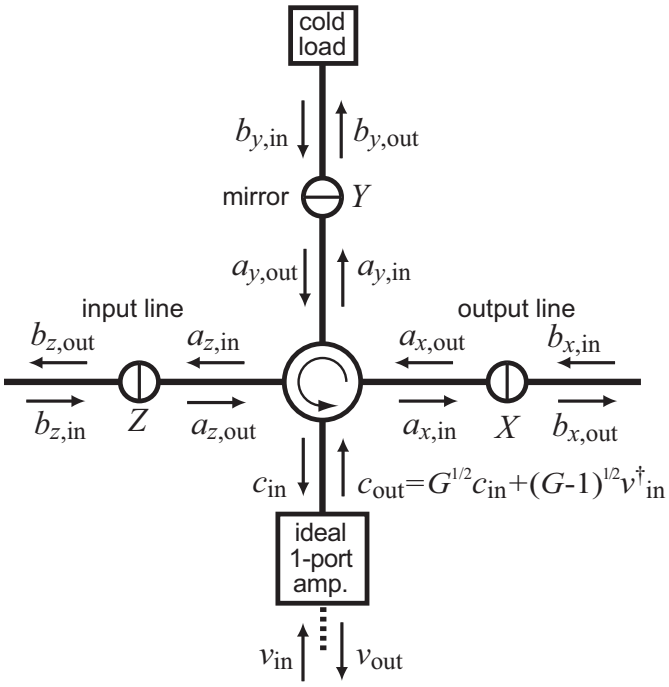

FIG. 7 Schematic of a modified minimal two-port amplifier, where partially reflecting mirrors have been inserted in the input and output transmission lines, as well as in the line leading to the cold load. By tuning the reflection coefficient of the mirror in the cold load arm (mirror Y), we can induce negative feedback which takes advantage of correlations between current and voltage noise. This then allows this system to reach the quantum limit as a weakly coupled voltage op amp. See text for further description

going to the cold load, and $j = x$ for the mirror in the output line. The mode a_j describes the "internal" mode which exists between the mirror and circulator, while the mode b_j describes the "external" mode on the other side of the mirror. We have taken the U_j to be real for convenience. Note that $\theta_j = 0$ corresponds to the case of no mirror (i.e. perfect transmission).

It is now a straightforward though tedious exercise to construct the scattering matrix for the entire system. From this, one can identify the reduced scattering matrix s appearing in Eq. (6.3), as well as the noise operators $\mathcal{F}_j$. These may then in turn be used to obtain the op-amp description of the amplifier, as well as the commutators of the added noise operators. These latter commutators determine the usual noise spectral densities of the amplifier. Details and intermediate steps of these calculations may be found in Appendix I.6.

As usual, to see if our amplifier can reach the quantum limit when used as a (weakly-coupled) op-amp , we need to see if it optimizes the quantum noise constraint of Eq. (5.88). We consider the optimal situation where both the auxiliary modes of the amplifier ($\hat{u}_{\text{in}}$ and $\hat{v}^{\dagger}_{\text{in}}$) are in the vacuum state. The surprising upshot of our analysis (see Appendix I.6) is the following: *if we include a small amount of reflection in the cold load line with the correct phase, then we can reach the quantum limit, irrespective of the mirrors in the input and output lines.* In particular, if $\sin\theta_y = -1/\sqrt{G}$, our amplifier optimizes the quantum noise constraint of Eq. (5.88) in the large gain (i.e. large G) limit, independently of the values of θ_x and θ_y. Note that tuning θ_y to reach the quantum limit does not have a catastrophic impact on other features of our amplifier. One can verify that this tuning only causes the voltage gain λ_V and power gain G_P to decrease by a factor of two compared to their $\theta_y = 0$ values (cf. Eqs. (I60) and (I64)). This choice for θ_y also leads to $Z_{\text{in}} \gg Z_a \sim Z_{\text{N}}$ (cf. (I62)), in keeping with our general expectations.

Physically, what does this precise tuning of θ_y correspond to? A strong hint is given by the behaviour of the amplifier's cross-correlation noise $\bar{S}_{VI}[\omega]$ (cf. Eq. (I65c)). In general, we find that $\bar{S}_{VI}[\omega]$ is real and non-zero. However, the tuning $\sin\theta_y = -1/\sqrt{G}$ *is exactly what is needed to have* $\bar{S}_{VI}$ *vanish.* Also note from Eq. (I65a) that this special tuning of θ_y decreases the back-action current noise precisely by a factor of two compared to its value at $\theta_y = 0$. A clear physical explanation now emerges. Our original, reflection-free amplifier had correlations between its back-action current noise and output voltage noise (cf. Eq. (6.18c)). By introducing negative feedback of the output voltage to the input current (i.e. via a mirror in the cold-load arm), we are able to use these correlations to decrease the overall magnitude of the current noise (i.e. the voltage fluctuations $\tilde{V}$ partially cancel the original current fluctuations $\tilde{I}$). For an optimal feedback (i.e. optimal choice of θ_y), the current noise is reduced by a half, and the new current noise is not correlated with the output voltage noise. Note that this is indeed negative (as opposed to positive) feedback– it results in a reduction of both the gain and the power gain. To make this explicit, in the next section we will map the amplifier described here onto a standard op-amp with negative voltage feedback.

2. Explicit examples

To obtain a more complete insight, it is useful to go back and consider what the reduced scattering matrix of our system looks like when θ_y has been tuned to reach the quantum limit. From Eq. (I58), it is easy to see that at the quantum limit, the matrix s satisfies:

$$s_{11} = -s_{22} \tag{H3a}$$

$$s_{12} = \frac{1}{G} s_{21} \tag{H3b}$$

The second equation also carries over to the op-amp picture; at the quantum limit, one has:

$$\lambda'_I = \frac{1}{G}\lambda_V \tag{H4}$$

One particularly simple limit is the case where there are no mirrors in the input and output line ($\theta_x = \theta_z = 0$),

only a mirror in the cold-load arm. When this mirror is tuned to reach the quantum limit (i.e. $\sin\theta_y = -1/\sqrt{G}$), the scattering matrix takes the simple form:

$$s \;=\; \begin{pmatrix} 0 & 1/\sqrt{G} \\ \sqrt{G} & 0 \end{pmatrix} \tag{H5}$$

In this case, the principal effect of the weak mirror in the cold-load line is to introduce a small amount of reverse gain. The amount of this reverse gain is exactly what is needed to have the input impedance diverge (cf. Eq. (6.7d)). It is also what is needed to achieve an optimal, noise-canceling feedback in the amplifier. To see this last point explicitly, we can re-write the amplifier's back-action current noise ($\tilde{I}$) in terms of its original noises $\tilde{I}_0$ and $\tilde{V}_0$ (i.e. what the noise operators would have been in the absence of the mirror). Taking the relevant limit of small reflection (i.e. $\tilde{r} \equiv \sin\theta_y$ goes to zero as $|G| \to \infty$), we find that the modification of the current noise operator is given by:

$$\tilde{I} \;\simeq\; \tilde{I}_0 + \frac{2\sqrt{G}\tilde{r}}{1-\sqrt{G}\tilde{r}}\frac{\tilde{V}_0}{Z_a} \tag{H6}$$

As claimed, the presence of a small amount of reflection $\tilde{r} \equiv \sin\theta_y$ in the cold load arm "feeds-back" the original voltage noise of the amplifier $\tilde{V}_0$ into the current. The choice $\tilde{r} = -1/\sqrt{G}$ corresponds to a negative feedback, and optimally makes use of the fact that $\tilde{I}_0$ and $\tilde{V}_0$ are correlated to reduce the overall fluctuations in $\tilde{I}$.

While it is interesting to note that one can reach the quantum limit with no reflections in the input and output arms, this case is not really of practical interest. The reverse current gain in this case may be small (i.e. $\lambda_I' \propto 1/\sqrt{G}$), but it is not small enough: one finds that because of the non-zero λ_I', the amplifier's input impedance is strongly reduced in the presence of a load (cf. Eq. (6.6)).

There is a second simple limit we can consider which is more practical. This is the limit where reflections in the input-line mirror and output-line mirror are both strong. Imagine we take $\theta_z = -\theta_x = \pi/2 - \delta/G^{1/8}$. If again we set $\sin\theta_y = -1/\sqrt{G}$ to reach the quantum limit, the scattering matrix now takes the form (neglecting terms which are order $1/\sqrt{G}$):

$$s \;=\; \begin{pmatrix} +1 & 0 \\ \frac{\delta^2 G^{1/4}}{2} & -1 \end{pmatrix} \tag{H7}$$

In this case, we see that at the quantum limit, the reflection coefficients s_{11} and s_{22} are exactly what is needed to have the input impedance diverge, while the reverse gain coefficient s_{12} plays no role. For this case of strong reflections in input and output arms, the voltage gain is reduced compared to its zero-reflection value:

$$\lambda_V \to \sqrt{\frac{Z_b}{Z_a}}\left(\frac{\delta}{2}\right)^2 G^{1/4} \tag{H8}$$

The power gain however is independent of θ_x, θ_z, and is still given by $G/2$ when θ_y is tuned to be at the quantum limit.

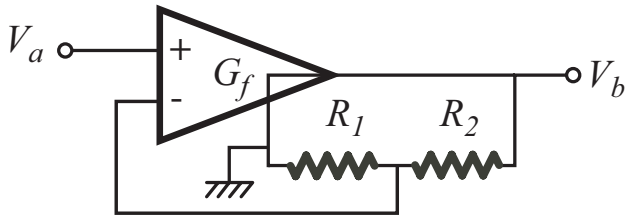

FIG. 8 Schematic of a voltage op-amp with negative feedback.

3. Op-amp with negative voltage feedback

We now show that a conventional op-amp with feedback can be mapped onto the amplifier described in the previous subsection. We will show that tuning the strength of the feedback in the op-amp corresponds to tuning the strength of the mirrors, and that an optimally tuned feedback circuit lets one reach the quantum limit. This is in complete correspondence to the previous subsection, where an optimal tuning of the mirrors also lets one reach the quantum limit.

More precisely, we consider a scattering description of a non-inverting op-amp amplifier having negative voltage feedback. The circuit for this system is shown in Fig. 8. A fraction B of the output voltage of the amplifier is fed back to the negative input terminal of the op-amp. In practice, B is determined by the two resistors R_1 and R_2 used to form a voltage divider at the op-amp output. The op-amp with zero feedback is described by the "ideal" amplifier of Sec. VI.B: at zero feedback, it is described by Eqs. (6.11a)- (6.11d). For simplicity, we consider the relevant case where:

$$Z_b \ll R_1, R_2 \ll Z_a \tag{H9}$$

In this limit, R_1 and R_2 only play a role through the feedback fraction B, which is given by:

$$B = \frac{R_2}{R_1 + R_2} \tag{H10}$$

Letting G_f denote the voltage gain at zero feedback ($B = 0$), an analysis of the circuit equations for our op-amp system yields:

$$\lambda_V \;=\; \frac{G_f}{1 + B\cdot G_f} \tag{H11a}$$

$$\lambda_I' \;=\; \frac{B}{1 + B\cdot G_f} \tag{H11b}$$

$$Z_{\text{out}} \;=\; \frac{Z_b}{1 + B\cdot G_f} \tag{H11c}$$

$$Z_{\text{in}} \;=\; (1 + B\cdot G_f)Z_a \tag{H11d}$$

$$G_P \;=\; \frac{G_f^2/2}{B\cdot G_f + 2Z_b/Z_a} \tag{H11e}$$

Again, G_f represents the gain of the amplifier in the absence of any feedback, Z_a is the input impedance at zero

feedback, and Z_b is the output impedance at zero feedback.

Transforming this into the scattering picture yields a scattering matrix s satisfying:

$$s_{11} = -s_{22} = -\frac{BG_f\left(Z_a - (2+BG_f)Z_b\right)}{BG_f Z_a + (2+BG_f)^2 Z_b} \quad \text{(H12a)}$$

$$s_{21} = -\frac{2\sqrt{Z_a Z_b}G_f\left(1+BG_f\right)}{BG_f Z_a + (2+BG_f)^2 Z_b} \quad \text{(H12b)}$$

$$s_{12} = \frac{B}{G_f}s_{21} \quad \text{(H12c)}$$

Note the connection between these equations and the necessary form of a quantum limited s-matrix found in the previous subsection.

Now, given a scattering matrix, one can always find a minimal representation of the noise operators $\mathcal{F}_a$ and $\mathcal{F}_b$ which have the necessary commutation relations. These are given in general by:

$$\hat{\mathcal{F}}_a = \sqrt{1-|s_{11}|^2-|s_{12}|^2+|l|^2}\cdot\hat{u}_{in} + l\cdot\hat{v}^\dagger_{in} \quad \text{(H13)}$$

$$\hat{\mathcal{F}}_b = \sqrt{|s_{21}|^2+|s_{22}|^2-1}\cdot\hat{v}^\dagger_{in} \quad \text{(H14)}$$

$$l = \frac{s_{11}s^*_{21}+s_{12}s^*_{22}}{\sqrt{|s_{21}|^2+|s_{22}|^2-1}} \quad \text{(H15)}$$

Applying this to the s matrix for our op-amp, and then taking the auxiliary modes $\hat{u}_{\rm in}$ and $\hat{v}^\dagger_{\rm in}$ to be in the vacuum state, we can calculate the minimum allowed $\bar{S}_{VV}$ and $\bar{S}_{II}$ for our non-inverting op-amp amplifier. One can then calculate the product $\bar{S}_{VV}\bar{S}_{II}$ and compare against the quantum-limited value ($\bar{S}_{IV}$ is again real). In the case of zero feedback (i.e. $B=0$), one of course finds that this product is twice as big as the quantum limited value. However, if one takes the large G_f limit while keeping B non-zero but finite, one obtains:

$$\bar{S}_{VV}\bar{S}_{II} \;\rightarrow\; (\hbar\omega)^2\left(1-\frac{2B}{G_f}+O\left(\frac{1}{G_f}\right)^2\right) \quad \text{(H16)}$$

Thus, for a fixed, non-zero feedback ratio B, it is possible to reach the quantum limit. Note that if B does not tend to zero as G_f tends to infinity, the voltage gain of this amplifier will be finite. The power gain however will be proportional to G_f and will be large. If one wants a large voltage gain, one could set B to go to zero with G_f i.e. $B \propto \frac{1}{\sqrt{G_f}}$. In this case, one will still reach the quantum limit in the large G_f limit, and the voltage gain will also be large (i.e. $\propto\sqrt{G_f}$). Note that in all these limits, the reflection coefficients s_{11} and s_{22} tend to -1 and 1 respectively, while the reverse gain tends to 0. This is in complete analogy to the amplifier with mirrors considered in the previous subsection, in the case where we took the reflections to be strong at the input and at the output (cf. Eq. (H7)). We thus see yet again how the use of feedback allows the system to reach the quantum limit.

Appendix I: Additional Technical Details

This appendix provides further details of calculations presented in the main text.

1. Proof of quantum noise constraint

Note first that we may write the symmetrized $\hat{I}$ and $\hat{F}$ noise correlators defined in Eqs. (4.4a) and (4.4b) as sums over transitions between detector energy eigenstates:

$$\bar{S}_{FF}[\omega] = \pi\hbar\sum_{i,f}\langle i|\hat{\rho}_0|i\rangle\cdot|\langle f|\hat{F}|i\rangle|^2\left[\delta(E_f-E_i+\hbar\omega)+\delta(E_f-E_i-\hbar\omega)\right] \quad \text{(I1)}$$

$$\bar{S}_{II}[\omega] = \pi\hbar\sum_{i,f}\langle i|\hat{\rho}_0|i\rangle\cdot|\langle f|\hat{I}|i\rangle|^2\left[\delta(E_f-E_i+\hbar\omega)+\delta(E_f-E_i-\hbar\omega)\right] \quad \text{(I2)}$$

Here, $\hat{\rho}_0$ is the stationary density matrix describing the state of the detector, and $|i\rangle$ ($|f\rangle$) is a detector energy eigenstate with energy E_i (E_f). Eq. (I1) expresses the noise at frequency ω as a sum over transitions. Each transition starts with an an initial detector eigenstate $|i\rangle$, occupied with a probability $\langle i|\rho_0|i\rangle$, and ends with a final detector eigenstate $|f\rangle$, where the energy difference between the two states is either $+\hbar\omega$ or $-\hbar\omega$. Further, each transition is weighted by an appropriate matrix element.

To proceed, we fix the frequency $\omega>0$, and let the index ν label each transition $|i\rangle\rightarrow|f\rangle$ contributing to the noise. More specifically, ν indexes each ordered pair of detector energy eigenstates states $\{|i\rangle,|f\rangle\}$ which satisfy $E_f-E_i\in\pm\hbar[\omega,\omega+d\omega]$ and $\langle i|\rho_0|i\rangle\neq 0$. We can now consider the matrix elements of $\hat{I}$ and $\hat{F}$ which contribute to $\bar{S}_{II}[\omega]$ and $\bar{S}_{FF}[\omega]$ to be complex vectors $\vec{v}$ and $\vec{w}$.

Letting δ be any real number, let us define:

$$[\vec{w}]_\nu = \langle f(\nu)|\hat{F}|i(\nu)\rangle \tag{I3}$$

$$[\vec{v}]_\nu = \begin{cases} e^{-i\delta}\langle f(\nu)|\hat{I}|i(\nu)\rangle & \text{if } E_{f(\nu)} - E_{i(\nu)} = +\hbar\omega, \\ e^{i\delta}\langle f(\nu)|\hat{I}|i(\nu)\rangle & \text{if } E_{f(\nu)} - E_{i(\nu)} = -\hbar\omega. \end{cases} \tag{I4}$$

Introducing an inner product $\langle\cdot,\cdot\rangle_\omega$ via:

$$\langle \vec{a}, \vec{b}\rangle_\omega = \pi \sum_\nu \langle i(\nu)|\hat{\rho}_0|i(\nu)\rangle \cdot (a_\nu)^* \, b_\nu, \tag{I5}$$

we see that the noise correlators $\bar{S}_{II}$ and $\bar{S}_{FF}$ may be written as:

$$\bar{S}_{II}[\omega]d\omega = \langle \vec{v}, \vec{v}\rangle_\omega \tag{I6}$$

$$\bar{S}_{FF}[\omega]d\omega = \langle \vec{w}, \vec{w}\rangle_\omega \tag{I7}$$

We may now employ the Cauchy-Schwartz inequality:

$$\langle \vec{v}, \vec{v}\rangle_\omega \langle \vec{w}, \vec{w}\rangle_\omega \geq |\langle \vec{v}, \vec{w}\rangle_\omega|^2 \tag{I8}$$

A straightforward manipulation shows that the real part of $\langle \vec{v}, \vec{w}\rangle_\omega$ is determined by the symmetrized cross-correlator $\bar{S}_{IF}[\omega]$ defined in Eq. (4.4c):

$$\text{Re } \langle \vec{v}, \vec{w}\rangle_\omega = \text{Re } \left[e^{i\delta}\bar{S}_{IF}[\omega]\right] d\omega \tag{I9}$$

In contrast, the imaginary part of $\langle \vec{v}, \vec{w}\rangle_\omega$ is independent of $\bar{S}_{IF}$; instead, it is directly related to the gain χ_{IF} and reverse gain χ_{FI} of the detector:

$$\text{Im } \langle \vec{v}, \vec{w}\rangle_\omega = \frac{\hbar}{2}\text{Re } \left[e^{i\delta}\left(\chi_{IF}[\omega] - [\chi_{FI}[\omega]]^*\right)\right] d\omega \tag{I10}$$

Substituting Eqs. (I10) and (I9) into Eq. (I8), one immediately finds the quantum noise constraint given in Eq. (4.16). As in the main text, we let $\tilde{\chi}_{IF} = \chi_{IF} - \chi^*_{FI}$. Maximizing the RHS of this inequality with respect to the phase δ, one finds that the maximum is achieved for $\delta = \delta_0 = -\arg(\tilde{\chi}_{IF}) + \tilde{\delta}_0$ with

$$\tan 2\tilde{\delta}_0 = -\frac{|\bar{S}_{IF}|\sin 2\phi}{(\hbar/2)|\tilde{\chi}_{IF}| + |\bar{S}_{IF}|\cos 2\phi} \tag{I11}$$

where $\phi = \arg(\bar{S}_{IF}\tilde{\chi}_{IF}*)$. At $\delta = \delta_0$, Eq. (4.16) becomes the final noise constraint of Eq. (4.11).

The proof given here also allows one to see what must be done in order to achieve the "ideal" noise condition of Eq. (4.17): one must achieve equality in the Cauchy-Schwartz inequality of Eq. (I8). This requires that the vectors $\vec{v}$ and $\vec{w}$ be proportional to one another; there must exist a complex factor α (having dimensions $[I]/[F]$) such that:

$$\vec{v} = \alpha \cdot \vec{w} \tag{I12}$$

Equivalently, we have that

$$\langle f|I|i\rangle = \begin{cases} e^{i\delta}\alpha\langle f|F|i\rangle & \text{if } E_f - E_i = +\hbar\omega \\ e^{-i\delta}\alpha\langle f|F|i\rangle & \text{if } E_f - E_i = -\hbar\omega. \end{cases} \tag{I13}$$

for *each* pair of initial and final states $|i\rangle$, $|f\rangle$ contributing to $\bar{S}_{FF}[\omega]$ and $\bar{S}_{II}[\omega]$ (cf. Eq. (I1)). Note that this *not* the same as requiring Eq. (I13) to hold for all possible states $|i\rangle$ and $|f\rangle$. This proportionality condition in turn implies a proportionality between the input and output (unsymmetrized) quantum noise spectral densities:

$$S_{II}[\omega] = |\alpha|^2 S_{FF}[\omega] \tag{I14}$$

It thus also follows that the imaginary parts of the input and output susceptibilities are proportional:

$$\text{Im } \chi_{II}[\omega] = |\alpha|^2 \text{Im } \chi_{FF}[\omega], \tag{I15}$$

as well as the symmetrized input and output noise (i.e. Eq. (4.18)). Finally, one can also use Eq. (I13) to relate the *unsymmetrized I-F* quantum noise correlator $S_{IF}[\omega]$ to $S_{FF}[\omega]$: (cf. Eq. (4.7)):

$$S_{IF}[\omega] = \begin{cases} e^{-i\delta}\alpha^* S_{FF}[\omega] & \text{if } \omega > 0, \\ e^{i\delta}\alpha^* S_{FF}[\omega] & \text{if } \omega < 0 \end{cases} \tag{I16}$$

Note that $S_{FF}[\omega]$ is necessarily real and positive.

Finally, for a detector with quantum-ideal noise properties, the magnitude of the constant α can be found from Eq. (4.18). The phase of α can also be determined from:

$$\frac{-\text{Im } \alpha}{|\alpha|} = \frac{\hbar|\tilde{\chi}_{IF}|/2}{\sqrt{\bar{S}_{II}\bar{S}_{FF}}}\cos\tilde{\delta}_0 \tag{I17}$$

For zero frequency or for a large detector effective temperature, this simplifies to:

$$\frac{-\text{Im } \alpha}{|\alpha|} = \frac{\hbar\tilde{\chi}_{IF}/2}{\sqrt{\bar{S}_{II}\bar{S}_{FF}}} \tag{I18}$$

Note importantly that to have a non-vanishing gain and power gain, one needs Im $\alpha \neq 0$. This in turn places a very powerful constraint on a quantum-ideal detectors: *all transitions contributing to the noise must be to final states $|f\rangle$ which are completely unoccupied.* To see this, imagine a transition taking an initial state $|i\rangle = |a\rangle$ to a final state $|f\rangle = |b\rangle$ makes a contribution to the noise. For a quantum-ideal detector, Eq. (I13) will be satisfied:

$$\langle b|\hat{I}|a\rangle = e^{\pm i\delta}\alpha\langle b|\hat{F}|a\rangle \tag{I19}$$

where the plus sign corresponds to $E_b > E_a$, the minus to $E_a > E_b$. If now the final state $|b\rangle$ was also occupied (i.e. $\langle b|\hat{\rho}_0|b\rangle \neq 0$), then the reverse transition $|i = b\rangle \rightarrow |f = a\rangle$) would also contribute to the noise. The proportionality condition of Eq. (I13) would now require:

$$\langle a|\hat{I}|b\rangle = e^{\mp i\delta}\alpha\langle a|\hat{F}|b\rangle \tag{I20}$$

As $\hat{I}$ and $\hat{F}$ are both Hermitian operators, and as α must have an imaginary part in order for there to be gain, we have a contradiction: Eq. (I19) and (I20) cannot both be true. It thus follows that the final state of a transition

contributing to the noise *must* be unoccupied in order for Eq. (I13) to be satisfied and for the detector to have ideal noise properties. Note that this necessary asymmetry in the occupation of detector energy eigenstates immediately tells us that *a detector or amplifier cannot reach the quantum limit if it is in equilibrium.*

2. Proof that a noiseless detector does not amplify

With the above results in hand, we can now prove assertions made in Sec. IV.A.4 that detectors which evade the quantum noise constraint of Eq. (4.11) and simply satisfy

$$\bar{S}_{FF}\bar{S}_{II} = |\bar{S}_{IF}|^2 \tag{I21}$$

are at best transducers, as their power gain is limited to being at most one.

The first way to make the RHS of Eq. (4.11) vanish is to have $\chi_{IF} = \chi_{FI}^*$. We have already seen that whenever this relation holds, the detector power gain cannot be any larger than one (c.f. Eq. (5.53)). Now, imagine that the detector also has a minimal amount of noise, i.e. Eq. (I21) also holds. This latter fact implies that the proportionality condition of Eq. (I13) also must hold. In this situation, the detector *must* have a power gain of unity, and is thus a transducer. There are two possibilities to consider here. First, $\bar{S}_{FF}$ and $\bar{S}_{II}$ could both be non-zero, but perfectly correlated: $|\bar{S}_{IF}|^2 = \bar{S}_{FF}\bar{S}_{II}$. In this case, the proportionality constant α must be real (c.f. Eq. (I17)). Using this fact along with Eqs. (I16) and (4.8b), one immediately finds that $S_{FF}[\omega] = S_{FF}[-\omega]$. This implies the back-action damping γ associated with the detector input vanishes (c.f. Eq. (2.12)). It thus follows immediately from Eq. (5.52) and Eq. (5.53) that the power gain $G_{P,\mathrm{rev}}$ (defined in a way that accounts for the reverse gain) is exactly one. The detector is thus simply a transducer. The other possibility here is that $\chi_{IF} = \chi_{FI}^*$ and one or both of $\bar{S}_{II}, \bar{S}_{FF}$ are equal zero. Note that if the symmetrized noise vanishes, then so must the asymmetric part of the noise. Thus, it follows that either the damping induced by the detector input, γ, or that induced by the output, γ_{out} (c.f. Eq. (5.48)) (or both) must be zero. Eqs. (5.52) and (5.53) then again yield a power gain $G_{P,\mathrm{rev}} = 1$. We thus have shown that any detector which has $\chi_{FI} = \chi_{IF}^*$ and satisfies $\bar{S}_{FF}\bar{S}_{II} = |\bar{S}_{IF}|^2$ must necessarily be a transducer, with a power gain precisely equal to one.

A second way to make the RHS of Eq. (4.11) vanish is to have $\bar{S}_{IF}/\tilde{\chi}_{IF}$ be purely imaginary and larger in magnitude than $\hbar/2$. Suppose this is the case, and that the detector also satisfies the minimal noise requirement of Eq. (I21). Without loss of generality, we take $\tilde{\chi}_{IF}$ to be real, implying that $\bar{S}_{IF}$ is purely imaginary. Eqs. (I10) and (I11) then imply that the phase factor $e^{i\delta}$ appearing in the proportionality relation of Eq. (I16) is purely imaginary, while the constant α is purely real. Using this proportionality relation in Eq. (4.8b) for $\tilde{\chi}_{IF}$ yields:

$$\begin{aligned}\tilde{\chi}_{IF} &= \frac{\alpha}{\hbar}\left(S_{FF}[\omega] - S_{FF}[-\omega]\right) \\ &= 2\alpha\left[-\mathrm{Im}\ \chi_{FF}[\omega]\right]\end{aligned} \tag{I22}$$

Using this result and the relation between χ_{FF} and χ_{II} in Eq. (I15), we can write the power gain in the absence of reverse gain, G_P (c.f. Eq. (5.52)), as

$$G_P = 1/\left|1 - \chi_{FI}/\chi_{IF}\right|^2 \tag{I23}$$

If the reverse gain vanishes (i.e. $\chi_{FI} = 0$), we immediately find that $G_P = 1$: the detector has a power gain of one, and is thus simply a transducer. If the reverse gain is non-zero, we must take the expression for G_P above and plug it into Eq. (5.53) for the power gain with reverse gain, $G_{P,\mathrm{rev}}$. Some algebra again yields that the full power gain is at most unity. We again have the conclusion that the detector does not amplify.

3. Simplifications for a quantum-limited detector

In this appendix, we derive the additional constraints on the property of a detector that arise when it satisfies the quantum noise constraint of Eq. (4.17). We focus on the ideal case where the reverse gain χ_{FI} vanishes.

To start, we substitute Eq. (I16) into Eqs. (4.8b)-(4.8a); writing $S_{FF}[\omega]$ in terms of the detector effective temperature T_{eff} (cf. Eq. (2.8)) yields:

$$\begin{aligned}\frac{\hbar\lambda[\omega]}{2} &= -e^{-i\delta}\hbar\left[-\mathrm{Im}\ \chi_{FF}[\omega]\right] \\ &\quad\left[(\mathrm{Im}\ \alpha)\coth\left(\frac{\hbar\omega}{2k_{\mathrm{B}}T_{\mathrm{eff}}}\right) + i\,(\mathrm{Re}\ \alpha)\right]\end{aligned} \tag{I24}$$

$$\begin{aligned}\bar{S}_{IF}[\omega] &= e^{-i\delta}\hbar\left[-\mathrm{Im}\ \chi_{FF}[\omega]\right] \\ &\quad\left[(\mathrm{Re}\ \alpha)\coth\left(\frac{\hbar\omega}{2k_{\mathrm{B}}T_{\mathrm{eff}}}\right) - i\,(\mathrm{Im}\ \alpha)\right]\end{aligned} \tag{I25}$$

To proceed, let us write:

$$e^{-i\delta} = \frac{\lambda}{|\lambda|}e^{-i\tilde{\delta}} \tag{I26}$$

The condition that $|\lambda|$ is real yields the condition:

$$\tan\tilde{\delta} = \frac{\mathrm{Re}\ \alpha}{\mathrm{Im}\alpha}\tanh\left(\frac{\hbar\omega}{2k_{\mathrm{B}}T_{\mathrm{eff}}}\right) \tag{I27}$$

We now consider the relevant limit of a large detector power gain G_P. G_P is determined by Eq. (5.56); the only way this can become large is if $k_{\mathrm{B}}T_{\mathrm{eff}}/(\hbar\omega) \to \infty$ while Im α does not tend to zero. We will thus take the large T_{eff} limit in the above equations while keeping both α and the phase of λ fixed. Note that this means the parameter $\tilde{\delta}$ must evolve; it tends to zero in the large T_{eff} limit. In

this limit, we thus find for λ and $\bar{S}_{IF}$:

$$\frac{\hbar\lambda[\omega]}{2} = -2e^{-i\delta}k_{\rm B}T_{\rm eff}\gamma[\omega]\,(\text{Im }\alpha)\left[1+O\left[\left(\frac{\hbar\omega}{k_{\rm B}T_{\rm eff}}\right)^2\right]\right] \tag{I28}$$

$$\bar{S}_{IF}[\omega] = 2e^{-i\delta}k_{\rm B}T_{\rm eff}\gamma[\omega]\,(\text{Re }\alpha)\left[1+O\left(\frac{\hbar\omega}{k_{\rm B}T_{\rm eff}}\right)\right] \tag{I29}$$

Thus, in the large power-gain limit (i.e. large $T_{\rm eff}$ limit), the gain λ and the noise cross-correlator $\bar{S}_{IF}$ have the same phase: $\bar{S}_{IF}/\lambda$ is purely real.

4. Derivation of non-equilibrium Langevin equation

In this appendix, we prove that an oscillator weakly coupled to an arbitrary out-of-equilibrium detector is described by the Langevin equation given in Eq. (5.41), an equation which associates an effective temperature and damping kernel to the detector. The approach taken here is directly related to the pioneering work of Schwinger (Schwinger, 1961).

We start by defining the oscillator matrix Keldysh green function:

$$\check{G}(t) = \begin{pmatrix} G^K(t) & G^R(t) \\ G^A(t) & 0 \end{pmatrix} \tag{I30}$$

where $G^R(t-t') = -i\theta(t-t')\langle[\hat{x}(t),\hat{x}(t')]\rangle$, $G^A(t-t') = i\theta(t'-t)\langle[\hat{x}(t),\hat{x}(t')]\rangle$, and $G^K(t-t') = -i\langle\{\hat{x}(t),\hat{x}(t')\}\rangle$. At zero coupling to the detector ($A=0$), the oscillator is only coupled to the equilibrium bath, and thus $\check{G}_0$ has the standard equilibrium form:

$$\check{G}_0[\omega] = \frac{\hbar}{m}\begin{pmatrix} -2\text{Im }g_0[\omega]\coth\left(\frac{\hbar\omega}{2k_{\rm B}T_{\rm bath}}\right) & g_0[\omega] \\ g_0[\omega]^* & 0 \end{pmatrix} \tag{I31}$$

where:

$$g_0[\omega] = \frac{1}{\omega^2-\Omega^2+i\omega\gamma_0/m} \tag{I32}$$

and where γ_0 is the intrinsic damping coefficient, and $T_{\rm bath}$ is the bath temperature.

We next treat the effects of the coupling to the detector in perturbation theory. Letting $\check{\Sigma}$ denote the corresponding self-energy, the Dyson equation for $\check{G}$ has the form:

$$\left[\check{G}[\omega]\right]^{-1} = \left[\check{G}_0[\omega]\right]^{-1} - \begin{pmatrix} 0 & \Sigma^A[\omega] \\ \Sigma^R[\omega] & \Sigma^K[\omega] \end{pmatrix} \tag{I33}$$

To lowest order in A, $\check{\Sigma}[\omega]$ is given by:

$$\check{\Sigma}[\omega] = A^2\check{D}[\omega] \tag{I34}$$

$$\equiv \frac{A^2}{\hbar}\int dt\; e^{i\omega t} \begin{pmatrix} 0 & i\theta(-t)\langle[\hat{F}(t),\hat{F}(0)]\rangle \\ -i\theta(t)\langle[\hat{F}(t),\hat{F}(0)]\rangle & -i\langle\{\hat{F}(t),\hat{F}(0)\}\rangle \end{pmatrix} \tag{I35}$$

Using this lowest-order self energy, Eq. (I33) yields:

$$G^R[\omega] = \frac{\hbar}{m(\omega^2-\Omega^2) - A^2\text{Re }D^R[\omega] + i\omega(\gamma_0+\gamma[\omega])} \tag{I36}$$

$$G^A[\omega] = \left[G^R[\omega]\right]^* \tag{I37}$$

$$G^K[\omega] = -2i\text{Im }G^R[\omega]\times \frac{\gamma_0\coth\left(\frac{\hbar\omega}{2k_{\rm B}T_{\rm bath}}\right)+\gamma[\omega]\coth\left(\frac{\hbar\omega}{2k_{\rm B}T_{\rm eff}}\right)}{\gamma_0+\gamma[\omega]} \tag{I38}$$

where $\gamma[\omega]$ is given by Eq. (2.12), and $T_{\rm eff}[\omega]$ is defined by Eq. (2.8). The main effect of the real part of the retarded $\hat{F}$ Green function $D^R[\omega]$ in Eq. (I36) is to renormalize the oscillator frequency Ω and mass m; we simply incorporate these shifts into the definition of Ω and m in what follows.

If $T_{\rm eff}[\omega]$ is frequency independent, then Eqs. (I36) - (I38) for $\check{G}$ corresponds exactly to an oscillator coupled to two equilibrium baths with damping kernels γ_0 and $\gamma[\omega]$. The correspondence to the Langevin equation Eq. (5.41) is then immediate. In the more general case where $T_{\rm eff}[\omega]$ has a frequency dependence, the correlators $G^R[\omega]$ and $G^K[\omega]$ are in exact correspondence to what is found from the Langevin equation Eq. (5.41): $G^K[\omega]$ corresponds to symmetrized noise calculated from Eq. (5.41), while $G^R[\omega]$ corresponds to the response coefficient of the oscillator calculated from Eq. (5.41). This again proves the validity of using the Langevin equation Eq. (5.41) to calculate the oscillator noise in the presence of the detector to lowest order in A.

5. Linear-response formulas for a two-port bosonic amplifier

In this appendix, we use the standard linear-response Kubo formulas of Sec. V.F to derive expressions for the voltage gain λ_V, reverse current gain λ'_I, input impedance Z_{in} and output impedance Z_{out} of a two-port bosonic voltage amplifier (cf. Sec. VI). We recover the same expressions for these quantities obtained in Sec. VI from the scattering approach. We stress throughout this appendix the important role played by the causal structure of the scattering matrix describing the amplifier.

In applying the general linear response formulas, we must bear in mind that these expressions should be applied to the *uncoupled* detector, i.e. nothing attached to the detector input or output. In our two-port bosonic voltage amplifier, this means that we should have a short circuit at the amplifier input (i.e. no input voltage, $V_a = 0$), and we should have open circuit at the output (i.e. $I_b = 0$, no load at the output drawing current). These two conditions define the uncoupled amplifier. Using the definitions of the voltage and current operators (cf. Eqs. (6.2a) and (6.2b)), they take the form:

$$\hat{a}_{\rm in}[\omega] = -\hat{a}_{\rm out}[\omega] \tag{I39a}$$

$$\hat{b}_{\rm in}[\omega] = \hat{b}_{\rm out}[\omega] \tag{I39b}$$

The scattering matrix equation Eq. (6.3) then allows us to solve for $\hat{a}_{in}$ and $\hat{a}_{out}$ in terms of the added noise operators $\hat{\mathcal{F}}_a$ and $\hat{\mathcal{F}}_b$.

$$\hat{a}_{\rm in}[\omega] = -\frac{1-s_{22}}{D}\hat{\mathcal{F}}_a[\omega] - \frac{s_{12}}{D}\hat{\mathcal{F}}_b[\omega] \quad \text{(I40a)}$$

$$\hat{b}_{\rm in}[\omega] = -\frac{s_{21}}{D}\hat{\mathcal{F}}_a[\omega] + \frac{1+s_{11}}{D}\hat{\mathcal{F}}_b[\omega] \quad \text{(I40b)}$$

where D is given in Eq. (6.8), and we have omitted writing the frequency dependence of the scattering matrix. Further, as we have already remarked, the commutators of the added noise operators is completely determined by the scattering matrix and the constraint that output operators have canonical commutation relations. The non-vanishing commutators are thus given by:

$$\left[\hat{\mathcal{F}}_a[\omega], \hat{\mathcal{F}}_a^\dagger(\omega')\right] = 2\pi\delta(\omega-\omega')\left(1-|s_{11}|^2-|s_{12}|^2\right) \quad \text{(I41a)}$$

$$\left[\hat{\mathcal{F}}_b[\omega], \hat{\mathcal{F}}_b^\dagger(\omega')\right] = 2\pi\delta(\omega-\omega')\left(1-|s_{21}|^2-|s_{22}|^2\right) \quad \text{(I41b)}$$

$$\left[\hat{\mathcal{F}}_a[\omega], \hat{\mathcal{F}}_b^\dagger(\omega')\right] = -2\pi\delta(\omega-\omega')\left(s_{11}s_{21}^* + s_{12}s_{22}^*\right) \quad \text{(I41c)}$$

The above equations, used in conjunction with Eqs. (6.2a) and (6.2b), provide us with all all the information needed to calculate commutators between current and voltage operators. It is these commutators which enter into the linear-response Kubo formulas. As we will see, our calculation will crucially rely on the fact that the scattering description obeys causality: disturbances at the input of our system must take some time before they propagate to the output. Causality manifests itself in the energy dependence of the scattering matrix: as a function of energy, it is an analytic function in the upper half complex plane.

a. Input and output impedances

Eq. (5.84) is the linear response Kubo formula for the input impedance of a voltage amplifier. Recall that the input operator $\hat{Q}$ for a voltage amplifier is related to the input current operator $\hat{I}_a$ via $-d\hat{Q}/dt = \hat{I}_a$ (cf. Eq. (5.83)). The Kubo formula for the input impedance may thus be re-written in the more familiar form:

$$Y_{\rm in,Kubo}[\omega] \equiv \frac{i}{\omega}\left(-\frac{i}{\hbar}\int_0^\infty dt \langle[\hat{I}_a(t), \hat{I}_a(0)]\rangle e^{i\omega t}\right) \quad \text{(I42)}$$

where $Y_{\rm in}[\omega] = 1/Z_{\rm in}[\omega]$,

Using the defining equation for $\hat{I}_a$ (Eq. (6.1b)) and Eq. (I39a) (which describes an uncoupled amplifier), we obtain:

$$Y_{\rm in,Kubo}[\omega] = \frac{2}{Z_a}\int_0^\infty dt e^{i\omega t}\int_0^\infty \frac{d\omega'}{2\pi}\frac{\omega'}{\omega}\Lambda_{aa}(\omega')\left(e^{-i\omega' t} - e^{i\omega' t}\right) \quad \text{(I43)}$$

where we have defined the real function $\Lambda_{aa}[\omega]$ for $\omega > 0$ via:

$$\left[\hat{a}_{\rm in}[\omega], \hat{a}_{\rm in}^\dagger(\omega')\right] = 2\pi\delta(\omega-\omega')\Lambda_{aa}[\omega] \quad \text{(I44)}$$

It will be convenient to also define $\Lambda_{aa}[\omega]$ for $\omega < 0$ via $\Lambda_{aa}[\omega] = \Lambda_{aa}[-\omega]$. Eq. (I43) may then be written as:

$$\begin{aligned} Y_{\rm in,Kubo}[\omega] &= \frac{2}{Z_a}\int_0^\infty dt \int_{-\infty}^\infty \frac{d\omega'}{2\pi}\frac{\omega'}{\omega}\Lambda_{aa}(\omega')e^{i(\omega-\omega')t} \\ &= \frac{\Lambda_{aa}[\omega]}{Z_a} + \frac{i}{\pi\omega}\mathcal{P}\int_{-\infty}^\infty d\omega' \frac{\omega'\Lambda_{aa}(\omega')/Z_a}{\omega-\omega'} \end{aligned} \quad \text{(I45)}$$

Next, by making use of Eq. (I40a) and Eqs. (I41) for the commutators of the added noise operators, we can explicitly evaluate the commutator in Eq. (I44) to calculate $\Lambda_{aa}[\omega]$. Comparing the result against the result Eq. (6.7d) of the scattering calculation, we find:

$$\frac{\Lambda_{aa}[\omega]}{Z_a} = \text{Re } Y_{\rm in,scatt}[\omega] \quad \text{(I46)}$$

where $Y_{\rm in,scatt}[\omega]$ is the input admittance of the amplifier obtained from the scattering approach. Returning to Eq. (I45), we may now use the fact that $Y_{in,scatt}[\omega]$ is an analytic function in the upper half plane to simplify the second term on the RHS, as this term is simply a Kramers-Kronig integral:

$$\begin{aligned} &\frac{1}{\pi\omega}\mathcal{P}\int_{-\infty}^\infty d\omega' \frac{\omega'\Lambda_{aa}(\omega')/Z_a}{\omega-\omega'} \\ &= \frac{1}{\pi\omega}\mathcal{P}\int_{-\infty}^\infty d\omega' \frac{\omega'\text{Re } Y_{\rm in,scatt}(\omega')}{\omega-\omega'} \\ &= \text{Im } Y_{\rm in,scatt}[\omega] \end{aligned} \quad \text{(I47)}$$

It thus follows from Eq. (I45) that input impedance calculated from the Kubo formula is equal to what we found previously using the scattering approach.

The calculation for the output impedance proceeds in the same fashion, starting from the Kubo formula given in Eq. (5.85). As the steps are completely analogous to the above calculation, we do not present it here. One again recovers Eq. (6.7c), as found previously within the scattering approach.

b. Voltage gain and reverse current gain

Within linear response theory, the voltage gain of the amplifier (λ_V) is determined by the commutator between the "input operator" $\hat{Q}$ and $\hat{V}_b$ (cf. Eq. (4.3); recall that $\hat{Q}$ is defined by $d\hat{Q}/dt = -\hat{I}_a$. Similarly, the reverse current gain (λ_I') is determined by the commutator between $\hat{I}_a$ and $\hat{\Phi}$, where $\hat{\Phi}$ is defined via $d\hat{\Phi}/dt = -\hat{V}_b$ (cf. Eq. (4.6)). Similar to the calculation of the input impedance, to properly evaluate the Kubo formulas for

the gains, we must make use of the causal structure of the scattering matrix describing our amplifier.

Using the defining equations of the current and voltage operators (cf. Eqs. (6.1a) and (6.1b)), as well as Eqs. (I39a) and (I39b) which describe the uncoupled amplifier, the Kubo formulas for the voltage gain and reverse current gain become:

$$\lambda_{V,\mathrm{Kubo}}[\omega] = 4\sqrt{\frac{Z_b}{Z_a}} \times \int_0^\infty dt\; e^{i\omega t}\mathrm{Re}\left[\int_0^\infty \frac{d\omega'}{2\pi}\Lambda_{ba}(\omega')e^{-i\omega' t}\right] \tag{I48}$$

$$\lambda'_{I,\mathrm{Kubo}}[\omega] = -4\sqrt{\frac{Z_b}{Z_a}} \times \int_0^\infty dt\; e^{i\omega t}\mathrm{Re}\left[\int_0^\infty \frac{d\omega'}{2\pi}\Lambda_{ba}(\omega')e^{i\omega' t}\right] \tag{I49}$$

where we define the complex function $\Lambda_{ba}[\omega]$ for $\omega > 0$ via:

$$\left[\hat{b}_{in}[\omega], \hat{a}^\dagger_{in}(\omega')\right] \equiv (2\pi\delta(\omega-\omega'))\,\Lambda_{ba}[\omega] \tag{I50}$$

We can explicitly evaluate $\Lambda_{ba}[\omega]$ by using Eqs. (I40a)-(I41) to evaluate the commutator above. Comparing the result against the scattering approach expressions for the gain and reverse gain (cf. Eqs. (6.7a) and (6.7b)), one finds:

$$\Lambda_{ba}[\omega] = \lambda_{V,\mathrm{scatt}}[\omega] - \left[\lambda'_{I,\mathrm{scatt}}[\omega]\right]^* \tag{I51}$$

Note crucially that the two terms above have different analytic properties: the first is analytic in the upper half plane, while the second is analytic in the lower half plane. This follows directly from the fact that the scattering matrix is causal.

At this stage, we can proceed much as we did in the calculation of the input impedance. Defining $\Lambda_{ba}[\omega]$ for $\omega < 0$ via $\Lambda_{ba}[-\omega] = \Lambda^*_{ba}[\omega]$, we can re-write Eqs. (I48) and (I49) in terms of principle part integrals.

$$\begin{aligned}\lambda_{V,\mathrm{Kubo}}[\omega] &= \frac{Z_b}{Z_a}\left(\Lambda_{ba}[\omega] + \frac{i}{\pi}\mathcal{P}\int_{-\infty}^{\infty} d\omega' \frac{\Lambda_{ba}(\omega')}{\omega-\omega'}\right)\\ \lambda'_{I,\mathrm{Kubo}}[\omega] &= -\frac{Z_b}{Z_a}\left(\Lambda_{ba}[\omega] + \frac{i}{\pi}\mathcal{P}\int_{-\infty}^{\infty} d\omega' \frac{\Lambda_{ba}(\omega')}{\omega+\omega'}\right)\end{aligned} \tag{I52}$$

Using the analytic properties of the two terms in Eq. (I51) for $\Lambda_{ba}[\omega]$, we can evaluate the principal part integrals above as Kramers-Kronig relations. One then finds that the Kubo formula expressions for the voltage and current gain coincide precisely with those obtained from the scattering approach.

While the above is completely general, it is useful to go through a simpler, more specific case where the role of causality is more transparent. Imagine that all the energy dependence in the scattering in our amplifier arises from the fact that there are small transmission line "stubs" of length a attached to both the input and output of the amplifier (these stubs are matched to the input and output lines). Because of these stubs, a wavepacket incident on the amplifier will take a time $\tau = 2a/v$ to be either reflected or transmitted, where v is the characteristic velocity of the transmission line. This situation is described by a scattering matrix which has the form:

$$s[\omega] = e^{2i\omega a/v}\cdot \bar{s} \tag{I53}$$

where $\bar{s}$ is frequency-independent and real. To further simplify things, let us assume that $\bar{s}_{11} = \bar{s}_{22} = \bar{s}_{12} = 0$. Eqs. (I51) then simplifies to

$$\Lambda_{ba}[\omega] = = s_{21}[\omega] = \bar{s}_{21}e^{i\omega\tau} \tag{I54}$$

where the propagation time $\tau = 2a/v$ We then have:

$$\lambda_V[\omega_0] = 2\sqrt{\frac{Z_b}{Z_a}}\bar{s}_{21}\int_0^\infty dt\; e^{i\omega_0 t}\delta(t-\tau) \tag{I55}$$

$$\lambda_I[\omega_0] = -2\sqrt{\frac{Z_b}{Z_a}}\bar{s}_{21}\int_0^\infty dt\; e^{i\omega_0 t}\delta(t+\tau) \tag{I56}$$

If we now do the time integrals and then take the limit $\tau \to 0^+$, we recover the results of the scattering approach (cf. Eqs. (6.7a) and (6.7b)); in particular, $\lambda_I = 0$. Note that if we had set $\tau = 0$ from the outset of the calculation, we would have found that both λ_V and λ_I are non-zero!

6. Details for the two-port bosonic voltage amplifier with feedback

In this appendix, we provide more details on the calculations for the bosonic-amplifier-plus-mirrors system discussed in Sec. H. Given that the scattering matrix for each of the three mirrors is given by Eq. (H2), and that we know the reduced scattering matrix for the mirror-free system (cf. Eq. (6.10)), we can find the reduced scattering matrix and noise operators for the system with mirrors. One finds that the reduced scattering matrix s is now given by:

$$s = \frac{1}{M}\times \begin{pmatrix} \sin\theta_z + \sqrt{G}\sin\theta_x\sin\theta_y & -\cos\theta_x\cos\theta_z\sin\theta_y \\ \sqrt{G}\cos\theta_x\cos\theta_z & \sin\theta_x + \sqrt{G}\sin\theta_y\sin\theta_z \end{pmatrix} \tag{I57}$$

where the denominator M describes multiple reflection processes:

$$M = 1 + \sqrt{G}\sin\theta_x\sin\theta_z\sin\theta_y \tag{I58}$$

Further, the noise operators are given by:

$$\begin{pmatrix} \mathcal{F}_a \\ \mathcal{F}_b \end{pmatrix} = \frac{1}{M} \begin{pmatrix} \cos\theta_y \cos\theta_z & \sqrt{G-1}\cos\theta_z \sin\theta_x \sin\theta_y \\ -\sqrt{G}\cos\theta_x \cos\theta_y \sin\theta_z & \sqrt{G-1}\cos\theta_x \end{pmatrix} \begin{pmatrix} u_{in} \\ v_{in}^\dagger \end{pmatrix} \tag{I59}$$

The next step is to convert the above into the op-amp representation, and find the gains and impedances of the amplifier, along with the voltage and current noises. The voltage gain is given by:

$$\lambda_V = \sqrt{\frac{Z_B}{Z_A}} \frac{2\sqrt{G}}{1-\sqrt{G}\sin\theta_y} \cdot \frac{1+\sin\theta_x}{\cos\theta_x} \frac{1-\sin\theta_z}{\cos\theta_z} \tag{I60}$$

while the reverse gain is related to the voltage gain by the simple relation:

$$\lambda_I' = -\frac{\sin\theta_y}{\sqrt{G}} \lambda_V \tag{I61}$$

The input impedance is determined by the amount of reflection in the input line and in the line going to the cold load:

$$Z_{\rm in} = Z_a \frac{1-\sqrt{G}\sin\theta_y}{1+\sqrt{G}\sin\theta_y} \cdot \frac{1+\sin\theta_z}{1-\sin\theta_z} \tag{I62}$$

Similarly, the output impedance only depends on the amount of reflection in the output line and the in the cold-load line:

$$Z_{\rm out} = Z_b \frac{1+\sqrt{G}\sin\theta_y}{1-\sqrt{G}\sin\theta_y} \cdot \frac{1+\sin\theta_x}{1-\sin\theta_x} \tag{I63}$$

Note that as $\sin\theta_y$ tends to $-1/\sqrt{G}$, both the input admittance and output impedance tend to zero.

Given that we now know the op-amp parameters of our amplifier, we can use Eq. (6.5) to calculate the amplifier's power gain G_P. Amazingly, we find that the power gain is completely independent of the mirrors in the input and output lines:

$$G_P = \frac{G}{1+G\sin^2\theta_y} \tag{I64}$$

Note that at the special value $\sin\theta_y = -1\sqrt{G}$ (which allows one to reach the quantum limit), the power gain is reduced by a factor of two compared to the reflection free case (i.e. $\theta_y = 0$).

Turning to the noise spectral densities, we assume the optimal situation where both the auxiliary modes $\hat{u}_{in}$ and $\hat{v}_{in}^\dagger$ are in the vacuum state. We then find that both $\hat{\tilde{I}}$ and $\hat{\tilde{V}}$ are independent of the amount of reflection in the output line (e.g. θ_x):

$$\bar{S}_{II} = \frac{2\hbar\omega}{Z_a}\left[\frac{1-\sin\theta_z}{1+\sin\theta_z}\right] \times \left(\frac{G\sin^2\theta_y + \cos(2\theta_y)}{\left(\sqrt{G}\sin\theta_y - 1\right)^2}\right) \tag{I65a}$$

$$\bar{S}_{VV} = \hbar\omega Z_a \left[\frac{1+\sin\theta_z}{1-\sin\theta_z}\right] \times \left(\frac{3+\cos(2\theta_y)}{4} - \frac{1}{2G}\right) \tag{I65b}$$

$$\bar{S}_{VI} = \frac{\sqrt{G}(1-1/G)\sin\theta_y + \cos^2\theta_y}{1-\sqrt{G}\sin\theta_y} \tag{I65c}$$

As could be expected, introducing reflections in the input line (i.e. $\theta_z \neq 0$) has the opposite effect on $\bar{S}_{II}$ versus $\bar{S}_{VV}$: if one is enhanced, the other is suppressed.

It thus follows that the product of noise spectral densities appearing in the quantum noise constraint of Eq. (5.88) is given by (taking the large-G limit):

$$\frac{\bar{S}_{II}\bar{S}_{VV}}{(\hbar\omega)^2} = \left(2-\sin^2\theta_y\right) \cdot \frac{1+G\sin^2\theta_y}{\left(1-\sqrt{G}\sin\theta_y\right)^2} \tag{I66}$$

Note that somewhat amazingly, this product (and hence the amplifier noise temperature) is completely independent of the mirrors in the input and output arms (i.e. θ_z and θ_x). This is a result of both $\bar{S}_{VV}$ and $\bar{S}_{II}$ having no dependence on the output mirror (θ_x), and their having opposite dependencies on the input mirror (θ_z). Also note that Eq. (I66) does indeed reduce to the result of the last subsection: if $\theta_y = 0$ (i.e. no reflections in the line going to the cold load), the product $\bar{S}_{II}\bar{S}_{VV}$ is equal to precisely twice the quantum limit value of $(\hbar\omega)^2$. For $\sin(\theta_y) = -1/\sqrt{G}$, the RHS above reduces to one, implying that we reach the quantum limit for this tuning of the mirror in the cold-load arm.

References

Amin, M. H. S., and D. V. Averin, 2008, Phys. Rev. Lett. **100**, 197001.

Arcizet, O., P.-F. Cohadon, T. Briant, M. Pinard, and A. Hedimann, 2006, Nature **444**, 71.

Billangeon, P. M., F. Pierre, H. Bouchiat, and R. Deblock, 2006, Phys. Rev. Lett. **96**, 136804.

Blais, A., R.-S. Huang, A. Wallraff, S. M. Girvin, and R. J. Schoelkopf, 2004, Phys. Rev. A **69**, 062320.

Brown, K. R., J. Britton, R. J. Epstein, J. Chiaverini, D. Leibfried, and D. J. Wineland, 2007, Phys. Rev. Lett. **99**, 137205.
Burkhard, G., R. H. Koch, and D. P. DiVincenzo, 2004, Phys. Rev. B **69**, 064503.
Caldeira, A., and A. Leggett, 1983, Ann. Phys. (NY) **149**, 374.
Clerk, A. A., S. M. Girvin, and A. D. Stone, 2003, Phys. Rev. B **67**, 165324.
Cohen-Tannoudji, C., J. Dupont-Roc, and G. Grynberg, 1989, *Photons and Atoms - Introduction to Quantum Electrodynamics* (Wiley, New York).
Courty, J. M., F. Grassia, and S. Reynaud, 1999, Europhys. Lett. **46**, 31.
Cover, T., and J. Thomas, 1991, *Elements of Information Theory* (Wiley, New York).
Deblock, R., E. Onac, L. Gurevich, and L. P. Kouwenhoven, 2003, Science **301**, 203.
Devoret, M., 1997, in *Quantum Fluctuations (Les Houches Session LXIII)* (Elsevier, Amsterdam), pp. 351–86.
Gardiner, C. W., A. S. Parkins, and P. Zoller, 1992, Phys. Rev. A **46**, 4363.
Gardiner, C. W., and P. Zoller, 2000, *Quantum Noise* (Springer, Berlin).
Gavish, U., Y. Levinson, and Y. Imry, 2000, Phys. Rev. B (R) **62**, 10637.
Gea-Banacloche, J., N. Lu, L. M. Pedrotti, S. Prasad, M. O. Scully, and K. Wodkiewicz, 1990a, Phys. Rev. A **41**, 369.
Gea-Banacloche, J., N. Lu, L. M. Pedrotti, S. Prasad, M. O. Scully, and K. Wodkiewicz, 1990b, Phys. Rev. A **41**, 381.
Gigan, S., H. Böhm, M. Paternostro, F. Blaser, J. B. Hertzberg, K. C. Schwab, D. Bauerle, M. Aspelmeyer, and A. Zeilinger, 2006, Nature **444**, 67.
Glauber, R. J., 2006, Rev. Mod. Phys. **78**, 1267.
Grassia, F., 1998, *Fluctuations quantiques et thermiques dans les transducteurs electromecaniques*, Ph.D. thesis, Universite Pierre et Marie Curie.
Harris, J. G. E., B. M. Zwickl, and A. M. Jayich, 2007, Review of Scientific Instruments **78**, 013107.
Höhberger-Metzger, C., and K. Karrai, 2004, Nature **432**, 1002.
Lang, R., M. O. Scully, and J. Willis E. Lamb, 1973, Phys. Rev. A **7**, 1788.
Lesovik, G. B., and R. Loosen, 1997, JETP Lett. **65**, 295.
Mallat, S., 1999, *A Wavelet Tour of Signal Processing* (Academic, San Diego).
Marquardt, F., J. P. Chen, A. A. Clerk, and S. M. Girvin, 2007, Phys. Rev. Lett. **99**, 093902.
Marquardt, F., J. G. E. Harris, and S. M. Girvin, 2006, Phys. Rev. Lett. **96**, 103901.
Meystre, P., E. M. Wright, J. D. McCullen, and E. Vignes, 1985, J. Opt. Soc. Am. B **2**, 1830.
Onac, E., F. Balestro, B. Trauzettel, C. F. J. Lodewijk, and L. P. Kouwenhoven, 2006, Phys. Rev. Lett. **96**, 026803.
Schliesser, A., P. Del'Haye, N. Nooshi, K. J. Vahala, and T. J. Kippenberg, 2006, Phys. Rev. Lett. **97**, 243905.
Schoelkopf, R. J., P. J. Burke, A. A. Kozhevnikov, D. E. Prober, and M. J. Rooks, 1997, Phys. Rev. Lett. **78**, 3370.
Schuster, D. I., A. Wallraff, A. Blais, L. Frunzio, R.-S. Huang, J. Majer, S. M. Girvin, and R. J. Schoelkopf, 2005, Phys. Rev. Lett. **94**, 123602.
Schwinger, J., 1961, J. Math. Phys. **2**, 407.
Teufel, J. D., C. A. Regal, and K. W. Lehnert, 2008, New J. Phys. **10**, 095002.
Thompson, J. D., B. M. Zwickl, A. M. Jayich, F. Marquardt, S. M. Girvin, and J. G. E. Harris, 2008, Nature (London) **452**, 06715.
Wallraff, A., D. I. Schuster, A. Blais, L. Frunzio, R.-S. Huang, J. Majer, S. Kumar, S. M. Girvin, and R. J. Schoelkopf, 2004, Nature (London) **431**, 162.
Walls, D. F., and G. J. Milburn, 1994, *Quantum Optics* (Springer, Berlin).
Wilson-Rae, I., N. Nooshi, W. Zwerger, and T. J. Kippenberg, 2007, Phys. Rev. Lett. **99**, 093901.
Yurke, B., 1984, Phys. Rev. A **29**, 408.
Yurke, B., and J. S. Denker, 1984, Phys. Rev. A **29**, 1419.